PREDICTION OF SATELLITE LINK RAIN ATTENUATION USING RADAR REFLECTIVITY FOR TROPICAL CLIMATE IN MALAYSIA

BY

KHAIRAYU BINTI BADRON

A thesis submitted in fulfillment of the requirement for the degree of Doctor of Philosophy (Engineering)

Kulliyyah of Engineering
International Islamic University Malaysia

MAY 2016

ABSTRACT

The requirements of wireless communications in Malaysia, both civilian and military will evidently include wideband capacity satellite systems. Prior to satellite launching, the precise rain fade margin has to be identified. At the moment, most prediction models for the link rain fade margin are not able to offer accurate estimation when compared to actual measurement. Current available rain attenuation prediction models are also regarded as "not universally applicable", and involve gross generalization as well as over simplification by using only point rainfall rate at 0.01% of time exceedance and speculated rain heights. Radar reflectivity data which are available at almost all points of the affected slant path link are believed to be capable of providing a more relevant rain attenuation estimation. This research was carried out in collaboration with the Malaysian National Space Agency (ANGKASA) and Malaysian Meteorology Department (MMD). RazakSAT's data and one-year radar data had been analyzed. The overall objective of this research is the derivation of a new technique using radar information, believed to be capable of generating a more reliable annual statistics of rain attenuation compared to previously proposed methods. In this research, the information from a radar had been exploited in estimating the rain attenuation using vertical and horizontal variability of rain events. The sub-objectives of the study involved quantification of knowledge concerning propagation effects, determination of climatological influences and production of refined propagation models for satellite communications. Tasks involved include derivation of relationship between radar reflectivity and actual satellite link attenuation at X-band frequency using the regression technique. The one-year rain events were classified where the characteristics had been deliberated to acquire vertical profile reflectivity (VPR) and the empirical rain height values. All information are important for attenuation predictions, link budget estimation, microwave system planning, slant path rain attenuation modelling and remote sensing of the Earth's surface. The new technique achieves reduced error of only 4.13% variation. This is certainly a great improvement as compared to the ITU-R estimation. ITU-R estimation has percentage error of 58.21% variation. The findings of this research will be valuable for the future designers in configuring the best communication establishment for satellite system operating in the tropics.

خلاصة البحث

من الواضح ان متطلبات الاتصالات اللاسلكية في ماليزيا ستشمل الاقمار الصناعية ذات النطاق الواسع سواء كان ذلك للتطبيقات المدنية او العسكرية على حد السواء. انه من الضرورة (wideband) بمكان ان يتم تحديد الحيز المسموح به للخسائر الناتجة عن المطر قبل اي عملية اطلاق لاي قمر صناعي. في الوقت الراهن، معظم النماذج المتوفرة عالميا لتحديد الحيز المسموح به للخسائر الناتجة عن المطر تعتبر غير دقيقة بالصورة المطلوبة اذا ما قورنت بقياسات حقيقية وفعلية. ومن المآخذ التي يمكن تؤخذ على هذه النماذج المقترحة والمستخدمة حاليا بانها غير عالمية بمعنى انه لا يمكن تطبيقها في جميع الدول، وايضا كذلك المبالغة في التبسيط، حيث انها اقترحت لنسبة مئوية معينة وهي 0.01% من معدل هبوط المطر، ومن ثم تم تعميمها لنسب مئوية اخرى لمعدل هبوط المطر ولحساب ارتفاع الغيوم الماطرة. البيانات المتوفرة من الرادار يمكن استغلالها في تحديد البيانات الافقية والعامودية لاي فترة مطر (بمعنى ارتفاع الغيم والمساحة الافقية المغطاة). حيث ان هذه البيانات متوفرة لمسار الاشارة المائل خلال هبوط المطر بين المحطة الارضية والقمر الصناعي. ومن خلالها يكن تحديد التلاشي في الاشارة بدقة اكثر.). حيث MMDاجريت هذه الدراسة بالتعاون مع وكالة الفضاء الماليزية وادارة الارصاد الجوية الماليزية ( ) وبيانات جمعت على مدار سنة من RazakSATتم تحليل بيانات جمعت من القمر الصناعي (خلال الرادار. تهدف هذه الدراسة الى معرفة الاثار الناتجة عن انتقال الاشارة في الفضاء، وتحديد والتاثيرات المناخية، واخيرا اصدار نموذج خاص بانتشار الاشارة للاتصالات الفضائية. حيث شملت المهام X-اشتقاق علاقة بين انعاكسية بيانات الرادار والتشتت الفعلي لاشارة الاتصالات ذات التردد (من ثم تم تحليل بيانات الرادالمتوفرة regression techn) باستخدام طريقة التحليل المعروفة (band كمحصلة، تم VPRللحصول على بينات ارتفاع الغيوم الماطرة والبيانات الانعكاسية العمودية للرادار اقتراح نموذج خاص بحساب التشتت السنوي الخاص باشارة الاتصالات الفضائية بحيث يعتبر اكثر موثوقية من النماذج السابقة. تعتبر جميع المعلومات التي تم استنتاجها من هذا البحث مهمة في: عملية حساب التشتت الناتج عن المطر، وحساب الميزانية التقديرية لعملية اطلاق القمر الصناعي، والتخطيط)، واخيرا الاستشعار عن بعد لسطح . نتائج هذا microwaveللانظمة التي تعمل على تردد (البحث مهمة لكل مصمم لاي نظام اتصالات فضائية مستقبلي في المناطق المدارية

APPROVAL PAGE

The thesis of Khairayu Binti Badron has been approved by the following:

_____
Ahmad Fadzil Ismail
Supervisor

_____
Md. Rafiqul Islam
Co-Supervisor

_____
Farhat Anwar
Internal Examiner

_____
Syed Idris Syed Hassan
External Examiner

_____
Tharek Abdul Rahman
External Examiner

_____
Tunku Mohar Tunku Mokhtar
Chairman

DECLARATION

I hereby declare that this dissertation is the result of my own investigations, except where otherwise stated. I also declare that it has not been previously or concurrentlysubmitted as a whole for any other degrees at IIUM or other institutions.

Khairayu Binti Badron

Signature .....Date .....

INTERNATIONAL ISLAMIC UNIVERSITY MALAYSIA

DECLARATION OF COPYRIGHT AND AFFIRMATION OF FAIR USE OF UNPUBLISHED RESEARCH

PREDICTION OF SATELLITE LINK RAIN ATTENUATION USING RADAR REFLECTIVITY FOR TROPICAL CLIMATE IN MALAYSIA

I declare that the copyright holders of this dissertation are jointly owned by the student and IIUM.

No part of this unpublished research may be reproduced, stored in a retrieval system, or transmitted, in any form or by any means, electronic, mechanical, photocopying, recording or otherwise without prior written permission of the copyright holder except as provided below

1. Any material contained in or derived from this unpublished research may be used by others in their writing with due acknowledgement.

2. IIUM or its library will have the right to make and transmit copies (print or electronic) for institutional and academic purposes.

3. The IIUM library will have the right to make, store in a retrieved system and supply copies of this unpublished research if requested by other universities and research libraries.

By signing this form, I acknowledged that I have read and understand the IIUM Intellectual Property Right and Commercialization policy.

Affirmed by Khairayu Binti Badron

……..…….. ……..
Signature Date

ACKNOWLEDGEMENTS

All glory is due to Allah, the Almighty, whose Grace and Mercies have been with me throughout the duration of my programme. Although, it has been tasking, His Mercies and Blessings on me ease the herculean task of completing this thesis.

I am most indebted to by supervisor, Assoc. Prof. Ir Dr. Ahmad Fadzil Ismail, whose enduring disposition, kindness, promptitude, thoroughness and friendship have facilitated the successful completion of my work. I put on record and appreciate his detailed comments, useful suggestions and inspiring queries which have considerably improved this thesis. His brilliant grasp of the aim and content of this work led to his insightful comments, suggestions and queries which helped me a great deal. The moral support he extended to me is in no doubt a boost that helped in building and writing this research work. I am also grateful to my co-supervisor, Prof. Dr. Md. Rafiqul Islam, whose support and cooperation contributed to the outcome of this work.

Last but not least, my gratitude goes to my husband, parents and children; for their prayers, understanding and endurance while away.

Once again, we glorify Allah for His endless mercy on us one of which is enabling us to successfully round off the efforts of writing this thesis. *Alhamdulillah.*

TABLE OF CONTENTS

LIST OFFIGURES

LIST OF TABLES

LIST OFABBREVIATIONS

BER	Bit Error Rate
DTH	Direct To Home
IEEE	Institute of Electrical and Electronics Engineers
ITU	International Telecommunication Union
ITU-R	International Telecommunication Union-Radiocommunication
LDR	Linear Depolarisation Ratio
MEASAT	Malaysia East Asia Satellite
MMD	Malaysian Meteorological Department
VPR	Vertical Profile Reflectivity
CDF	Cumulative Distribution Function
FSPL	Free Space Path Loss
RHI	Range Height Indicator
CAPPI	Constant Altitude Plane Position Indicator
QoS	Quality of Service

CHAPTER ONE

INTRODUCTION

1.1 Background ofthe Study

At present, the state of the telecommunication market is driven by the escalating demand by the end-users of multimedia services, which require broadband data rates. Hence the idea of deploying a new satellite system in millimetre wave frequency bands most likely will involve a complex co-ordination procedure (Gayrard, 2009). In tropical and sub-tropical areas, Malaysia included, the terrestrial infrastructure can be considered less developed and there are always strong incentives and supports by the government to develop satellite communication systems in the coming years, to serve wider territories and to reach a larger market size for economic profitability. Nonetheless, propagation impairments are expected to be quite acute in tropical climate. Copious heavy rain events in the tropics profoundly affect high frequency radio wave signals causing severe signal fading and interference (Yeo et al. 2012). It is very likely that 'standard performances' may not be achieved or very difficult to realize in these regions. Accurate and precise prediction of impairment statistics is very critical for the design and deployment of satellite systems in tropical regions.

The needs of Malaysian communications, both civilian and military will evidently include wideband capacity satellite systems. System operator/s apparently will have no choice but to resort in employing the microwave and millimetre-wave bands. The challenge of such high frequencies operation is that there exist stronger electromagnetic interaction between the signals and atmospheric hydrometeors (Pillai

et al. 2006). As the frequency increases, it loses more energy than lower frequency bands because of the increase interactions between the radio signals and the atmospheric particles at a particular place and time. In around the world, atmospheric hydrometeors that typically interfere along radio paths are fogs, snow, ice, rain and hail (Suddharsana et al. 2011). These instances substantially degrade the performance of the communication systems. The phenomenon of the signal amplitude depletion due to rain is called rain fading which factored by the scattering of the signals due to the incidence of the signal wavelength and the surface of rain droplets as well as by the absorption of the signal energy by the rain droplets (Crane, 2003). Communications developments are crucial for any country, regardless of its size if it is to grow economically (Brost and Cook, 2012). Key elements for economic growth in Malaysia are good national and international telecommunications. Underlined by the Economic Transformation Programme, the National Key Economic Area, the Communications, Content & Infrastructure aims at driving continued high growth in communications and enabling the paradigm shift from infrastructure to applications and content (National Key Economic, 2012).

The expanding communications requirements will evidently lead to frequency spectrum congestion (Kyung et al. 2011). Malaysian operators will also have to employ higher frequency bands. Theoretically, rain attenuation is the dominant factor that limits the use of higher frequencies for line-of-sight microwave links and satellite communications in Malaysia. Malaysian engineers must be aware that the integrity of microwave systems that have been designed for use in countries with temperate climate may not be capable to adapt conditions in our country. Excessive rainfall is a common phenomenon throughout the year in Malaysia hence the knowledge of the rain fade at an established frequency of operation is a critical requirement for the

design of a reliable communication link at a particular location.Radio wave propagation plays an important part in the design and eventually dictates the performance of Malaysian space communication systems.

The available path attenuation data for Malaysia and similar climatic regions are still insufficient for a comprehensive evaluation of propagation process even on an empirical basis. Bearing in mind, the profound effect of rain on microwave and millimetre wave links, initiatives were embarked accordingly.The study attempted to investigate and quantify the impacts of rain on the performance of satellite-Earth links starting from thelower end of microwave band namely the X-band (8.21 GHz) frequencies. It is hoped that the continuing efforts to collect the much-needed propagation data similar to this researchand at higher frequencies can be supported by more organizations; government and private alike. The analyses work deliberated in this research is hoped capableof satisfying some of the initial requirements. Endeavour will be initiated to identify the cause of inadequacies discovered in tropical regions in the existing established attenuation prediction procedures. New data can instigate the development of refined prediction techniques. There is an urgent need for continuous microwave propagation studies to be carried out in Malaysia where the effects of rainfall on microwave and millimetre-wave transmissions have not yet been fully quantified.

1.2 Problem Statement

In tropical regions, the future stratospheric and space based telecommunications systems are expected to operate with high elevation angle slant paths from the Earth stations' perspective. This is due to the fact that the corresponding space borne transmitters are likely to be orbiting along the equator (Pillai et al. 2006). These

systems will also be initially sharing frequency bands with other terrestrial and space services. From this standpoint, an accurate modelling of the vertical variation of precipitation (rain) parameters will be of great interest (Sudarshana and Samarasinghe, 2011) not only for improving the prediction of attenuation along the slant path in the tropics, but also for rain scattering interference calculations.

Propagation studies in the tropics are indeed extremely scarce. There are only about 10 studies per decade. They are extremely delicate, complicated and expensive to venture upon. Many rain attenuation models had been established and seem to offer a good estimation for temperate regions (Brost and Cook, 2012; Crane, 2003; Kyung et al. 2011). Inadequacies were discovered where the same recommendations failed to give a good approximationfor tropical regions. The findings from the research objectives will be applications of new expertise as well as new approaches to "established researches" previously exclusive only to temperate regions.

The conventional device for rain measurement at the ground is the rain gauge which measures the volume of water falling over a known area. The collection in a common rain gauge is typically measured manually at regular intervals. Since a gauge measurement is a point measurement andrainfall is not a continuously variable functionin space, a measurement by a gauge may not truly representits surroundings. Measurement inaccuracies in total of annual precipitation has been estimated to be as high as 70% (Groisman, 2012). Respected group of scientists (Ciach and Krajewski 1999;Sevruk and Klemm ,1989) had been unable to consenton what type of precipitation gauge is most effective for meteorological applications.

The utilization of a remote sensing method such as radar to measure or estimate precipitation would offer the equivalent of a very high density network, resolution limited only by that of the sensor. Such a high resolution device would

capture isolated heavy rain rates which may be missed or smoothed out by any practical network of rain gauges. Radar information can offer instantaneous estimation of precipitation rates. It will also enable real time collection of data for large areas from a few centralized locations. Data can also be collected over the sea area. Besides that, Vertical Profiles Reflectivity (VPR) can also be obtained. The high resolution data can be used as input to numerical models. Since relatively few sensors are needed, the operation may be less complex compare to a dense rain gauge network. Unlike a rain gauge which makes a measurement over a very small area at the ground, the radar measures reflectivity, Z (or some other parameters) integrated overthe pulse volume which is a function of the range and the beam width and is usually much larger than the volume sampled by a gauge. This is, therefore, more representative of a larger area but the sampled volume is at a height above ground which depends on range. In the caseof attenuation, it is measured by integration over a path length.

The biggest advantage of radar data is the large amount of data that is available in a short period of time. Radar data is also capable of providing aerial precipitation where it is almost impossible to do using rain gauges. As a result, a single parameter radar system can be a good tool for studying the finer detail of climate conditions in the tropics. The information from radars can be used to investigate the vertical variability of rain events. This is one of the practical technique of data collection that can furnish both the horizontal and vertical structure of precipitation in a way that is sensiblefor studying rain scatter and interference.

1.3 Research Scope

Rain induced attenuation study for satellite link is an important factor to be taken into serious consideration for the establishment of any future satellite link. This study will

embark on deriving the relationship between radar reflectivity and actual satellite link received power variations of RazakSAT i.e. the rain attenuation. Besides that, the classification of rain in Malaysia will be identified and the characteristics will be deliberated such as specific attenuation and vertical reflectivity profile. These characteristics will certainly operate as an important aspect of the rain attenuation prediction model especially in the tropical region. The findings of this research will be valuable for the future designers in the attempts of predicting the satellite link's performance from a radar reflectivity.

1.4 Research Objectives

The broad objective of this research encompasses the knowledge concerning propagation effects, climatological influences, and refined propagation modelling for satellite communications systems providing services in tropical regions.Specific objectives of the proposed study can be summarized as follows:

1. To developnovel rain attenuation prediction technique using radar data applicable in tropical region based on the characteristics of the vertical profile reflectivity
2. To derive specific attenuation, γ-Z relationship using the satellite data and radar dataincluding the distinction of stratiform and convective rain profile.
3. To validate the proposed technique for a more reliable fade margin.

1.5 Thesis Organization

The thesis is divided into seven main chapters. This chapter outlines the research motivations, objectives, and organization of the thesis. Chapter 2 presents theories and background studies on propagation mechanisms, classification of world climates,

classifications and characteristics of precipitation, and several related topics of the research. Chapter 3 consists of the methodology involved in the analyses. Results attained are included in Chapter 4 and 5. Chapter 4 concentrates on detail accounts of the technique in predicting rain induced attenuation using radar information. The rain scatter of the vertical profile reflectivity is studied.The fade margins for X-band and Ku-band are estimated using the newly proposed technique in this chapter.Chapter 5 describes subsequent research works and investigations carried out using radar data. The derivation of specific attenuation-reflectivity is highlighted.Measured attenuation statisticsusing RazakSAT satellite was compared with predicted attenuation statistics generated by radar information in Chapter 6. A second technique to estimate rain attenuation is outlined. The stratiform and convective rain profile had been distinguish. The thesis ends with Chapter 6 where it gives conclusion and suggestion of future works.

CHAPTERTWO

LITERATURE REVIEW

2.1 Introduction

Satellite-Earth communications systems in tropical regions are limited by attenuation due to rain. The following section presents delineated details about the communication satellite and the meteorology radar data that havebeen used as the main information that to be compared to the received power signal variations experienced by RazakSAT communication path. The section also focuses relevant awareness to the rain attenuation models proposed and applied in tropical region.

2.2 Satellite Communications System.

Satellites play a key role in the growth of global communications, media and technologyindustries. A communications satellite system is a setup of microwave receiver, repeater and regenerators placed in orbit around the Earth that receives, amplifies and redirects analogue and digital signals contained within a carrier frequency. It is one of the most essential development from the space programmes and has made a core contribution to the trends in international communications. The data transferred most often involvevoice (telephone), video (television) and digital information. The basic component of a communications satellite system are the two feature of the space segment and ground segment. The space segment consists of the spacecraft and launch mechanism while the ground segment typically comprises the Earth station and network control centre of the entire satellite system (Wood, 1994).

The first launch of a satellite into space; the Sputnik caught the world's attention in 1957. A year later, US launched Explorer I. Thereafter, there have been many more satellite launches by countries in various regions offering a wider range of services over greater coverage areas, with greater capacity upon more advanced technology. Emerging satellite services such as Broadband Global Area Network (BGAN), Earth ObservationSystems including Global Earth Observation System of Systems (GEOSS) and Global Monitoring for Environment and Security (GMES), hybrid triple play and digital signage, not only create prospect for satellite business to expand, but also exploit these medium in ways that previous satellite services were unable to accomplish (Kota et al. 2010). Satellite communications play an important role in the telecommunications industry, especially duringcatastrophe. Uncertainties such asdisturbance or congestion of cellular networks will definitely occur, and satellite can act as backhaul for emergency as well as"extensions" to cellular networks (ranging from 2G, 3G, 4G and upcoming 5G) (Satellite Industry Developments, 2008).

Malaysia's first regional satellite system MEASAT-1 was operated by MEASAT (Malaysia East Asia Satellite) Satellite Systems Sdn Bhd (MSS) and owned by MEASAT Global Berhad (MGB) (Malaysia Investment and Business Guide, 2007). The MEASAT fleet comprises MEASAT-2, MEASAT-3 and AFRICASAT-1 satellites covering 145 countries or 80% of the world's population across Asia Pacific, Middle East, Europe and Australia (Satellite Industry Developments,2007). The fleet had been further improvedwith the launch of MEASAT-3a (2009) and MEASAT-3B (2014). Other Malaysian satellites launched are TiungSat-1 (2000) and RazakSAT(2009) which are remote sensing or known as micro-satellites for Earth observation purposes. Urban districtsarecommonly linked with more economically viable communications services thatoffer better options in terms of quality of service,

bandwidth and limitless commercially robustapplications (Elbert, 2008). Satellite benefits including instant wide area coverage in a single sweep upon setup is usually more cost-effective for rural areas or areas where terrestrial means of communications is not available or in case of emergencies. In today's world where big populations and countries with geographic limitations for terrestrial options are demanding and can afford better communications, the satellite option is then a viable and opportune one for even mainstream communications.

In designing a new satellite link, the performance prediction of the satellite are vital step to ensure the reliability of the systems. It is very critical to be capable to predict accurately the impairment of the given link in order to devise the services efficiently. The predicted value of signal loss and fading are commonly used in the process of establishing the satellite design parameters(Ismail and Watson, 2001). Performance of the link is usually expressed as the expected quality of the channel for a very high percentage of time (at least a month and usually a year).The performance can be specified for instance, at availability of 99.99% of time at a given receiving locality or at a specified percentage of locations within a reception area. Availability is the percentage of total time a service is enabled or being used, or is available to be utilized. Table 2.1 shows the frequency band allocated for satellite transmission.

Clearly, satellite communication has a bright future due to new technologies, with ability to provide broad coverage, mobile services and direct services to consumers. It can also supply cost-effective broadcasting services, together with the ability to provide instantaneous re-deployment of capacity, instantly providing communications infrastructure, and avoid costly, time-consuming trenching operations, leading to overall flexibility and reliability.

Table 2.1Frequency Band Allocated to Satellite Transmission (Godard, 2001)

Frequency	Uplink/ Downlink	User	Service
UHF	400/225 GHz	Military	Mobile
L-band	1.6/1.2GHz	Commercial	Mobile
S-band	3/2 GHz	Commercial	Satellite Control
C-band	6/ 4 GHz	Commercial	Fixed
X-band	8/7 GHz	Military	Fixed/Mobile
Ku-band	14/12 GHz	Commercial	Fixed
Ka-band	30/20 GHz	Commercial	Fixed
Ka-band	44/20 GHz	Military	Fixed/Mobile

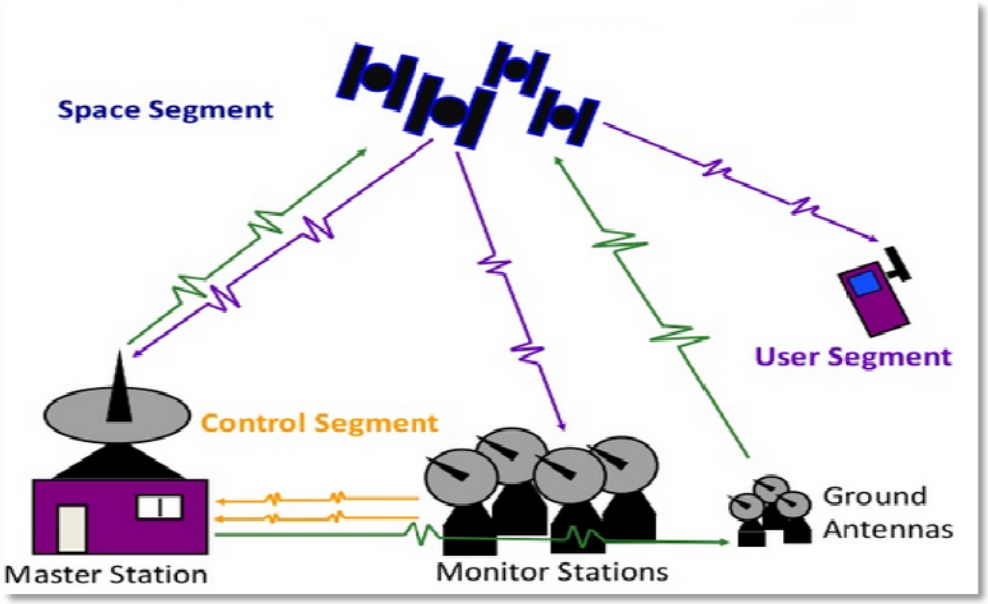

Figure 2.1: Satellite Segments(Dahiya, 2013)

2.2.1 Slant Range for Ground Stations of Near EquatorialOrbiting Satellites

Communication via satellite begins when the satellite is positioned in the desired orbitalspot (Roddy, 2006). A near equatorial orbit (NEqO) is an orbit that lies close to the equatorial plane of the object orbited under the category of Low Earth Orbit (LEO) satellite. This orbit allows for rapid revisit times (for a single orbiting spacecraft) of

near equatorial ground sites. Ground stations can communicate with NEqO satellites only when the satellite is in their visibilityterritory. Due to natural obstacle or very high buildings in urban areas, practical horizon plane differs from the ideal one (Cakaj et.al, 2011). The duration of the visibility and the communication duration varies for each NEqO satellite pass at the ground station, since NEqO satellites move very quicklyabove the Earth. NEqO satellites have very wide applications, fromremote sensing through analyses on Earth's climate changes, Earth's observation with high resolution and astronomical purposes (Zee and Stibrany,2002). NEqOs are just above Earth's atmosphere, where there is almost no air to cause drag on the satellite and reduce its speed. Less energy is required to launch a satellite into this type of orbit than into any other orbit (Richharia, 2009, Cakaj et al., 2007). NEqOs altitudes range from 275 km up to 1400 kmlimited by Van Allen radiation effects (Kirby and Stratton, 2013). At 90° elevation the shortest range occurs sincesatelliteappears perpendicularly above the ground station and it equals with satellites attitude (Cakaj and Malaric, 2007). The range between the ground station and the NEqO satellite depends on maximal elevation of satellite's path above the ground station. The position of the satellite within its orbit considered fromthe ground station point of view can be defined by *Azimuth* and *Elevation* angles. The concept of azimuth and elevation is presented in Figure 2.2.

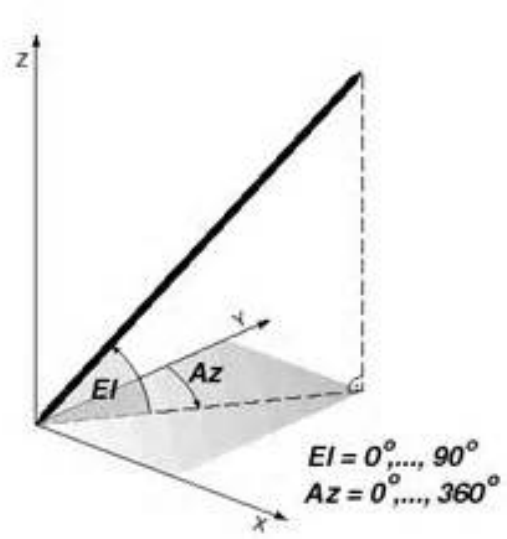

Figure 2.2: Azimuth and Elevation Illustration

The azimuth (*Az*) is the angle of the direction of the satellite, measured in the horizon plane from geographical north in clockwise direction. The range of azimuth is 0° to 360°. The elevation (*El*) is the angle between a satellite and the observer's (ground station's) horizon plane. The range of elevation is 0° to 90°.

For tracking the satellite, Kepler elements (space orbital parameters) are fed to orbit location (altitude and latitude) which calculates the actual position of the satellite (Richharia, 1999). A software process running at the ground station uses these parameters to precisely determine the time when the satellite will communicate with the ground station and prepares the ground station's antenna in advance to wait for the upcoming pass of the satellite (Cakaj et al. 2010). For NEqO satellites the communication is locked when the satellite shows up at the horizon plane. The respective software provides real-time tracking information, usually displayed in different modes (satellite view, radar map, tabulated, etc.). The basic geometry between a NEqO satellite and ground station is depicted in Figure 2.3.

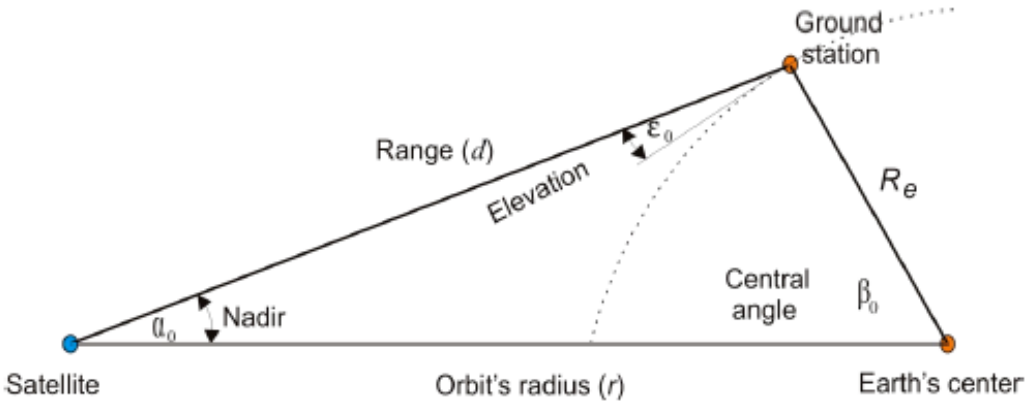

Figure 2.3: Ground Station Geometry (Cakaj et al. 2011).

Among the above parameters, the most inquired parameter is the slant range, d (distance from the ground station to the satellite). This parameter will be used during the free space path loss calculation and link budget calculation, and it is expressed through elevation angle, ε_0. Applying cosines law for triangle at Figure 2.3yields:

$$r^2 = R_E^2 + d^2 - 2R_E\, dcos\,(90 + \varepsilon_0) \qquad (2.1)$$

Solving Equation (2.1) by d, yields:

$$d = R_E \left[\sqrt{\left(\frac{r}{R_E}\right) - cos^2\varepsilon_0} - \sin\varepsilon_0\right] \qquad (2.2)$$

Substituting, $r = H + RE$ at equation (2.2) finally we will get the slant range as function of elevation angle ε_0:

$$d = R_E \left[\sqrt{\left(\frac{H+R_E}{R_E}\right) - cos^2\varepsilon_0} - \sin\varepsilon_0\right] \qquad (2.3)$$

In telecommunication, free-space path loss (FSPL) is the loss in signal strength of an electromagnetic wave that would result from a line-of-sight paththrough free space, with no obstacles nearby to cause reflection or diffraction (Sklar, 2005). The FSPL appears in vacuum under ideally conditions, e.g. a radio communication between satellites.The free path loss also can be calculated as Equation (2.4) below;

$$FSPL\ (dB) = 10\ log_{10}\left(\left(\frac{4\pi}{c}df\right)^2\right) \quad (2.4)$$

Where d is the distance the distance from the transmitter (in metres), f is the signal frequency (in hertz), and c is the speed of light in a vacuum, 2.99792458×10^8 metres per second.

2.3 Radar Data Processing

Radio Detection and Ranging (Radar), once developed for aircrafts detection during the World War II, was swiftly applied to tracking rain areas from the radar echoes (Roland 2000;Bechet al.2008). Information relating to rain is derived using radar echoes reflectivity values. A radar system can be an ideal tool for studying the climate conditions in the tropics. This is theonly feasible technique of collecting data that will furnish both the horizontal and vertical structure of precipitation in a way that is practical for studying rain scatter and interference in mass area (Currie and Brown, 1987; Kingsley and Shaun, 1992). The cross-polar and Doppler information from such radar could be used to determine the height of melting layer for all types of rain condition (Ladd et al. 1997; Eastment et al. 1995; Watson et al. 1998). It is of important to ascertain the correct height of the melting layer in a statistically valid way, rather than by studying specific events during short-term campaigns. The characterisation of the melting layer has always been of particular interest in the modelling of radiowave propagation for Earth-space communication path due to its different electromagnetic properties in comparison to those of underlying rain (Salonen et al., 1990).Most weather radars can perform measurements of the rain's spatial structure (Rinehart 1991). The technology extends from the idea of using pulses of energy for target detection during World War II. After the war, research into the uses of radar for weather studies (i.e., the detection of a volume of precipitation-

size particles instead of the detection of individual ships and planes) developed. A radar consists of a transmitter that generates an electromagnetic signal and an antenna to send out the signal and receive echo back from a target (Otto and Russchenberg, 2011). The total received radar power, P, can be expressed as:

$$P = Z - 20 \log r - C \quad (2.5)$$

where,*P* is measured in decibels referenced to 1 milliwatt (dBm); *Z* is the reflectivity factor referenced to 1 mm^6 m^{-3} (dBZ) and is determined by the number, size, and composition of the target; *r* is the range of the target from the radar in km; and *C* is a radar constant measured in decibels (dB) that is dependent on the hardware of the system such as wavelength and bandwidth (Battan, 1973). When measuring rain or cloud, a radar receives power from many targets in a sample volume. Assuming all of the scatterers are water, the effective radar reflectivity factor, Z_e, can be expressed as:

$$Z_e = \int_0^\infty N(D) D^6 dD \quad (2.6)$$

where,*D* is the diameter of the hydrometeor and *N(D)* is the drop concentration. Note the D^6dependence, which places a heavier weight on the size rather than the number of hydrometeors. Rain drop size ranges in size from 0.5-6 mm (or even larger for hail); electromagnetic wavelengths of 2-10 cm (or frequencies of 3-15 GHz) can be used to detect these size particles. Thus, radars that operate at these wavelengths are often called precipitation or weather radars. The most commonly used weather radar wavelengths are 10 cm (S-band), 5 cm (C-band), and 3 cm (X-band).

The S-band is typically used by weather radar (also by the Malaysian Meteorological Department (MMD)), surface ship radar, and some communications satellites, especially those used by NASA to communicate with the Space Shuttle and the International Space Station (Latef and Hasan, 2011). The 10 cm radar short-band ranges roughly from 1.55 to 3.2 GHz. The ability of a radar to scan a wide area around

the radar site and not just a particular path made it a very attractive for many types of investigations. Radar can be used to indirectly estimate the rainfall rate (Anagnostou et al. 2006). This is achieved by knowing the radar reflectivity and then converting them into rainfall rate. From the rainfall rate the rain attenuation can also be estimated (Battan, 1973). Figure 2.4 shows how a radar works and some of its characteristics during operation.

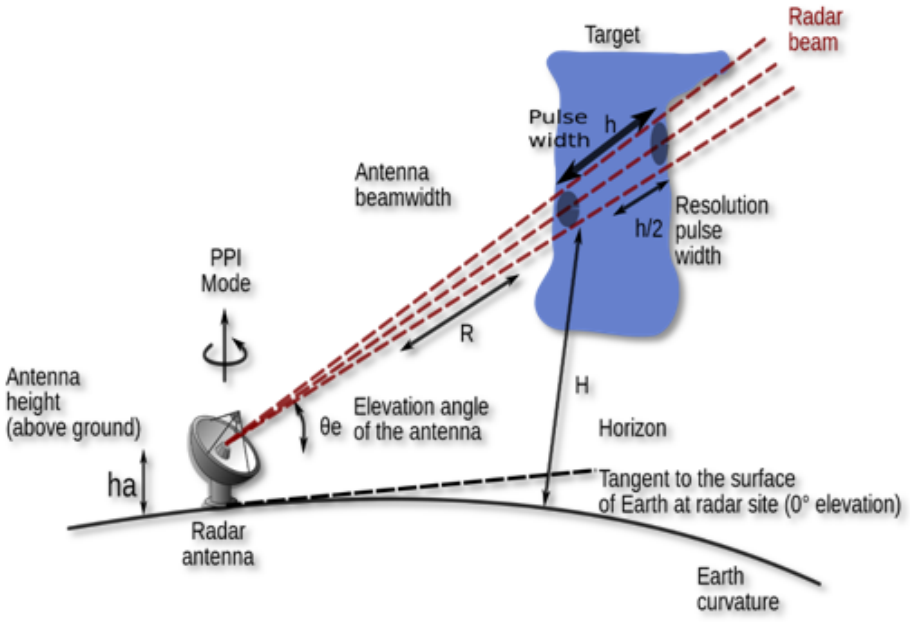

Figure 2.4: The Radar Beam Path with Height (Doviak and Zmic, 1993)

Radar provide valuable information that is relevant in modelling rain induced propagation effects. Radar also can provide spatially and temporally continuous measurements that are immediately available at one location (Romo et al. 2012). Currently, radar applications include continuous-wave, pulsed, single-polarization, dual-polarization, synthetic aperture radar, and phased arrays. Radar frequency sub-bands are used in civil, military, and government institutions for weather monitoring,

air traffic control, maritime vessel traffic control, defence tracking, and vehicle speed detection for law enforcement.

2.3.1 Reflectivity (in decibel or dBZ)

Return echoes from targets which are known as reflectivity were analyzed for their intensities to establish the precipitation rate in the scanned volume. The wavelengths used (1–10 cm) ensure that this return is proportional to the rate because they are within the validity of Rayleigh scattering which states that the targets must be much smaller than the wavelength of the scanning wave (by a factor of 10). Effective reflectivity perceived by the radar, Z_e varies by the sixth power of the rain droplets' diameter, D the square of the dielectric constant, K of the targets and the drop size distribution (e.g. $N\,[D]$ of Marshall and Palmer (1976)) of the drops (Yau and Rogers, 1989). This gives a truncated Gamma function of the form:

$$Z_{e=} \int_0^{Dmax} |K|^2 \, N_o e - \Lambda^D D^6 dD \qquad (2.7)$$

Precipitation rate (R), on the other hand, is equal to the number of particles, their volume and their fall speed, $v(D)$ as:

$$R = \int_0^{Dmax} N_0 e - \Lambda^D \left(\frac{\pi D^3}{6}\right) v(D) dD \qquad (2.8)$$

So Z_e and R have similar functions that can be resolved, giving a relation between the two of the form:

$$Z = aR^b \qquad (2.9)$$

where,a and b depend on the type of precipitation (snow, rain, convective or stratiform), which has different Λ, K, N_0 *and* v. The slant path attenuation for an Earth-satellite link is calculated through the numerically summation of

$$A = \sum_{i=0}^{n} kR_i^{\alpha} . \Delta L_i \qquad (2.10)$$

where $L = n\Delta L_i = h_R/sin(\theta)$ is the path length affected by rain, θ is the link elevation angle, h_R is the fixed yearly mean rain height, derived from ITU-R Rec. P. 839–3 (1996). The coefficients of specific attenuation, k and α can be obtained from the ITU-R Rec. P.838–3 (1999) and are dependent on the radio wave frequency and polarization. In (2.10), $R_i$is the rainfall rate value and $\Delta L_i$is the path length at each Cartesian pixel along the slant path between the Earth station and the melting layer. Therefore, the transmission link performance is strongly dependent on the precipitation characteristics along the slant path. In this case, precipitation can significantly affect the system performance.As the antenna radar scans the atmosphere, on every angle of azimuth it obtains certain strength of return from each type of target encountered. Reflectivity is then averaged for that target to have a better data set. Since variation in diameter and dielectric constant of the targets can lead to large variability in power return to the radar, reflectivity is expressed in dBZ (10 times the logarithm of the ratio of the echo to a standard 1 mm diameter drop filling the same scanned volume).When the beam encounters a target in the atmosphere such as a raindrop, a lot of interesting processes take place. The raindrop will attenuate the energy in two ways: scattering and absorption as shown Figure 2.5.

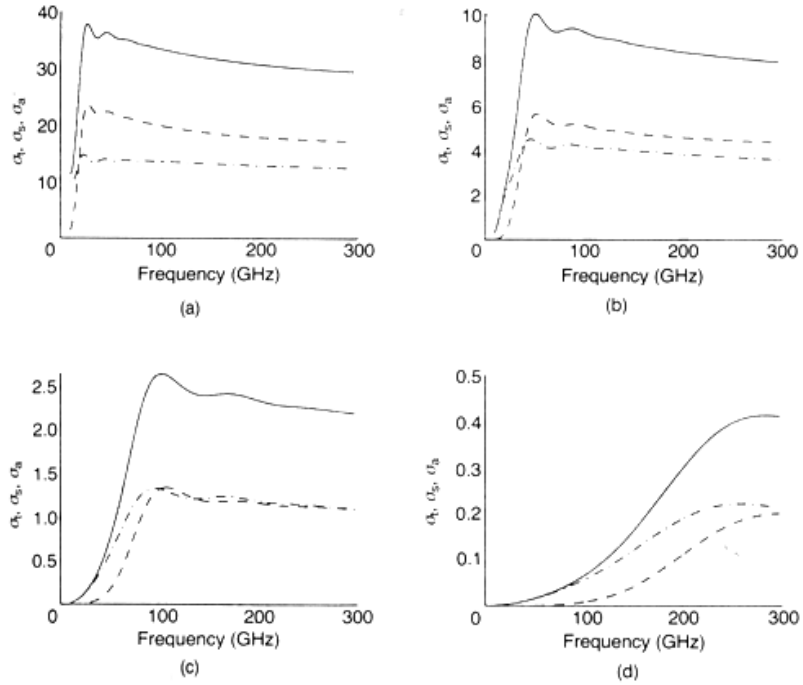

Figure 2.5: Scattering (---),Absorption (-·-) and Total (-) Cross-sections σ_s, σ_a and σ_t in mm^2 for Water Spheres of Various Sizes as a Function of Frequency: (a) a = 2 mm; (b) a = 1 mm; (c) a = 0.5 mm; (d) a = 0.2 mm. (Brussard and Watson, 1995)

Upon contact with the raindrop, the energy is scattered in all directions, so only a very small portion of the incident radiation is sent back in the direction of the radar. The raindrop will actually absorb some of the energy. These two processes, scattering and absorption, are collectively known as attenuation. However, it's not just raindrops to be concerned about. Atmospheric gases and small aerosols are responsible for some absorption (too small for scattering), but particles such as hail, snow, and insects are also responsible for both absorption and scattering. Attenuation becomes significant when the beam has to travel through a lot of targets and/or through a wide spacious area; i.e., through heavy precipitation and/or long distances (Doviak and Zmic, 1993). This means that the power received back at the antenna is even less than it would otherwise be. Scanning through a heavy thunderstorm, gaseous absorption might

cause a 5% reduction in backscattered power, while the intervening rain and hail could cause an 80% reduction.

2.4 Classification of Precipitation

The Earth's surface is a patchwork of climate zones. Climatologists, the scientists who study the climate have organised similar types of climates into groups. One of the earliest classifications was the division of Earth into tropical, temperate and polar climates, using the tropics 23.5°N and S and the arctic 66.5° N and Antarctic 66.5° S circles as dividing lines, with temperature conditions being the only one considered having any importance (Riley and Spolton, 1974). Since propagation characteristics depend clearly on the climate and type of rainfall, specific models should be considered separately. In this research, statistics of the stratiform and convective rain events had been analyzed and its influence on attenuation along slant paths had been assessed. Initial understanding of precipitation types has revealed two broad classes of precipitation event (Zvanovec and Pechac, 2006). One involves a very intense and relatively short-lived convective precipitation with variable rain heights that might go up to height of more than 10 km. Convective rain is being characterised by intense rainfall that occurs for a short period and covers a small or localised area (Das and Maitra, 2009). The stratiform rain on the other hand can be characterised by medium and low rate events that occurs for a longer period of time. This type of rain comprises a long period of stratiform precipitation with a very well developed melting layer at a constant height (Baldini et al. 2008).

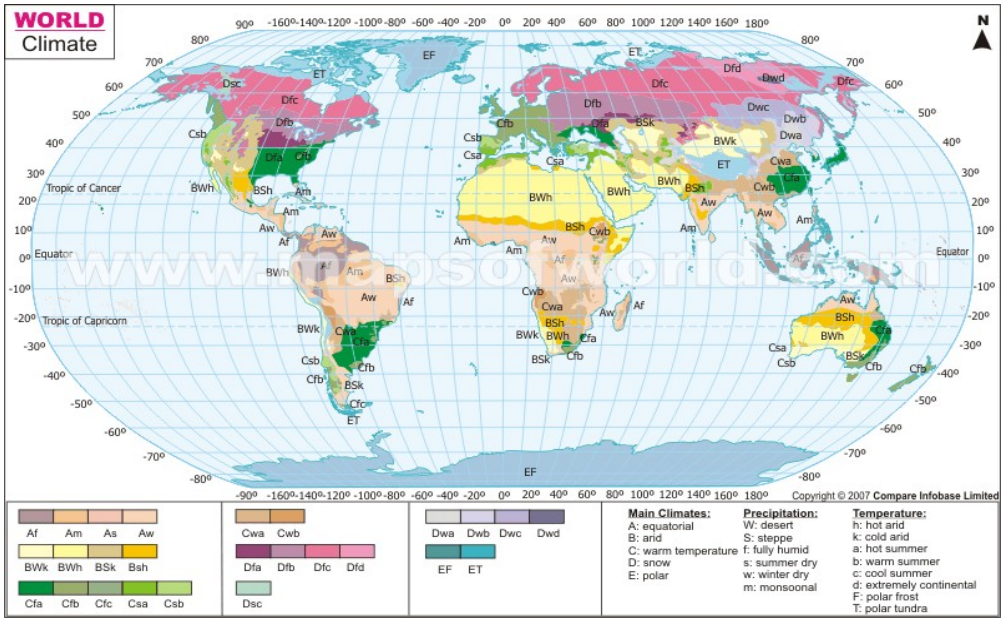

Figure 2.6: World Climatic Map (2007).

Further studies had been carried out by organisation such as Malaysian Meteorology Department (MMD) with radar data on precipitation events. Attempts were made to characterise the vertical distribution of ice and water regions, and to determine the rainfall rate from measurements of reflectivity. Both parameters are considered important for improved radiowave propagation modelling. According to the ITU Handbook on Radiometeorology (Recommendation ITU-R P.837-2, 1999) and Houze (1981) precipitation that occurs all over the world may be grouped into four different types inclusive of stratiform and convective.

2.5 Rain Induced Attenuation Model

Rain attenuation, caused by scattering and absorption by water droplets, is one of the most fundamental limitations to the performance of satellite communication links in the microwave region, causing large variations in the received signal power, with little predictability and many sudden changes.The challenge in operating at high

frequencies for communication purposes is that there exist stronger interaction between the radio signals and atmospheric hydrometeors. Hydrometeors are concentrations of water or ice particles that may exist in the atmosphere before being deposited on to the surface of the Earth (ITU-R PN.310-9, 1994). The prevailing propagation impairment at radio frequencies above 10 GHz is the rain attenuation and this is even more obvious in the tropical regions (Din, 2008; Pontes et al. 2005; Ajayi, 1985 and Rafiq, 1999). There are many factors such as frequency, elevation angle, polarization angle, rainintensity, raindrop size distribution and raindrop temperature that directly contribute to rain attenuation.

Many researchers have worked in the studies of predicting the radiowave signal attenuation due to rain. The prediction of microwave and millimetre wave signal degradation is an iterative procedure. Several models were proposed by the scientists and have been adopted by the International Telecommunication Union (ITU). The ITU was formed in 1932 from the International Telegraph Union, which originated in 1865. The ITU is a specialised agency of United Nations, with over 150 current member nations. Initial theoretical models are then verified against measured data. The prediction models are improved to match the data and in the process they become semi-empirical models.

Most ITU models seem to offer a good estimation for the lower frequency signal attenuation caused by rain in temperate regions as emphasized by Ventourus et al.(2000). However, inadequacies were discovered in the existing attenuation-prediction procedures where the models or recommendations for high frequency failed to give good approximation of the rain induced attenuation in tropical regions (Din, 2008; Mandeep, 2006; Watson et al. 1997; Ismail et al. 2000; Rafiq et al. 1999 and Ajayi, 1985). There are several popular prediction models used to estimate the rain

attenuation. Most of these models are based on statistical data of rain rate such as ITU-R model, Crane model and Garcia-Lopez model.

2.5.1 ITU-R Model

The most commonly implemented model from the international propagation community is the ITU-R rain attenuation model. The model was first admitted internationally in 1982 and is continuously updated as rain attenuation modelling is better understood. The input parameters required for the ITU-R Rain Model are: the frequency of operation, in GHz, the elevation angle to the satellite, in degrees, the latitude of the ground station and the altitude of the ground station above sea level, in km (ITU-R P.618-12, 2012; Tamrakar et al. 2010). The required information of the rainfall rate, $R_{0.01}$, exceeded in 0.01% of an average year, can be obtained from the map of rainfall rate available in the Recommendation ITU-R P.837 (ITU-R P.837-6, 2012). The specific attenuation, γ_R can be obtained using the frequency-dependent coefficients (k and α, these parameters are dependent on frequency, rain temperature, raindrop size distribution, and polarization) given in Recommendation ITU-R P.839-4 (2013).

$$\gamma_R = K(R_{0.01})^{\alpha} \tag{2.11}$$

In order to predict attenuation exceeded in 0.01% of an average year,$A_{0.01}$ the following formula is used;

$$A_{0.01} = \gamma_R L_E \tag{2.12}$$

where L_E is the effective path length, calculated from;

$$L_E = L_R V_{0.01} \tag{2.13}$$

where $v_{0.01}$is thevertical adjustment factor.

To calculate the vertical adjustment factor, $v_{0.01}$, for 0.01% of the time:

$$\xi = tan^{-1}\left(\frac{h_R - h_S}{L_G r_{0.01}}\right) \quad (2.14)$$

where,h_R= the height of the rain (km).

Mean rain height above mean sea level,h_R, can be obtained from 0°C isotherm h_0 given in (ITU-R P.839-3, 2001) as:

$$h_R = h_0 + 0.36\ km \quad (2.15)$$

The slant path length,$L_S$expressed in km, is determined from

$$L_S = \frac{(h_R - h_S)}{sin\theta} \quad \text{for } \theta \geq 5 \text{ degree} \quad (2.16)$$

where, h_S is the altitude of the receiver site from sea level (km) and θ is the elevation angle.The horizontal projection (L_G), of the slant path length is calculated:

$$L_G = L_S cos\theta \quad (2.17)$$

$$r_{0.01} = \frac{1}{1+0.78\sqrt{\frac{L_G \gamma_R}{f}} - 0.38\left(1-e^{-2L_G}\right)} \quad (2.18)$$

For, $\zeta > \theta$ $\quad L_R = \frac{L_G\ r_{0.01}}{\cos\theta}$ km (2.19)

Else, $\quad L_R = \frac{(h_R - h_s)}{\sin\theta}$ km (2.20)

If $|\varphi| < 36°$, $\quad \chi = 36 - |\varphi|$ degrees

Else, $\quad \chi = 0$ degrees

$$v_{0.01} = \frac{1}{1+\sqrt{\sin\theta}\left(31\left(1-e^{-(\theta/(1+\chi))}\right)\frac{\sqrt{L_R\ \gamma_R}}{f^2} - 0.45\right)} \quad (2.21)$$

φ: latitude of the earth station (degrees)

The estimated attenuation to be exceeded for other percentages of an average year, in the range 0.001% to 5%, is determined from the attenuation to be exceeded for 0.01% for an average year:

If $p \geq 1\%$ or $\lvert\varphi\rvert \geq 36°$:	$\beta = 0$
If $p < 1\%$ and $\lvert\varphi\rvert < 36°$ and $\theta \geq 25°$:	$\beta = -0.005(\lvert\varphi\rvert - 36)$
Otherwise:	$\beta = -0.005(\lvert\varphi\rvert - 36) + 1.8 - 4.25 \sin\theta$

$$A_P = A_{0.01}\left(\frac{p}{0.01}\right)^{-(0.655+0.033\,ln(p)-0.045\,ln(A_{0.01})-\beta(1-p)\sin\theta)} \quad (2.23)$$

where A_P, is estimated attenuation to be exceeded for other percentages of an average year.In the Ku and Ka-bands, the attenuation caused by rain is too severe to be accounted for by a fixed margin in the link budget. In order to provide the same performance as in lower frequency bands, an excessively large margin is expected to be required (Crane, 1993).

2.6 Rain Attenuation Prediction Using Radar Information

The potential of a radar to scan a wide area around the radar site and not just aparticular path made it a very helpful for many types of investigations. Radar information canalso be used tomeasure the rainfall rate indirectly. This is achieved by knowing the radarreflectivity and then converting them into rainfall rate. The S-band frequency of themeteorological radar ensures that propagation effects such as attenuation arenegligible (Goddard 1991). Many studies have utilized meteorological radar data (Battan, 1973; Puhakka,1974;.Goldhirsh, 1979; Wilson et al. 1979). A radar will actively probes a specificregion.This enables a large amount of data to be collected in ashort period of time. A large database can be used to provide statistical

informationby simulating particular systems. Compared to a rain gauge network, radar observeslarger variability of precipitation characteristics over a short period of time, and at afaster rate (Olsen, 1982). Radar provides valuable information that is relevant inmodelling rain-induced propagation effects (Goddard, 1991). Radar also providesspatially and temporally continuous measurements that are immediately available at one location. Through technology and computer software advancement, radar canscan 3-D space, seek out region of rain, and acquire a quasi-photograph of theprecipitation structure. Goldhirsh (1979) has noted that researchers have demonstrated that database of one whole summer radar reflectivity enabled the prediction ofrain rate distribution, which agreed in shape to the distribution acquired using 10years of continuous rain gauge data. Lahaie et al. (1993) suggested the use of 1000virtual links to an attenuation model. His study used more than 5 millions virtuallinks and that is just for the 1-km path lengths. Seed et al. (1990), utilized a month ofradar data for his study. Wilson (1964) used radar data that covered a periodof 19 days, while Jatila et al. (1973) used radar data taken during summer of 1969.Thus, by using radar information, adequate rain attenuation statistics can be obtained in a shorterror limited period of time.Techniques that utilize Doppler radar and polarimetric radar have also beenemployed (Hornbostel et al. 1979; Meneghini et al. 1997; Zhang et al. 2001). Using these kinds of radars, rain rate can be deduced, and hence attenuation can be calculated.

The most effective technique used to measure rain attenuation is to conduct experiments, where the received signal strength of a satellite beacon is monitored concurrently with radar data (Yeo et al. 2012; Goldhirsh, 1975). Weather radars have been routinely used for investigating propagation phenomena which affect satellite communication links. Weather radar signal strength returns can be used to estimate

both attenuation and depolarization produced by hydrometeors (Dissanayake and Lin, 2002). Radar data information can be used to predict attenuation along a slant path by inferring attenuation in each range gate/bin from the measured radar reflectivity. Higher reflectivity values, *dBZ* indicate greater intensity of precipitation and/or larger objects, such as large raindrops and hail (Horne and Ours, 2002). Using these values along with other information, meteorologists can estimate the instantaneous rain rate at a specific location. An approximate relationship between *dBZ*, *R*, and descriptive intensity is given in Figure 2.7.

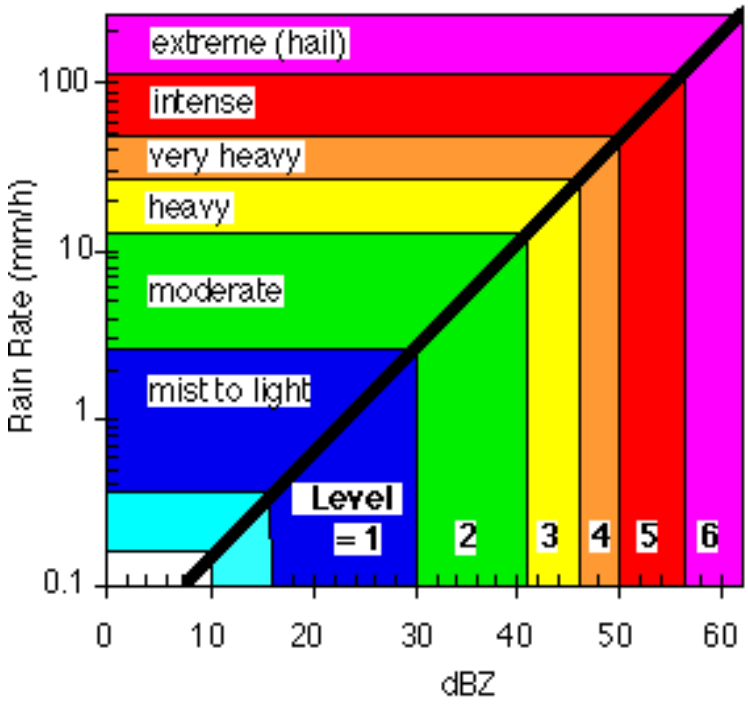

Figure 2.7: Rain Intensity Level Derived from Reflectivity Values (Roland, 2002)

The rain rate will be able to estimate the rain attenuation, *A*. The prediction process can be improved by using dual polarized radar, which makes possible a more accurate assessment of the parameters of the rain in each range gate. Successful prediction of

attenuation on a slant path from radar reflectivity measurements allows the radar to be used to determine slant path attenuation for any path, and obviates the need for satellite beacon or radiometer observations (Stuzman et al. 1986). Some of the early radar measurements resulted in the discovery of high altitude ice particles as a potential source for depolarization and the development of models for the melting layer or the radar bright band. The radar signals return from precipitation particles is proportional to the number density of particles in the radar pulse volume. The reflectivity can be converted to equivalent rain rate or signal attenuation through appropriate assumptions on the particle size distribution. Researches experiments involving radar data to estimate satellite path attenuation in tropical regions are indeed limited. The earliest work comparing satellite rain attenuation with radar data is by Goldhirsh (1975) recorded at Wallops Island. A series of plan-position indicator (PPI) sweeps over these intervals were implemented at a sequence of elevation angles starting from 0.5°up to an angle above which the reflectivity values were below a designated threshold level. Using the above data base, reflectivity profiles along representative Earth-satellite paths were determined from which attenuation and space diversity statistics were calculated at the frequencies of 13 and 18 GHz using ATS-6 satellite (Goldhirsh, 1976). Specifically, the form $Z= aR^b$ was used to deduce the total path attenuation, where a is the attenuation coefficient (dB/km), and Z is the reflectivity factor (mm^6/m^3). The constants a and b were calculated using the raindrop distribution for thunderstorm activity as proposed by (Joss and Waldvogel, 1968). For each slant PPI's scan or vertical plane, series of hypothetical Earth-satellite paths separated a distance d_o at a fixed elevation angle $\theta_p$as shown in Figure 2.8. Goldhirsh also published a sequence of results and findings in predicting rain attenuation using radar data in 1979 and 1980 using COMSTAR satellite. Attenuation coefficient

reflectivity factor using regression relationships were determined from measured raindrop spectra and injected into the radar attenuation estimation technique. Individual attenuation events as well as cumulative conditional fade distributions are compared with corresponding beacon measured cases (Goldhirsh 1979). Radar is shown to be capable of permitting the prediction of rain attenuation as measured directly along a ground to satellite path. Comparison of radar and beacon measurements demonstrates that radar can be a good estimator of fade events both on a case-by-case basis and statistically during the fall and winter months (Goldhirsh, 1980). Figure 2.9 shows experimental configuration for 13 and 18 GHz transmitters analyzed by Goldhirsh which is 26 km from the radar, SPANDAR. While, in this research, the location of the satellite Earth station and the radar station is about 19.5 km.

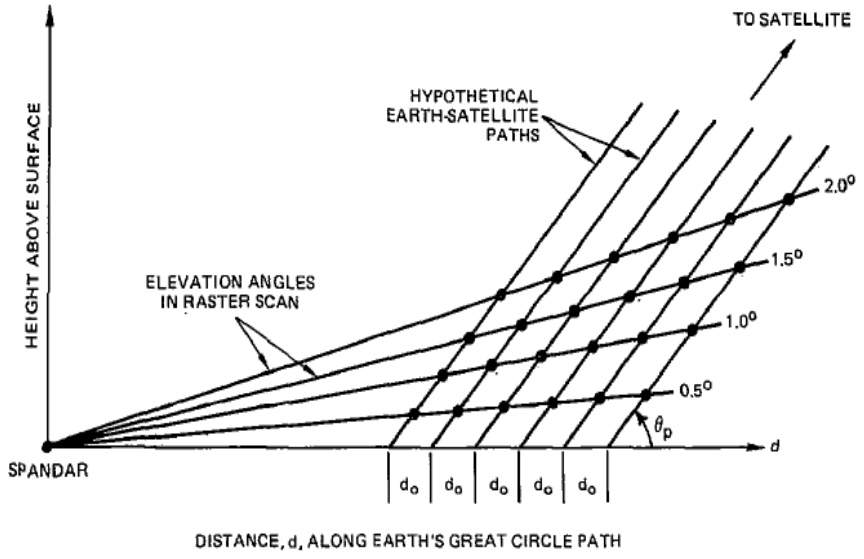

Figure 2.8: Series of Hypothetical Earth-Satellite Paths at Predetermined Azimuth of Raster Scan (Goldhirsh, 1975)

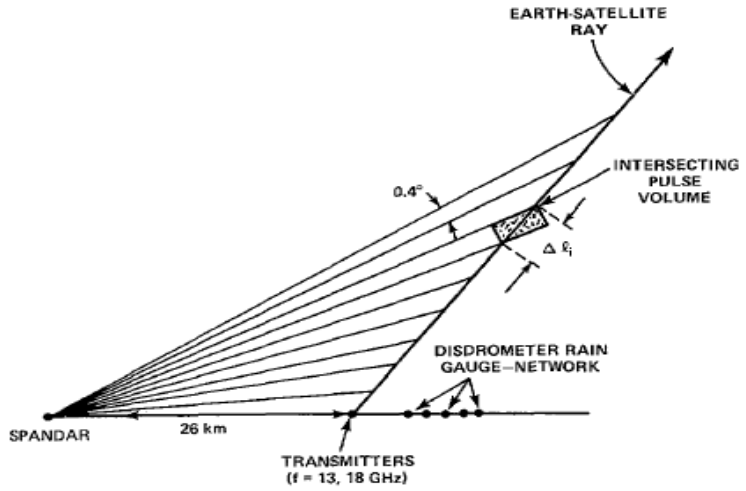

Figure 2.9: Experimental Configuration Showing 13 and 18 GHz Transmitters 26 km from SPANDAR. Beams are Directed in Uplink Mode Toward ATS-6 Satellite (Nominal Elevation = 42.3') (Goldhirsh, 1980).

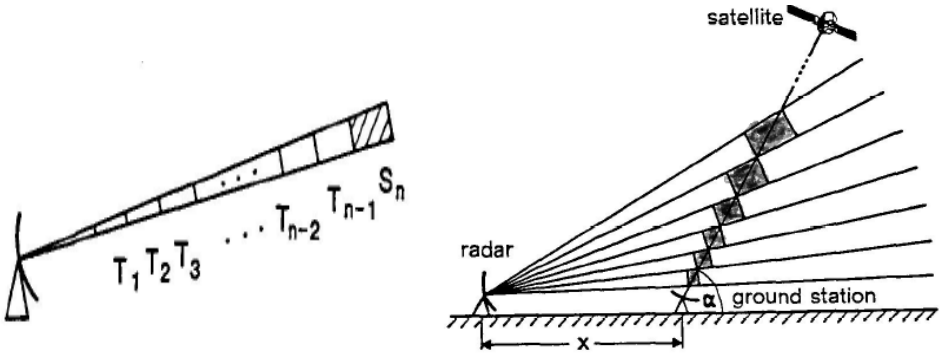

a) b)

Figure2.10:

a) Scattering Geometry of the Radar

b) Scattering Geometry of the Radar and the Satellite-Earth Link (Schanbl, 1988)

Scnabl (1988) proposed radar measurements of a rain volume as marked as the line shaded (S_n) in the figure 2.10 is affected by satellite propagation. Let S_j and T_j be the mean scattering and transmission matrix of say the j_{th} scatter volume, j = 1,2,...n. S_{total} would be measured as;

$S_{total} = T_1T_2 \ldots T_{n-1}S_nT_{n-1} \ldots T_2T_1$.

Hornbostel and Schroth (1995) derived an equation for measuring rain attenuation using radar information such as horizontal reflectivity, Z_h, differential reflectivity, Z_{DR} and linear depolarization ratio, LDR as;

$$A = \alpha(Z_{DR}, LDR)e^{b(Z_{DR},LDR)-Z_h} \qquad (2.27)$$

Where α and b is the attenuation coefficient. Also, an empirical correction of the reflectivity factor Z_h by 2 dB was made to take into account uncertainties in the absolute calibration of the radar and other system effects. Lahaie et al. (1993) presented a way to use meteorological radar data to improve the reliability of rain attenuation prediction models. The method is based on the properties ofmeteorological radar images and on the fact that those images could be obtained every five minutes over a large area. This procedure permits to obtain images of the rain at about an altitude of five kilometres. The resolution of the radar is 1 km, so that each pixel of the image corresponds to onesquare kilometre. While the resolution in rain rate is as much as 0.1 mm/hour,there is however an imprecision in the estimate as high as 20%. This imprecision is independent from pixel to pixel so that, on a statistical basis, it should not greatly affect the outcome of the calculations. According to Lahaie et al.(1993) there are two ways to use such radar images. The first method (Austin and Austin, 1975)consists in placing virtual microwave links and in using successive images in order to estimate the speed intensity and direction of raincells and to calculate in this way the attenuation in space and time by interpolation of the cell movement. The second way is to place a large number of virtual communication links; to calculate for each image the attenuation that each system would have suffered and

then to put those values into a database. Eastment et al. (1996) suggested that the radar reflectivity height profile *Z(h)* can be used to predict the path attenuation via the relationship:

$$A = \left(\sum_{h=0}^{hr} \alpha_R \, Z(h)^{\beta_R} \delta h\right) + \left(\sum_{h=0}^{hm} \alpha_m \, Z(h)^{\beta_m} \delta h\right) \quad (2.28)$$

where δh is the height resolution of the *Z* profile, $h_R$and $h_m$are the heights of the upper extent of the rain and the melting layer respectively, α_R and β_R are coefficients in rain required for attenuation scaling to higher frequencies α_m and β_m are the corresponding coefficients in the melting layer. The vertical extent of the rain is a significant factor in determining the attenuation on an Earth-space path. For calculation of slant path attenuation predictions, one needs only to integrate up to the top of the melting layer. A radar-based attenuation model was developed from simulations that were obtained by varying the parameters of a gamma DSD (John and Bringi, 1997). Using a Mie solution for spherical water particles, propagation variables such as Ka-band specific attenuation and S-band reflectivity were computed over a wide range of DSD parameters. Bolen and Chandrasekar (1998) developed a theoretical model to estimate the specific attenuation, α in the vertical direction from specific differential phase, K_{DP} in the horizontal propagation direction. From this propagation radar (PR) model, attenuation is derived from ground-measured K_{DP} along the space radar beam. The total two-way path-integrated-attenuation (PIA) along the beam is then calculated which can also be used to determine an α corrected PR return. Their results indicate a significant level of attenuation in the space-radar during high rainfall events – as much as 12 dB when storm levels reach 50 dBZ near the surface. Maekawa also compares the Superbird-C satellite links with radar data in Japan and Indonesia (Maekawa et al. 2009). Yeo et al. (2012) as well presented a comparison of S-Band radar attenuation

prediction with 3 satellitesmeasurements in Singapore. They suggested that long term radar observation of precipitation can be very effective to estimate the attenuation statistics of satellite propagation path when Earth stations or satellite signals are not available.

2.6.1 Vertical Profile Reflectivity (VPR) For Convective and Stratiform Rain

Knowledge of the rain vertical profiles is very useful in fields like microwave communication, radar/satellite meteorology and cloud micro-physics. Vertical structure of rain that is obtained using radar can provide information that includes themelting layer's height and thickness.The characterisation of the melting layer has always been of particular interest in the modelling of radiowave propagation for Earth-space communication path due to its different electromagnetic properties. The melting layer is the transition zone between snow and rain, and its distinctiveness aresignificantly important to remote sensing and rain fade estimation prediction. This is due to the fact that it definesthe rain height and the impact of melting particles onsatellite radar profiles(Wilsonet al. 2001). The concept of rain heightplays an important role in propagation modelling forsatellite communication because rain significantlyattenuates millimeter wave signals. Information pertaining to attenuation from the melting layer downwards is crucial in order to properly estimate the required fade margin for short wavelength wireless transmission links.However, such measurements and information on the melting process in the tropics are stillvery limited. Heavy rain in the tropical region can affect radiowave signals profoundly, causing signal fading and interference. Therefore, more campaigns to preciselymeasure the atmospheric parameters caused by heavy rain using remote sensing techniques are certainly required. The radar can play an important part

inimproving atmospheric phenomenon knowledge in this area. This is one of the practical techniques of collecting data that can furnish both the horizontal and vertical structure of precipitation in a way that is practical for studying rain scatter and interference (Steiner et al.1995;Geerts and Teferi, 2005). The cross-polar and Doppler information from such radar could be used to determine the height of melting layer for all types of rain condition (Tan and Goddard, 1999). Figure 2.11 shows a schematic diagram of a possible satellite path link illustrating the vertical view of the rain height and the effective path length.

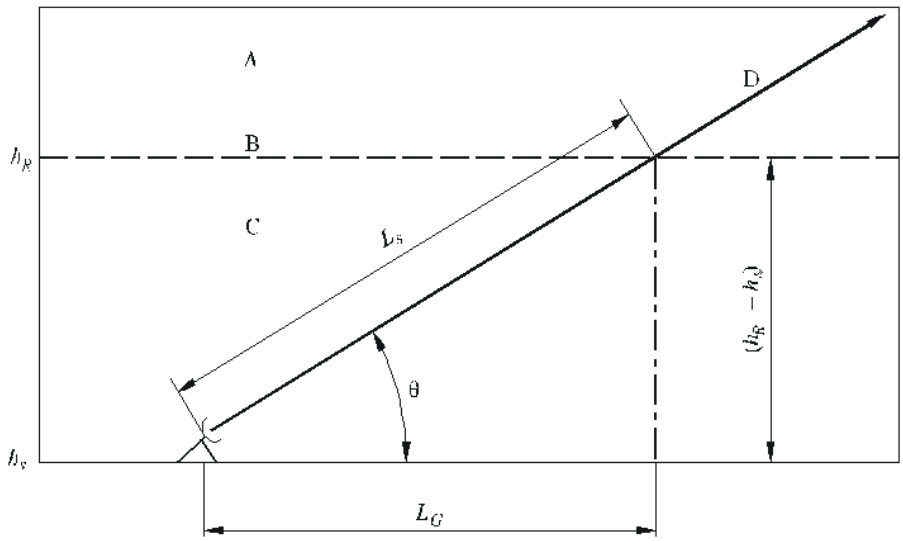

Figure 2.11: Satellite Path Length. A: Frozen Precipitation; B, h_R:Rain Height; C:Liquid Precipitation; D: Earth-Space Path (ITU-R P618-10, 2012)

Height information of melting layer is critical in the estimation of the rain affected transmission path. For slant-path propagation applications, such as satellite communications, the height of the rain structure is important. A region known as the 'melting layer' or the bright band' must be identified. Below this region, rain occurs and microwave propagation suffers attenuation due to rain. Losses in the ice region

above the bright band are negligible for the purposes of most calculations (Eastment et al. 1996). Above this region, no rain occurs and the propagation suffers only spatial attenuation. Studies (Pontes et al. 1995; ITU-R P.839-2) have shown that convective rain in tropical region often has bright band above 10 km and also suffers from severe updraft. However, the bright band region usually exists at the height of 4.5 – 10 km. The ITU recommended that rain height for tropical region is ~4.86km (ITU-R P.839-2). A study (Ong et al. 2000) has shown that the variability of rain height is subjected to seasonal period and types of rain. Identification of the melting layer can be done through radar reflectivity measurement. The uncertainty of the difference in height between rain event and the melting layer need to be investigated so that a reliable prediction of attenuation can be made. Figure 2.12 shows the characteristics of the melting layer as illustrated by Khamis et.al (2006).

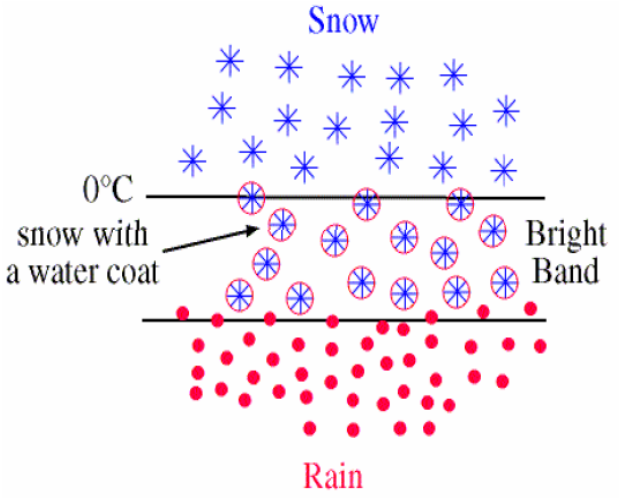

Figure 2.12: Melting Layer Characteristics (Khamis et al. 2006).

Understanding of the characteristics of melting layer is also very practical for weather forecasters in predicting and monitoring the snow level, defined as the lowest

level in a melting layer where snow or ice completely changes to rain. This information can also be useful to hydrologists, aviators and the skiing industry(Harikumar, 2005). The information of the freezing height and the melting layer are critically essentialin making decision whether to do seeding experiment or not and in establishing an optimal seeding strategy that may lead to the most profitable output (Cha et al. 2007). In the case of weather adjustment, cloud seeding is used in an effort to change the amount or type of precipitation that falls from clouds. Substances are being disperse into the air to serve as cloud condensation or ice nuclei. This will alter the microphysical processes within the cloud to increase precipitation (rain or snow). Cloud seeding is also widely practiced in airports for hail and fog suppression (Das et al. 2011). Different reflectivity profiles imply differences in latent heating profiles, and in the convective fraction. The convective-stratiform distinction is important because of differences in Z-R relationships (Das et al. 2009), which affects not only the radar-based rainfall estimation, but also the latent heat release profile, and hence the energy balance of the tropical atmosphere (Creutin and Jean, 1995). Determining vertical profile of rainfall matters because it helps to understand the dynamics of rainfall systems in response to diurnally varying surface energy fluxes and wind profiles.The reflectivity of the radar can be utilised to characterise the vertical variation of rain specific attenuation. This is because reflectivity is proportional to the back scattering properties of the hydrometeors in which the volume is being detected. It is normally assumed for practical calculations that the variation of reflectivity with height in the rain region of a precipitation process is height independent and in general, very small (Goldhirsh, 1979; Hall, 1978). However, especially for high elevation angles; such small variation should be taken into consideration for an improved rain attenuation model (Crane, 1990). Researchers have

studied the climatology of vertical profiles of radar reflectivity and have listed several factors that influence this gradient. (Joss and Pittini, 1991; Joss and Waldvogel, 1989). Among the factors are the growth or evaporation of precipitation and the air motion (Ismail, 2002). Other investigators have also hypothesised that this variation with height can also be attributed to the variation of drop velocities with atmospheric pressure (Leitao and Watson 1986). This means, with assumption that vertical continuity of rainfall rate, larger particle concentrations are found near the ground than above. However, another investigators (Crane, 1990) highlighted that for places across the Tropics (20°N-20°S) involving transmission at high elevation angles; regardless of how small the variation is, it should be taken into consideration for an improved rain attenuation model due to the fact that the bright band phenomenon is a challenge to the knowledge of precipitation physics and scattering theory.

2.7 Summary

The technology of radar for precipitation measurement is very stable and the results of observations are highly accurate (Japan Meteorology Agency, 1979;Goddard, 1991). Radar data are also said to be a better tool to build a rain attenuation prediction model for Earth-satellite link communication (Luini & Jeannin, 2008). In temperate region, many researchers have been concluded, on the other hand, the research conducted in tropical region still requires validation and inspection.

CHAPTER THREE

METHODOLOGY

3.1 Introduction

The research has been carried out in collaboration with Malaysian National Space Agency (ANGKASA) and Malaysian Meteorology Department (MMD). One year radar data were provided by MMD. The data were acquired from an S-band (2.75 GHz) MMD's weather radar located at Bukit Tampoi, Sepang, Selangor. X-band (8.21 GHz) signalsfrom Malaysian RazatSATdetected at ANGKASA space centerwereanalysed and studied. Consequent received signal drop i.e. sudden signal fade detected by ANGKASA Earth station might suggest presence of rain event. The MMD's radar scans were examined to confirm existence of precipitations hence validating that the recorded satellite signals variation were due to attenuation by rain. The distance betweenthe location of the MMD radar and the ground station of RazakSAT satellite is 19.4 km as shown in Figure 3.1. Figure 3.2 displays the configuration of the system setup.Table 3.1lists the latitude, longitude, bearing and distance. Figure 3.3 shows the flow chart of the study.

Table 3.1: TDW Radar and Satellite Ground Station Location and Distance

	Latitude	Longitude	Distance
Satellite Ground Station, Banting	2°47'2.69"N	101°30'26.74"N	19.5 km
KLIA Radar Station	2° 51' 0"N	101°40' 0.014"E	

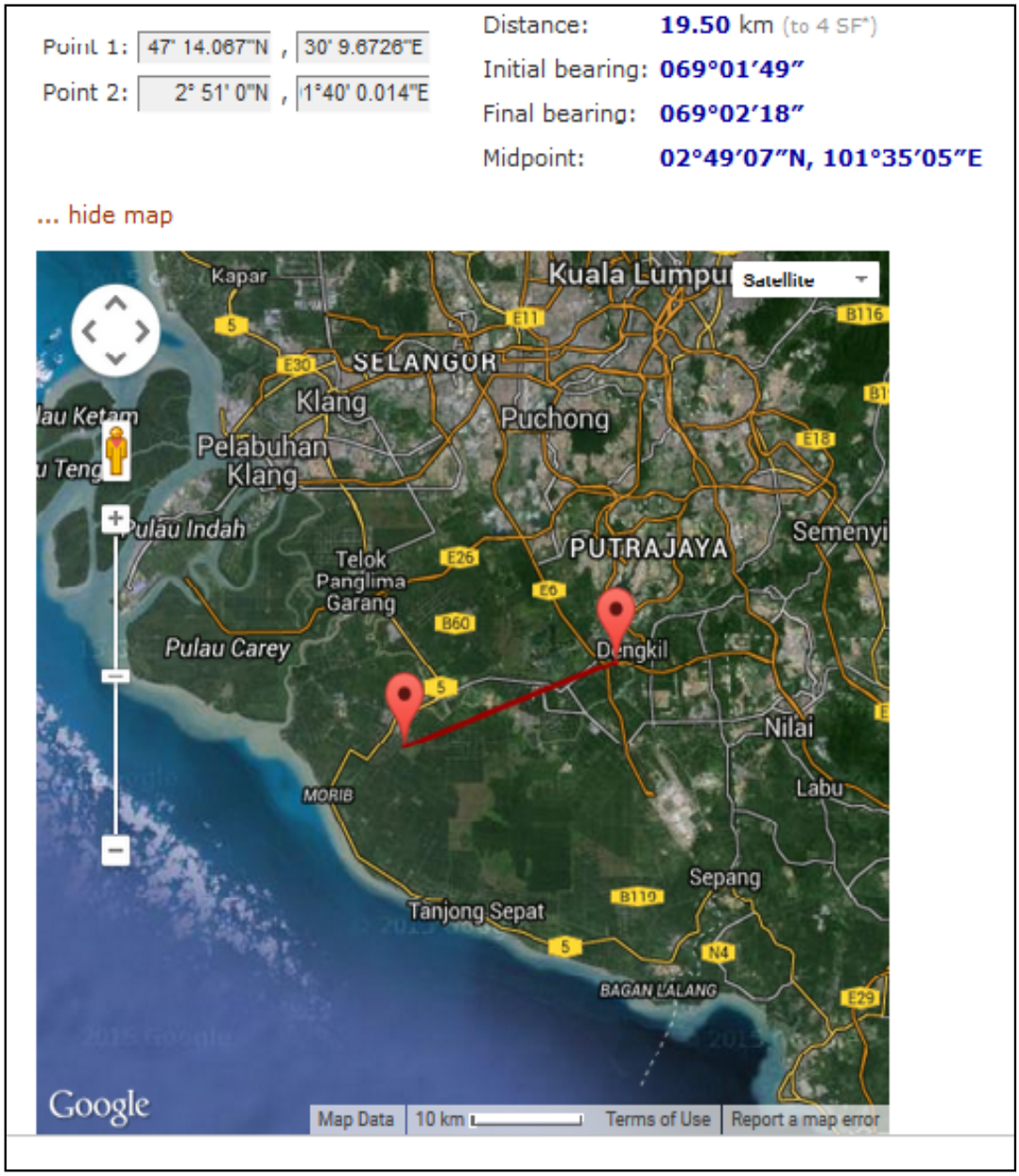

Figure 3.1: RazakSAT and MMD Radar Location Map

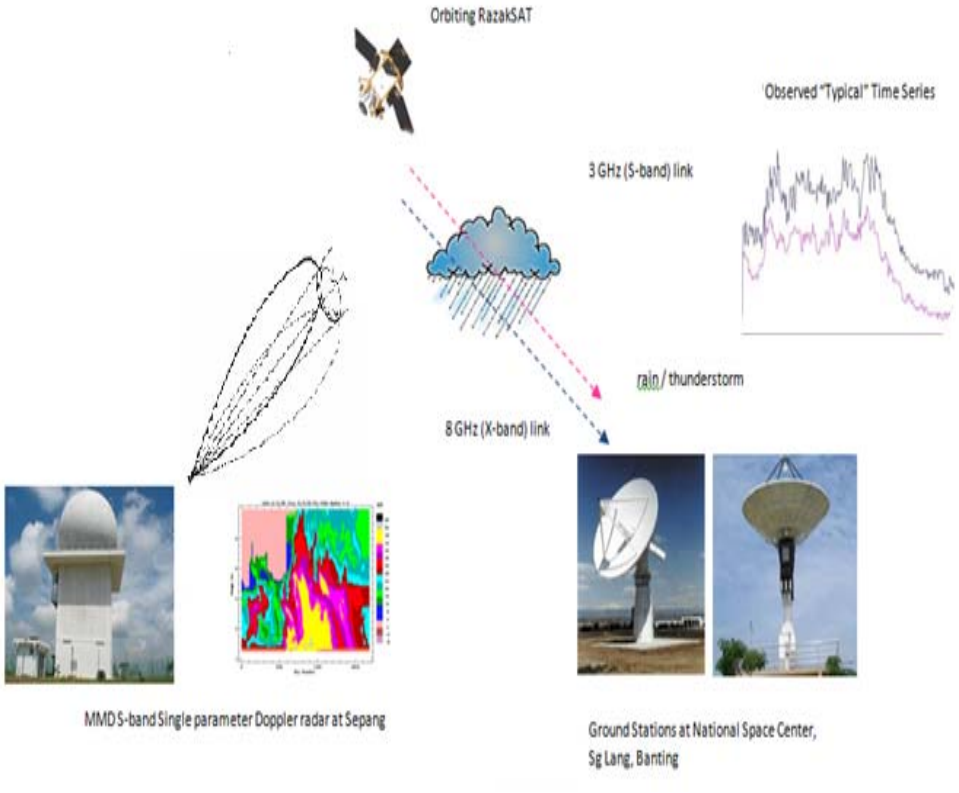

Figure 3.2: Overview of System Set-up

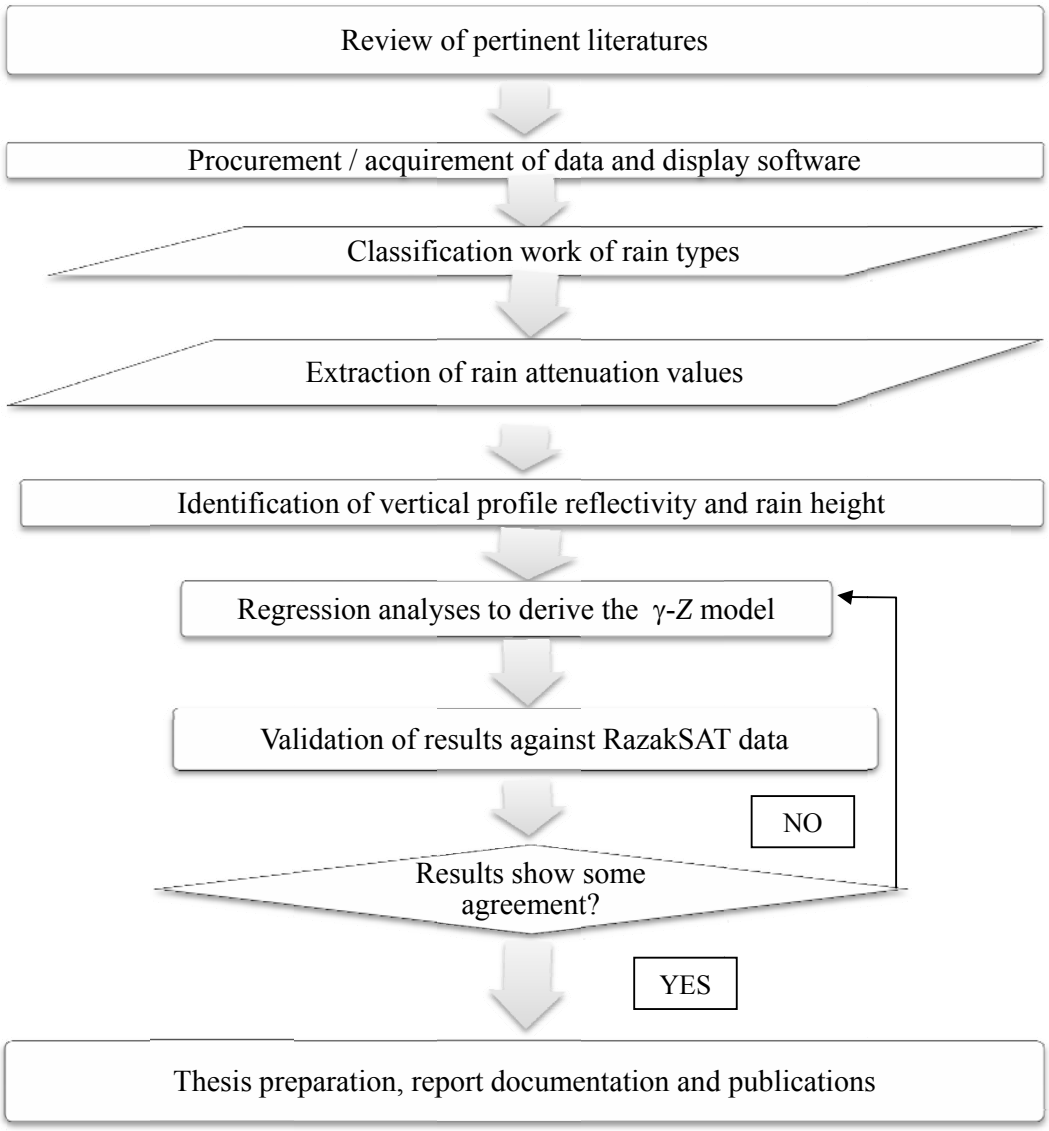

Figure 3.3: Flow Chart of Research Methodology

3.2 Phase 1: Literature Review

The first phase was to conduct pertinent literature review on Earth-satellite link's propagation characteristics and radar reflectivity. It is of great importance to understand thoroughly how signals are being attenuated as well as the principles of the

return echoes from targets. Reflectivity attributes were analyzed to determine their intensities in establishing the specific values in the scanned volume. The wavelength involved of about 10 cm (S-band radar) ensures that this return is proportional to the rate because they are within the validity of Rayleigh scattering. Rayleigh states that the targets must be much smaller than the wavelength of the scanning wave (maximum drop diameter rarely exceeded 4 mm (Brusssard and Watson, 1995). Some of critical information was deliberated in Chapter 2.

3.3 Phase 2: Measurement Setup and Data Collection.

a. RazakSAT Satellite System.

RazakSAT is the Malaysian's second remote sensing or known as Earth observation satellitelaunched in July, 14, 2009. The imageof the satellite is shown in Figure 3.4. It is a small Low Earth Observation (LEO) satellite orbiting the Earth in a unique Near Equatorial Orbit (NEqO) at nominal altitude of 685 km and 9 degrees inclination.The X-band (8.21 GHz) transmitted signals from RazakSAT were received, monitored, and tracked by the Hexapod antenna. The recorded data of the 8.21 GHz QPSK modulated transmission were used in this study. RazakSAT wasoperated from its ground segment located at 2° 47' 14.067"N, 101° 30' 9.6726"E in Kampung Sg.Lang, Banting Selangor.The ground segment physique is shown in Figure 3.5. The ground segment i.e. Malaysian Space Center consists of a Mission Control Station (MCS) and an Image Receiving and Processing Station (IRPS).The RazakSAT revisited Malaysian territory every 90 minutes, potentially maximizing its ability to exploit gaps in the clouds (RazakSAT, 2012). It carries the Medium-sized Aperture Camera (MAC) which is an electro-optical payload of a push broom camera type with 5 linear detectors (1 panchromatic, 4 multi-spectral).

Figure 3.4: RazakSAT with Solar Panel Deployment

Figure 3.5:ANGKASAGround Station at Sg. Lang, Banting, Selangor.

The RazakSAT mission plan, command generation and telemetry receiving, archiving and analyses were executed accordingly at the MCS by a dedicated team of satellite engineers. They archive and analyze received data, then process and distribute accordingly to the users. The receiving and archiving images for post processing are

carried out at IRPS. Figures3.6 - 3.8 show the RazakSAT satellite orbits during its lifetime. Table 3.2 listed the countries in the equatorial region that covered by the satellite.

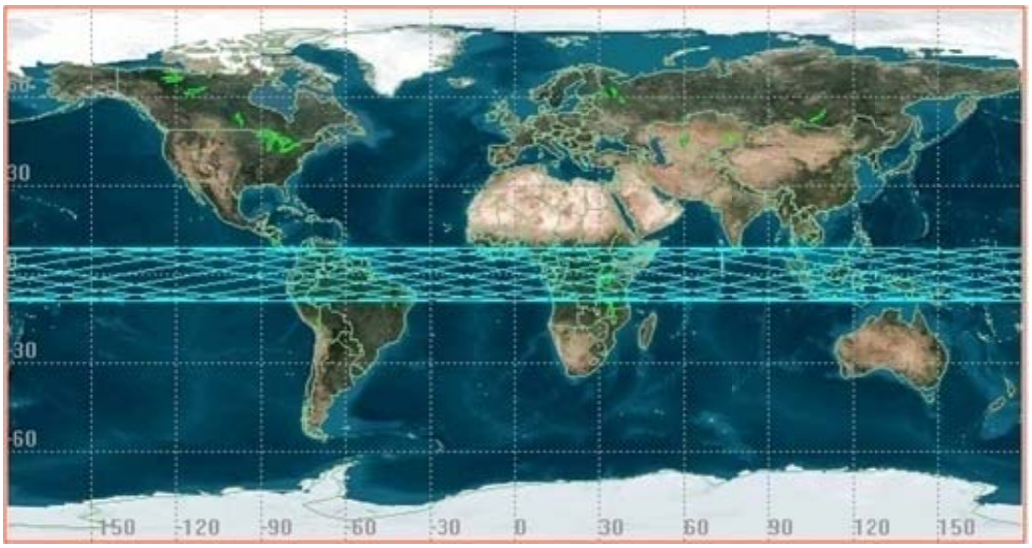

Figure 3.6: RazakSAT Orbits on World Map (RazakSAT, 2012)

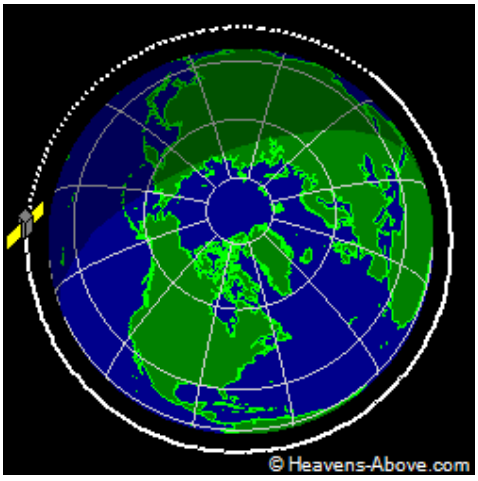

Figure 3.7: View from Above Orbital Plane

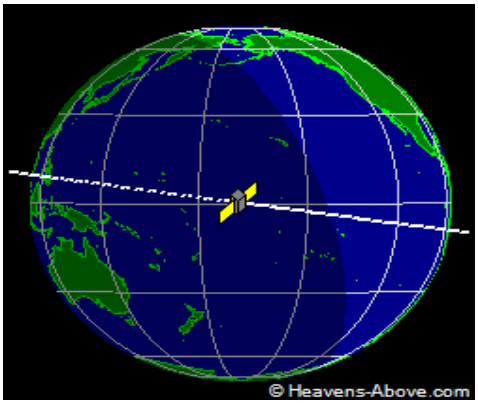

Figure 3.8: View from Above Satellite

Table 3.2: List of Countries Covered by NEqO (9°Inclination)

Continent	Countries
Asia	India, Indonesia, Malaysia, Maldives, Philippines, Sri Lanka, Thailand
Africa	Angola, Benin, Burundi, Cameroon, Central African Republic, Chad, Cote d'Ivoire, Ethiopia, Gabon, Guinea, Kenya, Liberia, Nigeria, Rwanda, Sierra Leone, Somalia, Sudan, Tanzania, Uganda, Zaire
Latin America	Brazil, Colombia, Ecuador, French Guiana, Guyana, Panama, Peru, Surinam, Venezuela

RazakSAT offers a high number of passes (14 times per day over Malaysia) for communication with ground station. With Near-Equatorial Low Earth Orbit (NEqO) at 685 km altitude, imaging opportunity increases by 3 times more compared to a sun-synchronous orbit. It is in contact with the Earth station for about 20 minutes each passes, and will be in contact again about 93 minutes later. During communication, Earth station receives a certain power signal level and this received power signal wereexploited for this intended research. Each time either rains or clear sky condition, the signal received were measured and the differences during these two

states were calculated as rain attenuation. In order to give user quality assurance of the operational imagery, ground calibration (pre-flight calibration) had been conducted (Wai et al. 2007). Table 3.3-3.5 itemised the specifications of the satellite and the ground station power received data used in the study.

Table 3.3: RazakSAT Specification (www.atsb.com.my, 2012)

Item	**Specifications**
Orbit	Near Equatorial Low Earth Orbit
Altitude	685 km
Inclination	9°
Mass	187.6 kg
Envelope	f1200mm ´ H1200mm
Attitude Control Accuracy	0.2°
Power	> 300 W
Payload	Medium-sized Aperture Camera
Mass Storage Capacity	32 Gbits
Data Down Link	30 Mbps (X-Band)

Table 3.4: RazakSAT® Data Characteristics (www.atsb.com.my, 2012)

Subsystems	Specifications
Altitude	685 km
Inclination	9 °
Payload (MAC)	GSD : 2.5 m (PAN), 5 m (MS) Swathwidth : 20 km @ 685 km
Attitude Determination & Control Subsystem (ADCS)	Three-axis stabilization based on four reaction wheels Pointing Accuracy : < 0.2° (2 s) Pointing Knowledge : 1 arcmin (2 s)
Electrical Power Subsystem (EPS)	GaAs/Ge solar cells on honeycomb substrate NiCd batteries (18 hr) Peak Power Tracking (PPT) & constant current control Solar Power : >300 W @ EOL
Command & Data Handling Subsystem (C&DH)	Two on-board computers Telemetry and command interface modules Analog Telemetry channels : up to 90 Digital Telemetry channels : up to 120
Telecommunication Subsystem (TS)	9,600 bit/s / 1,200 bit/s S-band TT&C uplink 38.4 kbs / 9,600 bit/s / 1,200 bit/s S-band TT&C downlink
Payload Data Management	32 Gbit On-board solid-state memory 30 Mbit/s X band payload data downlink
Structure & Thermal	Ø1,200 × 1,200 mm Hexagonal shape Mass : 180 kg Modular structure Passive & Active thermal control
Mission Lifetime	> 3 Years

Table 3.5: Ground Station/Earth Station Characteristics (www.angkasa.gov.my, 2012)

Antenna Size and Type	X band-7.3 meter, S band -5.3 meter, full hemispherical monopulse autotracker with SGP4 based program track capability
Coordinates	Lat = 2°47'2.69"N, Lon = 101°30'26.74"E, Alt = 10.00 metres
Antenna axis speed	AZ =10˚/sec EL = 10˚/sec
Overhead pass	3rd axis tilt ±10˚
Receive RF bands	8000 – 8400MHz
Receive G/T	30.0 dB/K
Modulations supported	BPSK, QPSK, OQPSK, UQPSK, 8PSK
Receive Data rate range	1 Mbps to 150 Mbps (upgradable up to 470 Mbps via license upgrade)
Polarizations supported	Selectable RHCP/LHCP
Space Data protocols	CCSDS
Connectivity protocols	TCP/IP
Link Coding	Descrambling,Reed-Solomon, Convolutional,Viterbi
Short Term Recording media	Hard disk
Removable Recording Media	Mission Specific
Metric tracking	Doppler and angles

b. MMDRadar

The investigation of rain attenuation made use of single polarization S-band terminal Doppler weather radar (TDWR) data with operating frequency of 2.75 GHz. The radar stationis shown in Figure 3.9.It is located at latitude 2°51'00"N and longitude 101°39'60"E, in Bukit Tampoi, Sepang about 10 km north from the Kuala Lumpur International Airport (KLIA). The radar system is programmed to operate in two scanning modes; Airport and Aerial mode. The radar automatically shifts from Aerial mode to Airport mode when its sensor detects rain of more than 0.1mm/hr within the 20 square km vicinity from KLIA.Each mode consists of three different volume scans called TASKs. Volume A (Vol-A) is for long range observation at low elevation angles. Volume B (Vol-B) is for medium range observation and Volume C (Vol-C) is for short range observation at high elevation angles. Both the Pulse Repetition Frequency (PRF) and antenna scan rate are different for each task. Higher PRF is use in the short range mode. Approximately 300 volume raster scans are acquired per day in which each scan is generated within the duration of 5 minutes. The calibration of the TDWR radar made by Enterprise Electronics Corporation (EEC),USA are carried out two times per year in July and December. The local corporation contracted out to carry the task is Malaysia Airport Technologies Sdn. Bhd, one of the subsidiaries of Malaysia Airport Holdings Berhad. ISO/IEC 17025 document pertaining to "General Requirements for the Competence of Testing and Calibration" are observed during the process. Both transmitted and received signal power are verified with the use of test instruments namely oscilloscope, power meter, power sensor, frequency counter, signal generator, spectrum analyzer, attenuators and crystal detectors. Data acquired were from 1/1/2009 to 31/12/2009. Ideally, radar scans of 1-minute should be used. However, the present system requires 10 sweeps i.e. 5 minute in order to be able to

generate a full volume scan. This is the only available data option that can be acquired from Malaysia Meteorology Department (MMD). Should 1-minute scanning time data are available in the future, a more refine technique can be attempted.Each mode includes sweeps of the surrounding area at a predetermined elevation angles. Each elevation contains 360 rays of data corresponding to 360 azimuth angles with no interlaced beams. The radar antenna rotates at the speed of 2 revolution per minute (RPM) with pulse repetition frequency (PRF) equals to 300 Hz for scanning elevation angles of less than 5°. The radar rotates at a speed of 4 revolution per minute (RPM) with PRF equals to 1000 Hz for angles of elevation between 5° to 40°. Figure 3.12and 3.13 are the information provided by the MMD. This radar can cover the Malaysian environment up to 480 km radius from the radar station at Bukit Tampoi, Selangor.Since the location of the radar to the Earth Station of the RazakSAT is only 19.4 km, the data collected are very much synchronized.

Figure 3.9: MMD Radar Station at Bukit Tampoi, Selangor, Malaysia

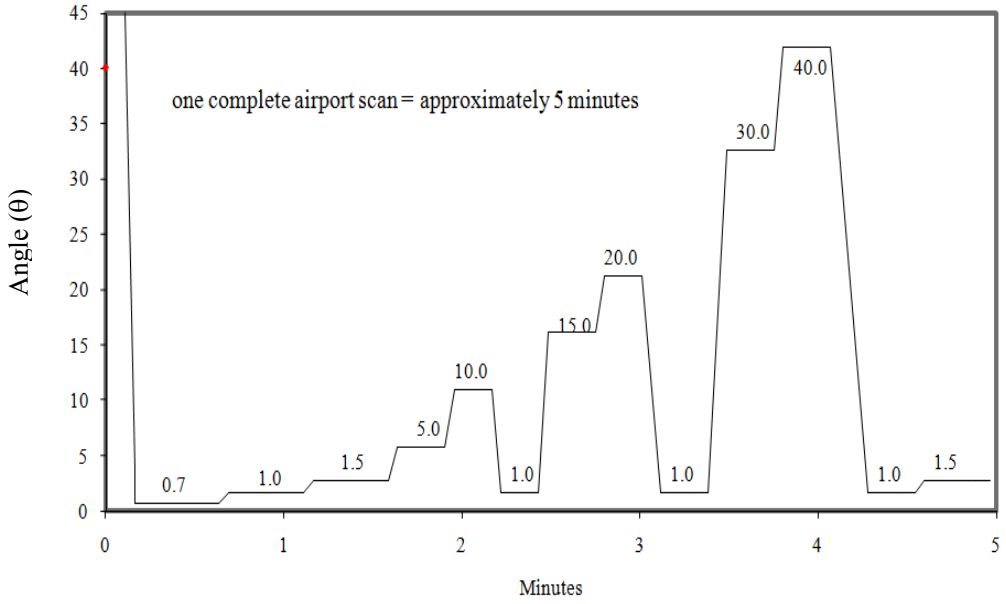

Figure 3.10: Airport Mode Radar Scanning Configuration

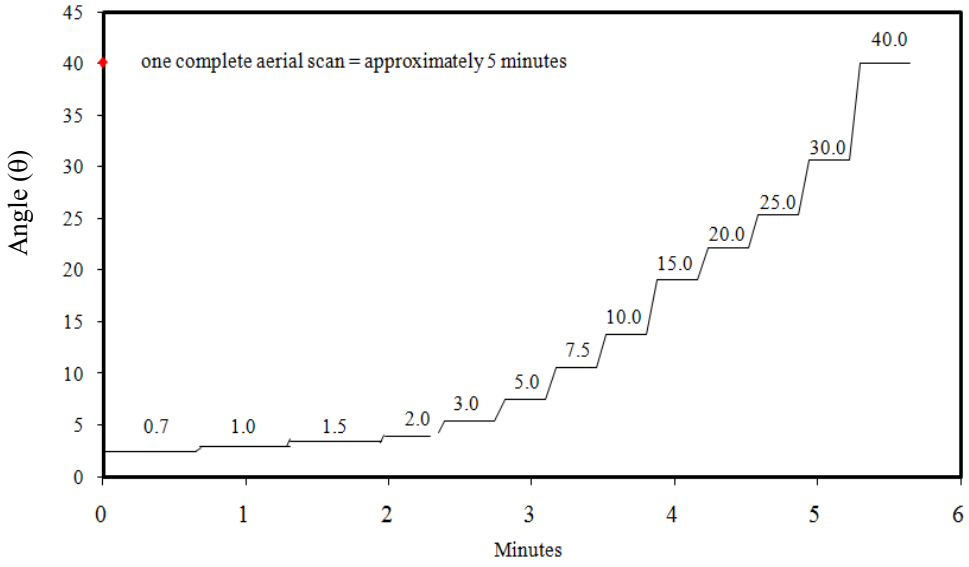

Figure 3.11: Aerial ModeRadar Scanning Configuration

The plan position indicator (PPI) is the most common type of radar display. The radar antenna is usually represented in the centre of the display, so the distance

from it and height above ground can be drawn as concentric circles. As the radar antenna rotates, a radial trace on the PPI sweeps in unison with it about the centre point. When a radar is scanning in only one direction vertically, it obtains high resolution data along a vertical cut of the atmosphere. The output of this sounding is called a Range Height Indicator (RHI) which is excellent for viewing the detailed vertical structure of a storm. The PPI scan of the radar during rain is shown in Figure 3.12 below. Whilst, Figure 3.13 is an example of the RHI scan that has been used to study the vertical profile of the rain events using cross section configuration at the intended location of the RazakSAT link to the Earth station.There are different angles during the transmission of signal received at the Earth station from the RazakSAT satellite. Based on RazakSAT databases, the RHI scan were generated to outline cross-sectionsfor each event. The primary objective of such system was to obtain information of the vertical structure of precipitation in tropical climate (Eastment et al. 1995). This was in a way very useful for example toestimate attenuation due to rain along the Earth-space paths at high frequencies.

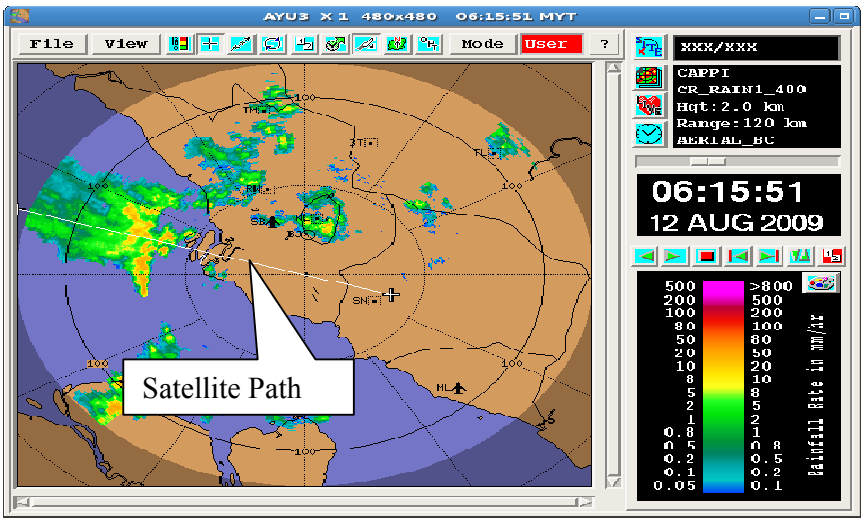

Figure 3.12: PPI Views for Rain Events Confirmed on 12/08/2009.

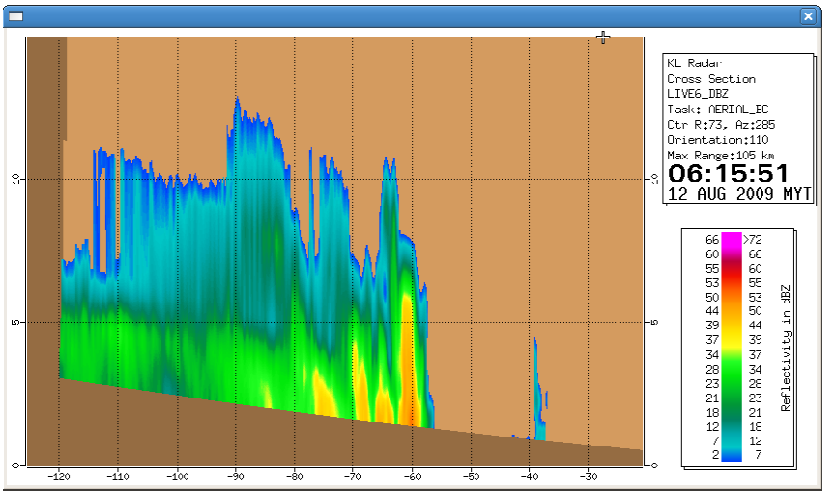

Figure 3.13: RHI Scans on 12/08/2009.

The radar specification used in the research is outlined in Table 3.6 as follows;

Table 3.6: MMD Radar Specification

Tasks	**AERIAL /AIRPORT SCAN**
Elevation Angle(s)	2.0, 3.0, 5.0,7.5,10.0,15.0, 20.0, 25.0, 30.0, 40
PRF (Hz)	1000
RPM	4
Wavelength (cm)	10.43
Pulse width (sec)	1 μ
Polarization	Vertical
Max range (km)	120
Bin width (m)	125
Scan rate (deg/sec)	24
Output bins	960
Start range (km)	0.00
End range Up to (km)	480.00

The system incorporates Gaussian Model Adaptive Processing (GMAP), the most advanced form of clutter filtering and moment estimation for anomalous propagation. The algorithms have included data quality thresholds such as;

i. Signal-to-noise ratio (SNR) - to reject bins for having weak signals

ii. Signal Quality Index (SQI) - to reject bins having for incoherent signals,

iii. Clutter-to-signal ration (CSR) - to reject range bins having very strong clutter

iv. Speckle Filter - to remove single bin targets such as aircraft or noise

Therefore, the value of dBZ obtained are already Clutter Corrected Reflectivity.Further details of the algorithms are given in the IRIS/Open user's manual, version 7.05 (SIGMET 1999).

c. MMD Rain Gauge

The ground truth measurement data were collected from the rain gauge located at MMD station KLIA with 2°44' N and 101°42' E, about 5km from the airport and 16.3m above mean sea level. The rain gauge used by MMD consists of standard tipping bucket in order to collect the measured rainfall values. The tipping bucket rain gauge follows the standard by World Meteorological Organization (WMO). This tipping bucket collects data every 60 minutes. Therefore, integration time for the measured data is 60 minutes.The tipping bucket comprises of two components; funnel-shaped at the top supported by a cylindricalshaped at the bottom. This funnel has a water filter at the end of the funnel opening. As rain falls it lands in the funnel of the tipping bucket rain gauge. Water flowing into the funnel will be screened and will

be collected by two metal water collectors (tipping buckets). The raindrops is poured into the cylinder when one of the collectors receives the raindrops of amount 0.2mm and the next rain will then fall to the other metal collectors. This process is repeated and this repetition process is connected to a computing system (counter) that will count the number of times the rain that falls into the water collector metal. The amount of rainfall rate is calculated based on multiplication of the number of times the precipitation that falls on the metal rain collector with 0.2mm of rain droplets. Maximum rainfall amount that can be obtained is 200mm/hr. Table 3.7summarized the specifications of the tipping bucket rain gauge operated by MMD and Figure 3.14 shows the tipping bucket that is located at KLIA.

Table 3.7: Specifications of Tipping Bucket Rain Gauge

Item	**Specifications**
Location (Latitude, Longitude)	KLIA, Sepang (2°44’ N and 101°42’ E)
Distance from KLIA	±5km
Receiving collector	203mm ±0.2mm
Accuracy	±1% to 200mm/hr
Bucket capacity	0.2mm
Dimensions	300 mm height 230mm body diameter 280mm base diameter
Physical	5.5kg net weigh

Figure 3.14: MMD Tipping Bucket at KLIA

3.4 Phase 3: Data Processing

IRIS Display is the industry software package for the graphical presentation of MMD radar data. Procurement / acquirement of the data and IRIS software are the elementary steps to get familiarize on how meteorology radar system works. The reflectivity measurement data were recorded every 5minute. There are two important types of data available, Constant Altitude Plan Position Indicator (CAPPI)data and volumetric data. The CAPPI data contain from two to four PPI scans at different elevation angle. The CAPPI is made by the signal processor at the radar site where the number of scan and elevation of scan selected depend on the local topography. Meanwhile the Volumetric data consists of 15 PPI scans. Data are archived in ASCII format, which 16 level encoding systems employ a deviation system to compress the data. There are sixteen characters which define sixteen video levels absolutely, and 49 characters which allow a deviation of up to 3 levels for two successive range bins to be encoded. Referring to Table 3.8, the *dBZ* level is givenin the value of *dB*, and its corresponding reflectivity, *Z*. In this study, the reflectivity data is only cropped to only

20km rangein order to ensure high quality reflectivity data, because at a great distance from radar, the signal received by radar can be influenced by noise (Sebastianelliet al. 2010).

Table 3.8: Reflectivity Values Shown in the Software

Reflectivity, dBZ (mm^6m^{-3})		
Level	Start	Stop
16	66	>72
15	60	66
14	55	60
13	53	55
12	50	53
11	44	50
10	39	44
9	37	39
8	34	37
7	28	34
6	23	28
5	21	23
4	18	21
3	12	18
2	7	12
1	2	7

Radar reflectivity were converted into rainfall rate. From the rainfall rate the rain attenuation were also estimated. The reflectivity *Z*was expressed on a logarithmic scale in unit *dBZ*, which was calculated using:

$$dBZ = 10 \log Z \tag{3.1}$$

The reflectivity, *Z*was then converted to rainfall rate, *R* using the Equation(2.9).

Marshall and Palmer proposed the Z-R relation using the exponential DSD with a set of parameters of $a = 200$ and $b = 1.6$ for general worldwide application. The

slant path attenuation for Earth-satellite link was then calculated through the numerically summation ofEquation (2.10)

The Range Height Indicator (RHI) cross section from the MMD radar were based on the RazakSAT link during stipulated time. The reflectivity values based on each bin of the RHI cross section were calculated and totalledup from each bin up to the link affected by the RazakSAT transmission. These estimated rain attenuation values from MMD radar were then compared to the attenuation from the differences of the power received signal from RazakSAT link during rain and no rain events. An example of the RazakSAT rain attenuation can be observed in Figure 4.5 in Chapter 4. Figure 3.15 shows an impression of a bin with its associated reflectivity value.

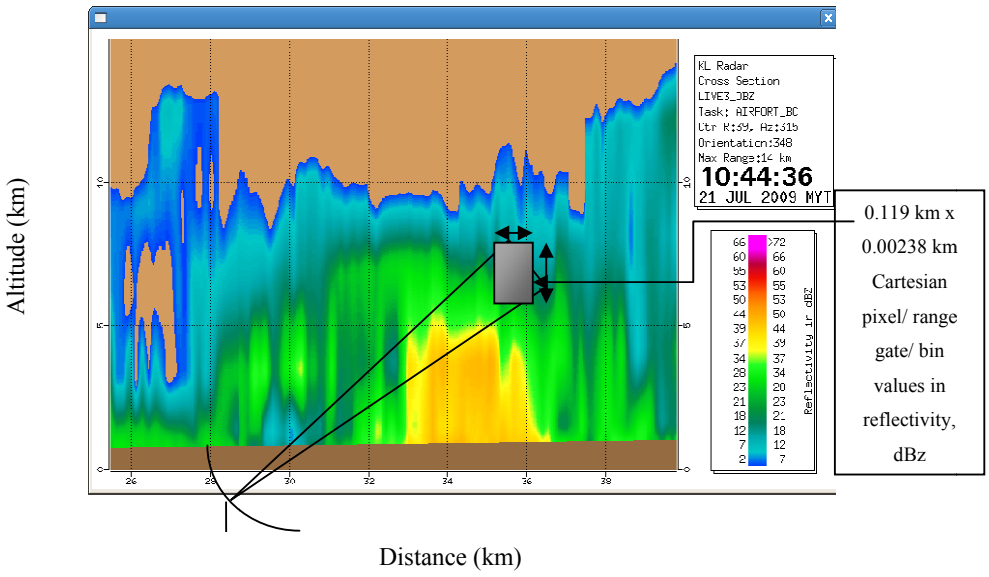

Figure 3.15: Illustration ofReflectivity ValuesRead from Radar Data.

3.5 Phase 4: Data Analysis

Characterization of stratiform and convective events within the one year duration from the Sepang facility have been carried-out in this study. Stratiform and convective

events have been grouped according to the following procedure. First, sequences of radar scans were visually inspected using the IRIS software. Those events with a clear bright-band in their range-height indicator (RHI) scans and having widespread characteristics in their PPI scans were classified as stratiform. Other events with localized rain cells of small dimensions and sharp gradients of reflectivity with range were classified as convective.

The final classification was achieved by monitoring carefully the history of the development of the rainstorm.By adopting such rigorous classification methodology, rain events were formally classified as stratiform and convective.

In short, the MMD radar scans of rain event in Sepang have been used to characterise the rain type and the ANGKASA RazakSAT's signal data were utilised to ascertain the rain attenuation level. The rain attenuation distributions were then applied to derive the relationship between specific attenuation,γ and the radar reflectivity, Z. Using regression analysis technique, matching measured rain attenuation against estimated radar derived attenuation, correction factor has been identified.

3.6 Phase 5: Development of Innovative Technique of Rain attenuation prediction

Using the measured rain attenuation values and the appropriate scattering properties at frequencies of interest, the specific attenuation and the radar reflectivity weretabulated at different attenuation level. The γ-Z model of specific attenuation and reflectivity calculations have been deduced using the standard regression assessment. Regression assessment models the relationship between an independent variable (γ) and a dependant variable (Z) using an equation that express γ as a function of Z. Such

modelwas then applied to estimate the specific attenuation using radar reflectivity from radar scans.

Subsequent workshave involvedthe utilization of the co-polar reflectivity of the radar to characterise the vertical variation of rain specific attenuation. This is because reflectivity is proportional to the back scattering properties of the hydrometeors in which the volume being detected. Regardless of how small or big the variation, it should be identified and taken into consideration for the development of an improved rain attenuation model for high elevation angles Earth-space communications.

Innovative technique of rain attenuation prediction have been configured by exploiting the derived γ-Z relationship. Instead of converting from Z-R-γ-A as per carried out in the first technique,which requires several processes and involving multiple equations, the newly derived γ-Z relationship is much simpler and based on empirical satellite link value and matched with the exact time and area of the radar data. In this study, the RazakSAT link's rain attenuation value was paired with the MMD radar data in thedevelopment of the said relationship.

For both types of rain events, observations concerning the radar reflectivity versus height have beendocumented.The research findings was compared with values obtained in temperate climate, hence validate (or dispute) common assumption that the variation of reflectivity with height in the rain region of a precipitation process is not dependent on height. The variation of Z with height in the rain region of a precipitation process in temperate climate has been reported to be generally small (Mori et al., 2011) and a height independent profile is normally assumed for ease of calculations. Nonetheless, similar conclusion has to be confirmed for precipitation rain

events in the tropics. Empirical values of rain height were derived from the mentioned exercise.

3.7 Phase 7: Validation of the Prediction Model

The newly discovered rain attenuation prediction models using the proposedγ-Z relationship were validated. The standard deviation and the variations were identified.The analyses of signals using RazakSAT data as expected, shed lights about the tangible signal fluctuation experienced by a satellite to Earth link in tropical environment. In this study, reflectivity has been exploited to characterize the vertical variation of rain specific attenuation.

3.8 Summary

The available path attenuation data for tropical and equatorial regions of the world are still insufficient for a comprehensive evaluation of attenuation process in the tropical regions even on empirical basis.Additional data would permit refinement of the prediction models.

CHAPTER FOUR

ANALYSES OF RAZAKSAT PATH LINK MEASUREMENTS

4.1 Introduction

The nations in the tropical regions today are undergoing a rapid expansion in satellite communications with the increase in demand for long distance telecommunications, broadcastings and data channel requests. Due to rapidly increasing demand for more bandwidth, the radio frequencies used by the current satellite communication systems in these regions have been gradually shifted toward higher bands. Despite such phenomenal growth, available data to describe how the high frequency radiowaves will behave in tropical conditions is still lacking.

In other words, there are insufficient measured data in the tropical region to accurately model the Earth-space propagation at microwave and millimetre wavelengths. Reliable propagation models are required to support the optimal design of the future satellite communication systems in the high rainfall rate climatic zones (Eastment, 1999). The introduction of Direct-to-Home (DTH) satellite services in tropical regions at K_u-band frequency and above could be hampered by signal attenuation due to heavy rainfall if the correct margin or fade mitigation technique are not engaged. This heavy rain in the tropical region can affect radiowave signals profoundly, causing signal fading and interference.

4.2 Signal Attenuation from RazakSAT Satellite

The measured received power signal from RazakSAT satellite during rainy event has been measured and compared with clear sky condition where no rain existed. The variation of the signal level was calculated and the measured values wereregarded as the attenuation of the X-band during rain. Since the satellite transmit the signal in many angle ranging from 0° up to 80°, the attenuation has to be compared based on the same positioning i.e. elevation angle, latitude and longitude. Figure 4.1 and 4.2 shows an example of one of the event where rainy and clear sky was occurring.

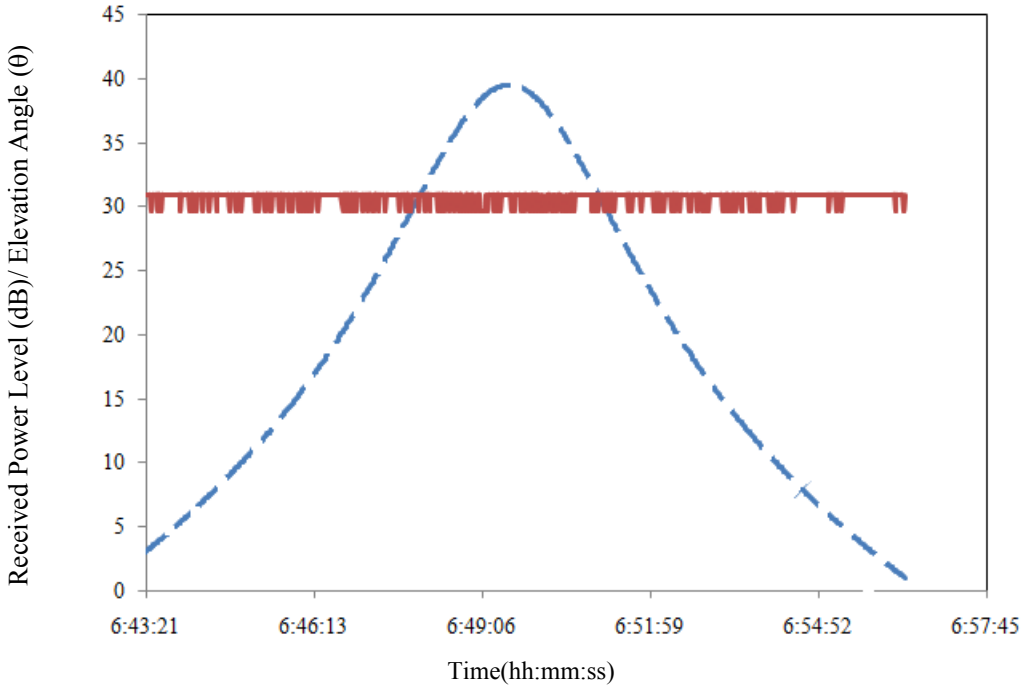

Figure 4.1: RazakSAT received power (-) and elevation angle (- -) during rainy condition.

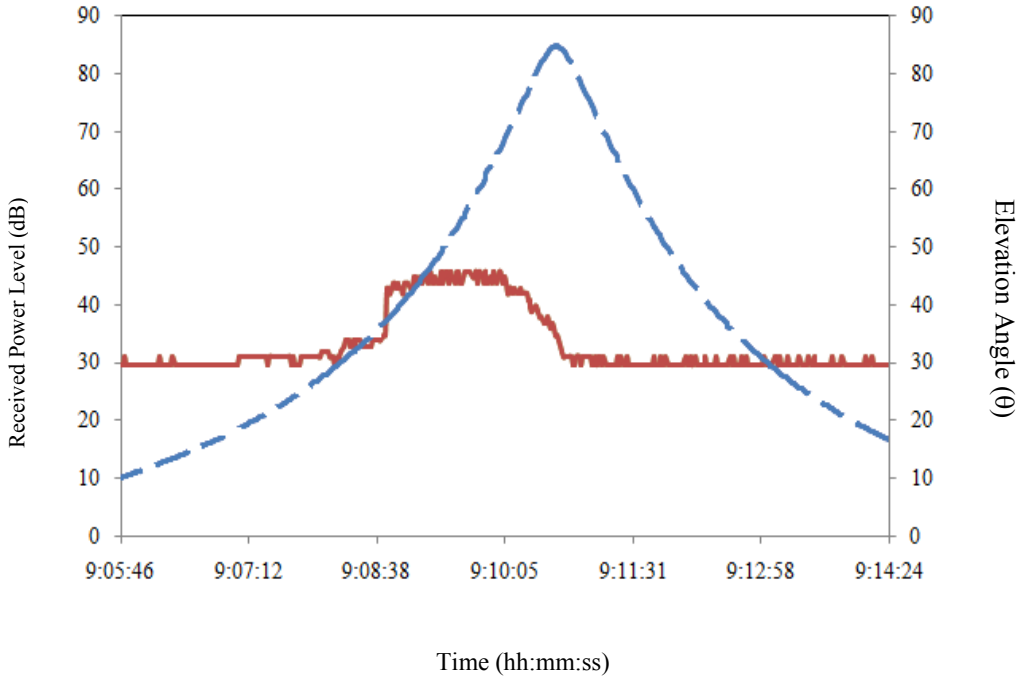

Figure 4.2: RazakSAT Received Power (-) and Elevation Angle (- -) During Clear Sky Condition

In this study, rain attenuation is indeed the difference between the received power during clear sky and rain events. Subsequently, the attenuation from all the events can be measured and compared to the attenuation prediction values of ITU-R and other prediction models for tropical region. Figure 4.3shows an example of the rain attenuation during rain eventson 21/7/2009. All the rain attenuations during RazakSAT X-band operation were compared to the TDWR radar data from MMD at the same location, date and time. The findings are presented in the next Chapter.

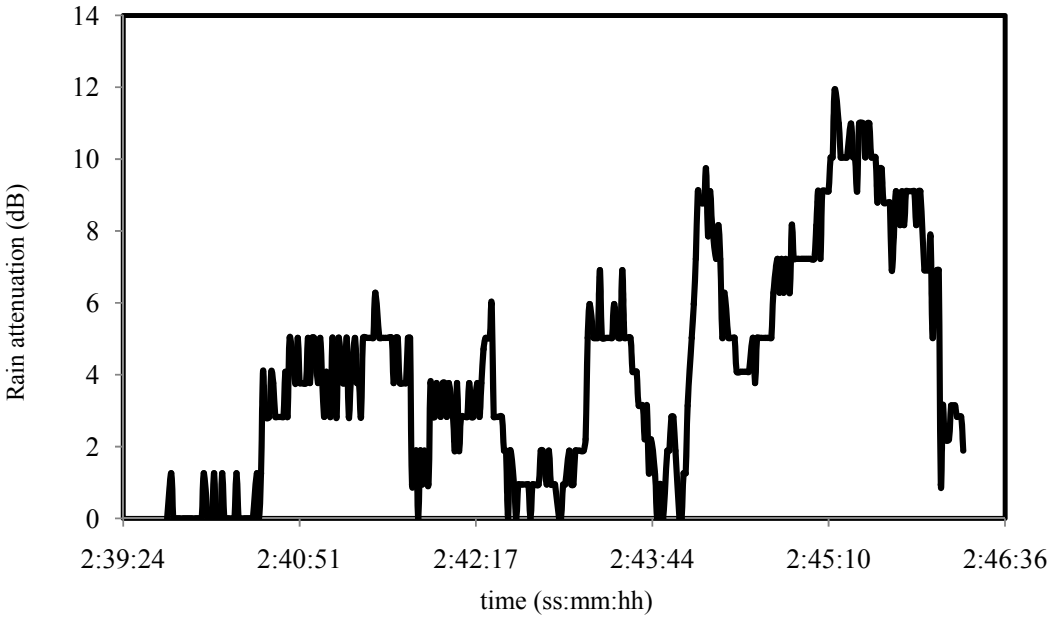

Figure 4.3: Power Level Differences Showing the Rain Attenuation on 21/7/2009 at 2:39:24 - 2:46:36

The convective rain and stratiform rain during the transmission can be observedin Figure 4.4 and 4.5 respectively. The results clearly show that convective rain inflictshigher rain attenuationthan thatof stratiform rain.The values areprovided in Table 4.1. The type of rain was validated using rain gauge and radar data information. The detailsarefurther explained in Chapter 5.

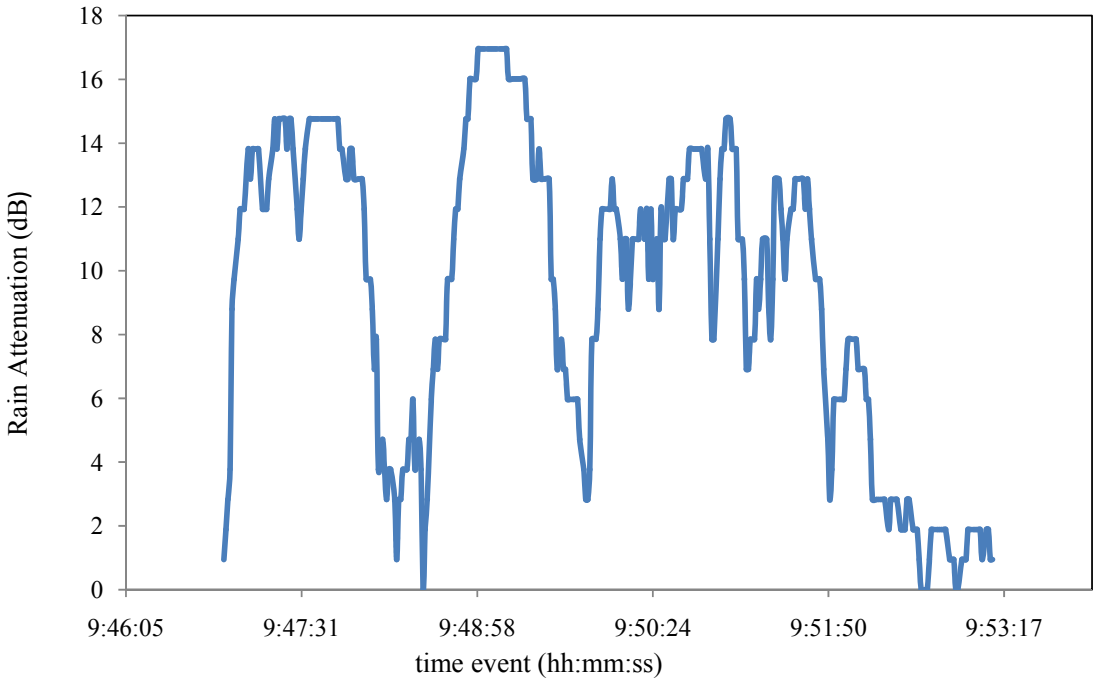

Figure 4.4: Convective RainAttenuation on 24/8/2009 from Satellite Data

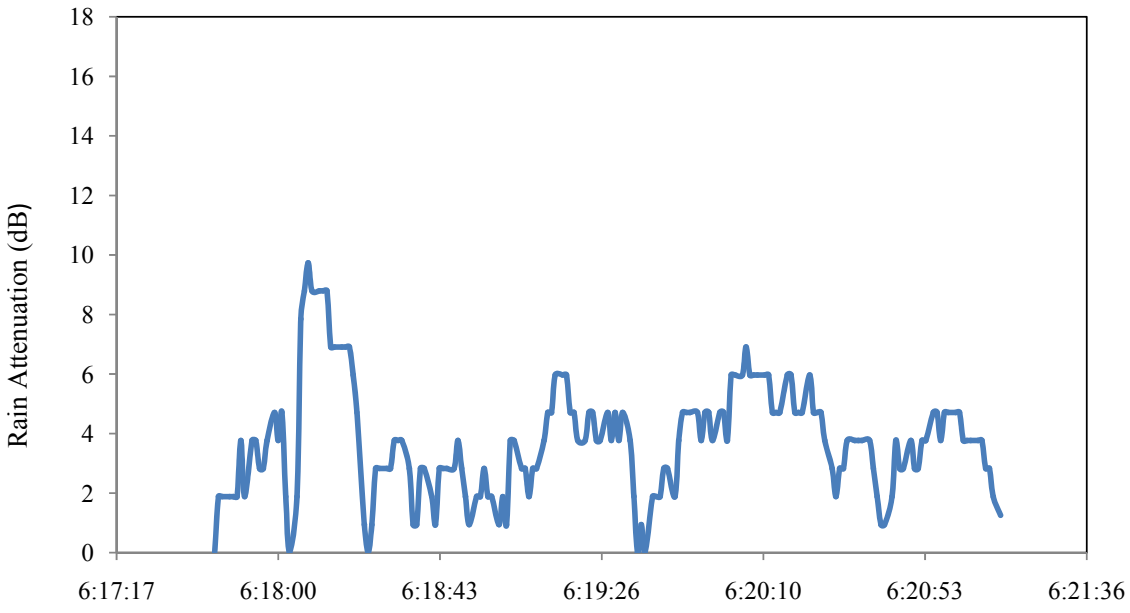

Figure 4.5: Stratiform RainAttenuation on 12/8/2009 using Satellite Data

Table 4.1: Comparisons of Convective and Statiform Rain Attenuation from RazakSAT Data on 21/7/2009

Elevation Angleθ, (°)	Stratiform Rain Attenuation (dB)	Convective Rain Attenuation (dB)
5	9.73	16.01
10	8.79	14.76
20	7.85	13.82
30	6.91	12.87
40	5.97	11.93
50	3.77	9.73
60	2.83	8.79
70	1.88	7.85
80	1.26	6.91
90	0.94	4.71

4.3 The Slant Range for Ground Stations of Near EquatorialOrbiting (NEqO) Satellites

Thetheoretical and empirical slant range, *d*and its Free Space Path Loss (FSPL) calculation on 28/07/ 2009 (clear sky condition) based on different elevation angle is shown in Table 4.2.Figure 4.6 shows the slant path differences between empirical and theoretical values and the correction factor. Figure 4.7 shows the FSPL for RazakSAT link; theoretical and empirical values for slant path range. The variation of the theoretical and empirical values show that the variation is higher for high elevation angle, therefore mindful calculation should be considered for higher elevation angle especially in tropical countries. Figure 4.8 shows the illustration of the satellite to ground station visibility at different angle.

The range under the lowest elevation angle representing the radius of the circle of an ideal horizon plane seen from the ground station. This is also signifies the worst link budget case, since that range represents the maximal possible distance between the ground station and the satellite. More power is required to overcome longer

distance. Thus, a tradeoff should be applied, in order to optimize the required transmit power and the designed horizon plane. The ideal horizon planes of ground stations dedicated to communicate with NEqO satellites of attitudes from (600 - 1200) km may be considered as ideal flat circles with diameter from 5660 km to 8176 km. Within these horizon planes the communication can be locked between the NEqO satellites and appropriate ground stations.

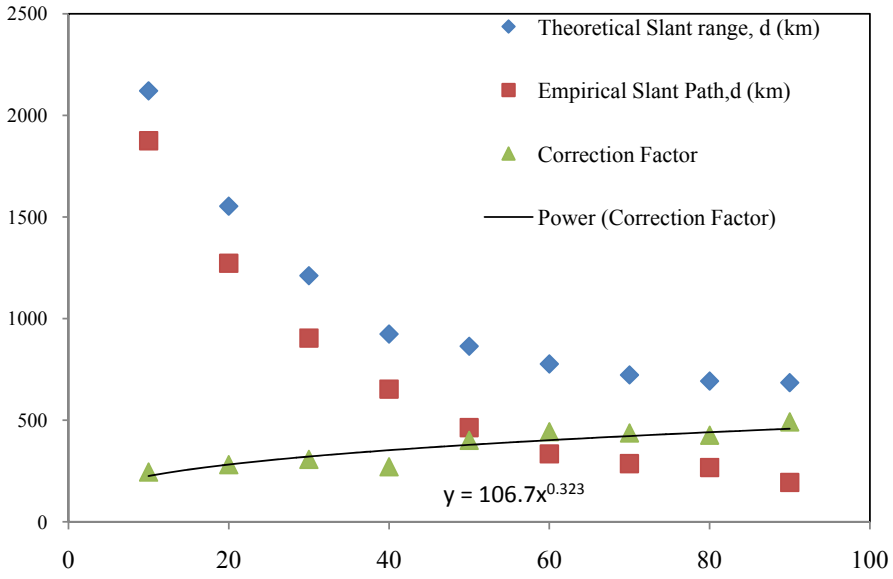

Figure 4.6: Theoretical and Empirical Slant Range, *d*Associated with theCorrection Factor.

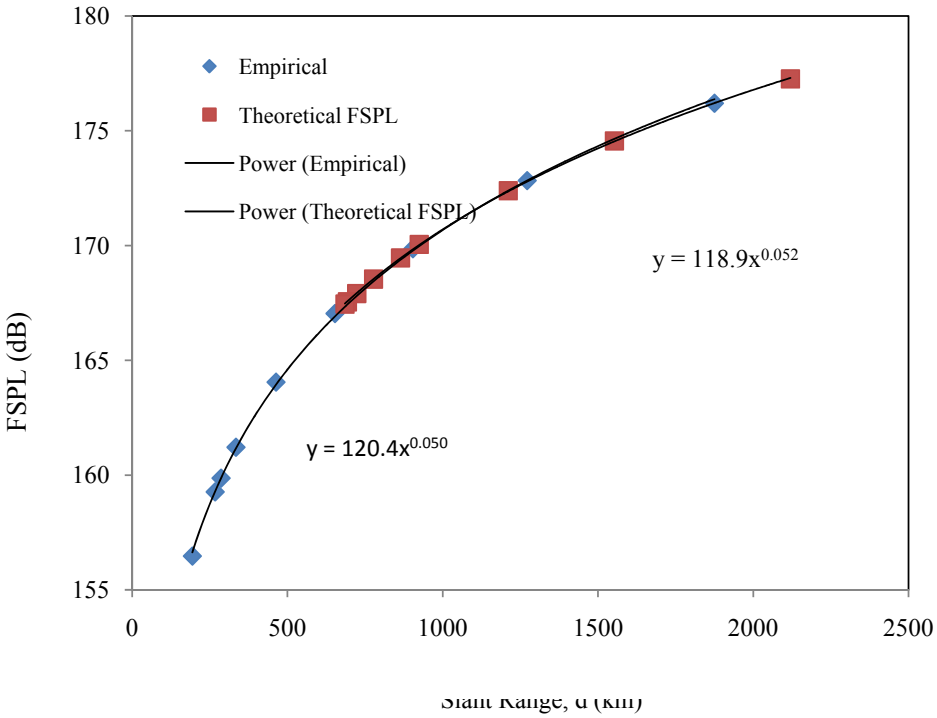

Figure 4.7: Theoretical and Empirical FSPL for RazakSAT Link at 8.21 GHz

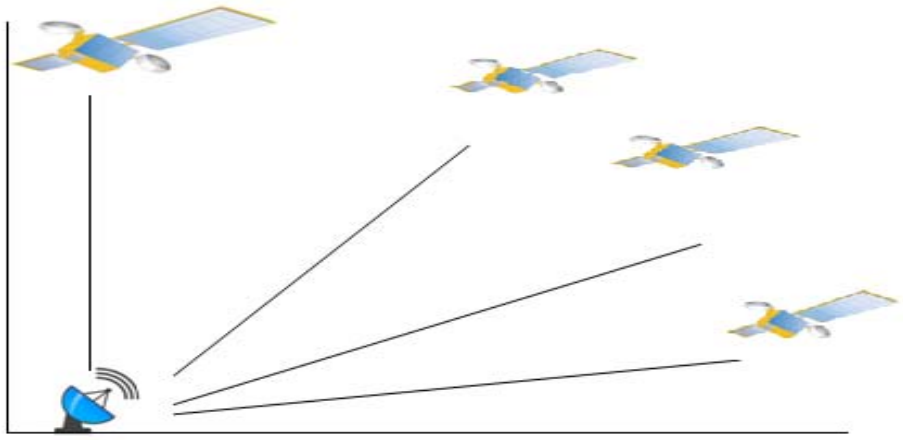

Figure 4.8: Illustration of Satellite to Ground Station Visibility at Different Angle

Communication duration will depend on maximal elevation of satellite's path above the respective horizon plane. Considering above analysis, the communication duration between NEqO satellites and the appropriate ground station usually takes (5 - 20) minutes, few times (6 - 8) during the day. Due to extremely short visible duration, this makes it necessary to determine the horizontalplane as precondition of optimized communication (data download) between the NEqO satellite and respective ground station.

Table 4.2: Theoretical and Empirical Slant Path Range and Free Space Propagation Loss Estimation

Elevation Angle, θ	Theoretical Slant range, d (km)	Empirical Slant Path, *d* (km)	Theoretical FSPL (dB)	Empirical FSPL (dB)	FSPL Variation
10	2120	1875	177.26	175.87	1.39
20	1553	1272	174.56	170.634	3.926
30	1211	904	172.39	168.46	3.93
40	924	653	170.05	164.88	5.17
50	864	463	169.46	162.35	7.11
60	777	434	168.54	161.52	7.02
70	723	386	167.91	159.86	8.05
80	693	367	167.55	159.27	8.28
90	685	295	167.45	156.47	10.98

4.4 Summary

After processing the available RazakSAT data, the number of rainy days was detected of 62 days and the numbers of rainy events are 181 events. Among these events, 46 days were convective rain and 136 days were stratiformrain. The preliminary determination of correction factor for the slant path is suggested to be $d_{cr}=106.7\theta^{0.323}$ to be included in the calculation of the slant range depended on the elevation angle.The Earth-satellite transmission link performance is strongly dependent on the precipitation characteristics along the slant path and affects the system performance significantly depends on the slant range and elevation angle.

CHAPTER FIVE

DEVELOPMENT OF RAIN ATTENUATION PREDICTION TECHNIQUE USING RADAR DATA

5.1 Introduction

The knowledge of rain fade level at a specific frequency of operation is critical for the design of a reliable terrestrial and/or Earth-space communication link.Development of a dedicated Earth to space communication link exclusively for the purpose of propagation research, can be indeed very expensive. One of the possible strategies in identifying the likely attenuation due to rain is by acquiring the detailed statistical descriptions in terms of its horizontal and vertical structure. Observation data generated by a radar operating in volume-scan surveillance mode can be used in the rain attenuation estimation. This is because the data offer spatial and temporal information relating to the precipitation process. The information provided by the radar can play important roles in the estimation of the rain-induced propagation effects (Rinehart 1991). Radar reflectivity values therefore becomean attractive alternativefor rain attenuation estimation.

5.2 Selection of Z-R Relation

In the study of radar meteorology, the accurate determination of the rainfall rate from the measured reflectivity is extremely critical. The *Z-R* relation associates the value of the measured reflectivity to the value of the rainfall rate. Rainfall rate (*R*) can be defined as the rate of increase of depth of water measured in mm/hour. Over the years,

several different *Z-R*relationships had been developed and proposed. These are mostly empirical models that were developed using co-located and simultaneous rainfall rate measurements and radar reflectivity measurements. There has been significant variability in the suggested models (Battan, 1973;Doviak and Zrnic, 1993). It has been highlighted that the Z-R relation are site-specific and that they do not apply universally to different locations around the world(Savageot, 1992;Marshal and Palmer, 1948). Pioneer investigator such as Marshall and Palmer published their *Z-R* relation with a set of generic parameters of a= 200 and b = 1.6. The succeeding researcher(Battan, 1973) on the other hand, presented a list with 69 different *Z-R* relations for different climatic conditions in various parts of the world. In the past, research work was carried out in the attempt to improve the applicability of *Z-R* relations by classifying the rain into different types(Tokay and David, 1995). In the interest of this work, several *Z-R* relationships claimed to be applicable for tropical climate have been taken into consideration and analyzed. Ladd et al.(1997) and Ismail (2001)proposed *Z-R* relations for tropical climate using data acquired from Papua New Guinea. Wilson and Tan (Wilson & Tan, 2001)used radar data and distrometer data to derive the *Z-R* relations for Singapore. Kumar et al. (2011), later in 2011 proposed a revised general *Z-R* relation for Singapore. Table 5.1 shows the parameters of selected *Z-R* relations identified from literature review. Yeo et al. (2012) highlight that RMS error between beacon measurement and the radar estimated attenuation using Z-R relation that was proposed by Kumar et al.(2011) has the smallest value when compare to that of others. Due to climate similarity and close proximity between Singapore and the location of interest (about 358 km), the *Z-R* relation proposed by Kumar et al.(2011) was adopted in this study.

Table 5.1: *Z-R*Relation Parameters

	Convective		Stratiform	
	a	*b*	*a*	*b*
Singapore (Kumar, et al. 2011)	285	1.33	285	1.33
Singapore (Wilson and Tan, 2001)	139	1.50	330	1.35
Papua New Guinea (Ismail, 2001)	281	1.31	296	1.38
Papua New Guinea (Ladd et al. 1997)	93	1.36	132	1.36
Kalingamari (Tokay and David,1995)	139	1.43	367	1.30
Ottawa (Marshal and Palmer, 1948)	200	1.6	200	1.6

5.3 Technique to Estimate Rain Attenuation on an Earth-Satellite link

One year full volumetric radar echoes reflectivity data of 2009 were exploited in the development of rain attenuation approximation technique per event basis. The procedure or technique that can be used to estimate the rain attenuation are explained below;

Step 1:

Raw radar data for the specific time range and location of interest have to be acquired. In this study, relevant data were ingested using the IRIS software. The rainy conditions were confirmed using the rain gauge installed at the KLIA.All dates and times where rain gauge data with values of more than 0.1 mm/hr were inspected. Figure 5.1 showslocation map of relevant sites that had been analyzed, involvingthe KLIA radar station and the ANGKASAground station. Bearing and distance were calculated using the latitude and the longitude of the two places.

ANGKA

Figure 5.1: Location Map of the KLIA Radar and the Ground Station of the Satellite

Step 2:

In order to determine the rain attenuation of the satellite path, the associated satellite path route needs to be drawn on the Plan Position Indicator (PPI)display. In this study, the azimuth angle,ϕ from the ground station to the satellite depicted in horizontal view (PPI) is shown in Figure 5.2. The cross section of the satellite path on vertical plane or known as Range Height Indicator(RHI) has to be generated in order to distinguish the rainfall rate features. The RHI display can be analysed to extract the rain's characteristics where the yellow and orange colour indicates heavy rainfall or convective rain. The green or blue colour implies light or stratiform rain. The image of the cross section of the satellite path (RHI) mentionedin Figure 5.2 is shown in Figure 5.3.

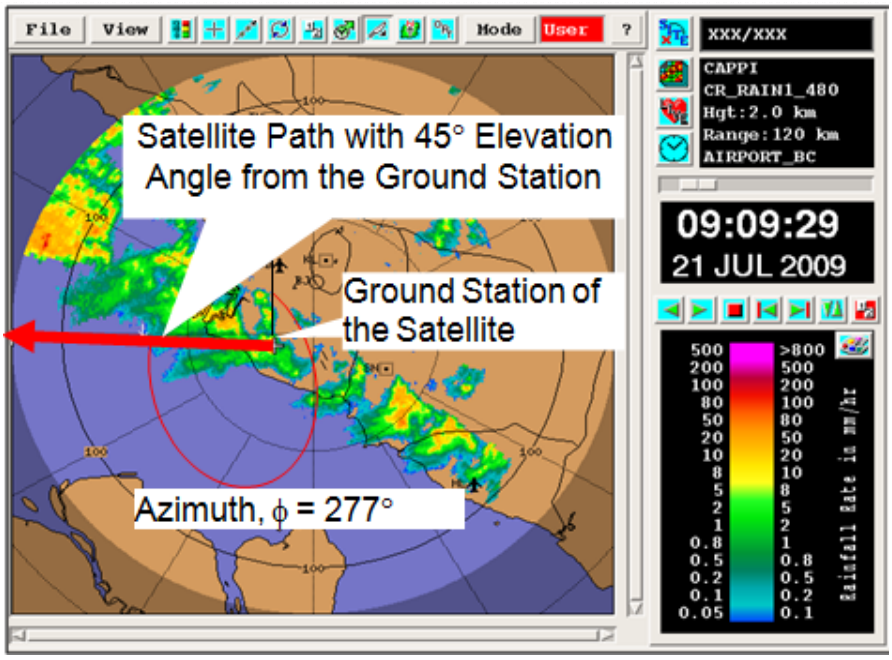

Figure 5.2: Ground Station Location, Satellite Path Link and Azimuth Angle from the Ground Station to the Satellite

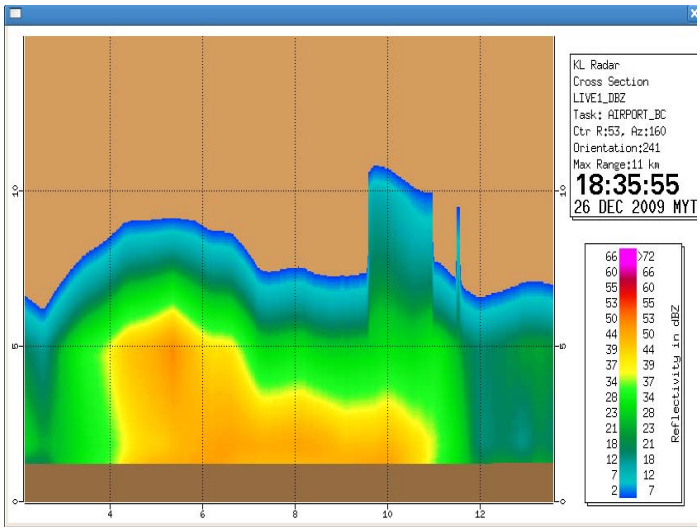

Figure 5.3: Example of the RHI Image of the Satellite Path at the Specified Time and Angle Based on the RazakSAT Databases

Step 3:

The values of the height from the ground, *z* azimuth angle,ϕ and the distance, *x* and *y* from the ground station is required in the estimation technique. The x and y values can be obtained based on the latitude and the longitude values using the 'Haversian' formula to calculate the great-circle distance between two points. The technique adapted from Mohr and Vaughan (Mohr and Vaughn, 1979) to estimate the equivalent radar reflectivity data in an orthogonal coordinate systems can be used in the application to calculate the rain attenuation for the Earth-Satellite link. The desired Cartesian coordinate system (*x, y, z)*can be defined and converted into effective path length, L_e, elevation angle, θ, and azimuth angle, ϕ according to the relations;

$$L_{e=\sqrt{x^2+y^2+z^2}} \tag{5.1}$$

$$\phi = tan^{-1}\frac{x}{y} \tag{5.2}$$

where the satellite ground station is at the origin. Figure 5.4 shows the Cartesian coordinates with reference to the Earth-satellite link. Standard adjustment had been made in the calculation of the elevation angle,θ to take into account the Earth's curvature and beam refraction (Mohr and Vaughn, 1979). The height of a given point (*x*,*y*,*z*) above the perceived horizon, z_h can be computed using (5.3);

$$z_h = z - \frac{x^2-y^2}{iD} \tag{5.3}$$

where i is the standard compensating factor (1.33) for beam refraction in the troposphere and D is the diameter of the Earth ≅ 12 756.2 km. The elevation angle, θcan be then computed as;

$$\theta = sin^{-1}\frac{z_h}{L_e} \tag{5.4}$$

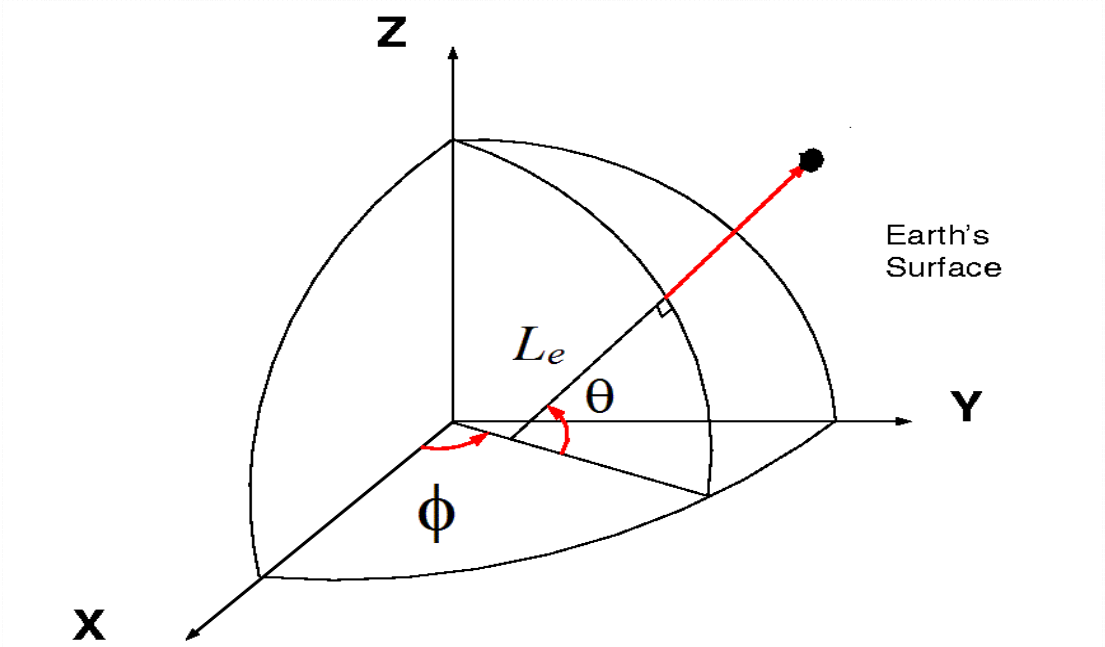

Figure 5.4. The Structure of the Earth-Satellite Link Projected to Cartesian Coordinate to Assist the Radar Data Estimation.

Step 4:

In this analysis, after the production of the cross-section, based on the coordinate, the subsequent product by IRIS software identified as "productx" was generated. Productx displays the data in 1-byte reflectivity format. Productx was generated from radar reflectivity values derived from pixels of the cross-section views. Typical colour bar in the PPI and RHI comprises of only 16 levels. Productx on

the other hand, is capable of providing the actual reflectivity values for each range bin without involving any interpolation. For the analysis involved, the bin size is 119 m x 23.8 m determined by the IRIS software shown in the productx. Once the productx along the satellite path was generated, the actual *dBZ* value in each range bin for the cross-section product was further processed.

Step 5:

The relevant bin has to be identified and analyzed accordingly. Figure 5.5 shows the selected event with satellite path link at 45° elevation angle from the ground station viewed in the cross-section scan form. Figure 5.6shows the "zoomed out" productx's reflectivity values that originate from the red square of Figure 5.5 (a small fraction of the total path). The shadowed area shows the relevant satellite path length. The relevant range bins depend on the elevation angle of the satellite path link as shown in both figures.

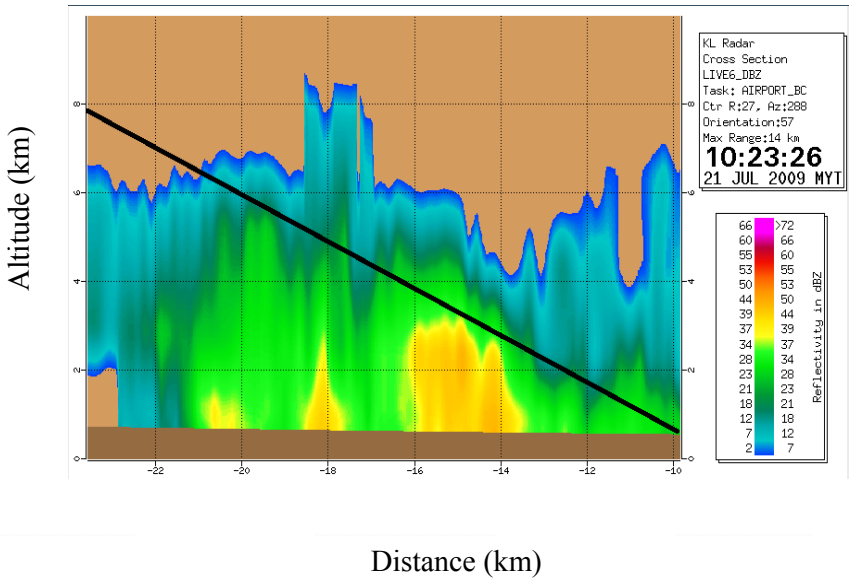

Figure 5.5: Satellite Path Link Previewed in XSECT Product at 45° Elevation Angle from the Satellite Ground Station

29	29	30	31	32	32	32	32	32
29	29	29	30	31	32	32	32	31
28	28	29	30	31	31	31	31	31
27	27	28	29	30	31	31	31	30
27	27	28	29	30	30	30	30	30
26	26	27	28	29	30	30	30	29
25	26	27	28	29	29	29	29	29
25	26	26	27	28	29	29	29	28

Figure 5.6:' productx' Derived dBZ for Reflectivity Values from XSECT Product

Step 6:

The reflectivity values (in dBZ) can be then converted to rainfall rate according to theselected *Z-R* relationship. In this investigation, the *Z-R* relation

proposed by Kumar *et al.* (2011) was adopted. The *Z-R* relation uses a set of parameters of a = 285 and b = 1.33 for both convective and stratiform events. By rearranging the formulation, the value of the rainfall rate was inferred from the value of the measured reflectivity as in Equation (5.5);

$$R = \sqrt[b]{\frac{Z}{a}} \tag{5.5}$$

Larger values of *dBZ* typically correspond to heavier rain from more intense thunderstorms, while small values correspond to light rain from shallow clouds.

Step 7:

Once the rainfall rate was calculated, the specific rain attenuation, γ_i(dB/km) for each specific range bin (i^{th}) can be then determined using the Equation (5.6);

$$\gamma_i = kR_i^{\alpha} \tag{5.6}$$

where R_i is the rainfall rate at the indicated bin and the coefficients of k and α, were obtained from the ITU-R Rec. P.838–3 (2012) and are dependent on the link elevation angle (θ), the radiowave frequency and the polarization tilt angle relative to the horizontal (τ) as shown;

$$k = [k_H + k_V + (k_H - k_V)cos^2\theta \cos 2\tau]/2 \tag{5.7}$$

$$\alpha = [k_H\alpha_H + k_V\alpha_V + (k_H\alpha_H - k_V\alpha_V)cos^2\theta \cos 2\tau]/2k \tag{5.8}$$

where the constants for the coefficient k_H for horizontal polarization, k_V for vertical polarization, α_H for horizontal polarization, and α_V for vertical polarization are given in (ITU-R P.838-3, 2012). Table 5.3 lists the value suggested by ITU-R Rec. P.838–3

for the RazakSAT link at 8.21 GHz. The conversion of rain rate into specific attenuation is carried out using the customary power-law relationships. The *k* and α coefficients do not only rely on frequency, polarization and link elevation, but also on the Drop Size Distribution (DSD). Kumar et al. (2009) suggested that truncated gamma DSD model is more appropriate for tropical region based on campaign carried out in Singapore. The use of ITU-R derived coefficients in the proposed technique is indeed in contrast with the employment of the Z-R relationship derived by Kumar et al. (2009), because the two equations were obtained from different DSD. Exhaustive search have been carried out and yet no derivation of *k* and α for tropical region for truncated gamma DSD can be found. Therefore, ITU parameters were adopted.

Table 5.3: ITU-R Rec. P838-3 Suggested Values for *k* and α

Frequency(GHz)	**8.21**
k_H	0.00412
α_H	1.39050
k_V	0.00345
α_V	1.37970

The rain attenuation for each range bin A_i(dB) can be calculated by using;

$$A_i = \gamma_i L_{ei} \tag{5.9}$$

where L_{ei} is the affected path length within the range bins. L_{ei} is calculated based on the elevation angle (θ) from the Earth station to the satellite location for each bin. Therefore L_{ei}(in km) for each bin is equal to:

$$L_{ei} = \frac{0.0238}{\sin(\theta)} = \csc(\theta) * 0.0238 \tag{5.10}$$

Figure 5.7shows the elevation angle affecting the bin's path length in the case of MMD radar bin.

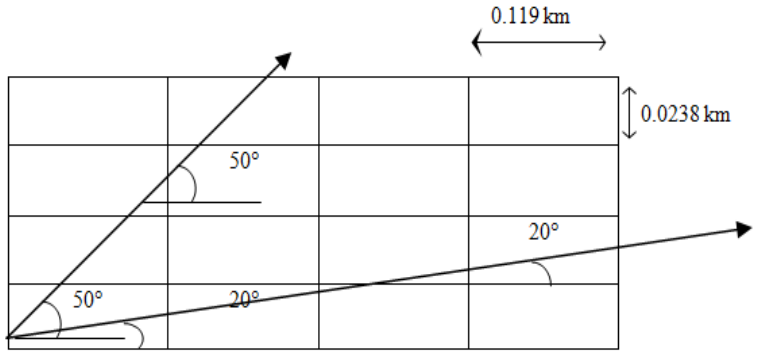

Figure 5.7: The Bin's Angle Configuration to Calculate the Effective Path Length, L_{ei}

The total rain attenuation along the slant path, A_{total}can then calculated through the numerically summation of (5.9);

$$A_{total} = \sum_{i=0}^{n} A_i \tag{5.11}$$

Where *i* is the bin's number that was affected by rain and *n* is the total number of bins based on the elevation angle. Therefore, the total attenuation of a particular link were estimated. Table 5.4 shows the conversion of values involved in the investigation on 28/8/2009.

Table 5.4: Radar Derived Attenuation Example for Each Bin at 20° and 50°Elevation Angle

Bin No.	Reflectivity (dBz)	Rainfall Rate, R (mm/hr)	Specific Attenuation, γfrom RazakSAT data (dB/km)	L_{ei} for each bin at 20° Elevation Angle	Attenuation per bin for 20° Elevation Angle	L_{ei} for each bin at 50°Elevation Angle	Attenuation per bin for 50° Elevation Angle
1	45	34.491	0.301	0.070	0.040	0.031	0.018
2	43	24.397	0.282	0.070	0.025	0.031	0.011
3	40	14.51	0.265	0.070	0.012	0.031	0.005
4	41	17.25	0.249	0.070	0.015	0.031	0.007
…	…	…	…	…	…		…
...	….	…	…	...	…	NA	NA
300	42	20.51	0.322	0.070	0.019	NA	NA
Total Attenuation (dB)					2.87		1.27

5.5 Classification of Rain Events

The radar data from KLIA radar station during the year2009were classified into two groups namely stratiform and convective. Previous studies (Tokay and Short, 1996; Ladd et al. 1997) also utilise these two rain classifications. Figures 5.10 – 5.11 below depict time series displays of *Z* vertical scan recorded on selected days during stratiform events within the period of campaign.The melting layers are the transition regions between snow and rain. They usually start at the 0° C and finish a few degrees above 0° C where the entire snow particles melted and become raindrops. Examples of convective events can be observed in figures labelled as Figure 5.12 - 5.13. Even though the radar reflectivity measurements do not exhibit existence of a melting layer, such enhancement can be seen in the cross-polar reflectivity that indicative of the melting process. Based on the one year radar data, the radar scans were inspected and rain events were identified and recorded. After all events were scanned and viewed using the MMD radar data, the rain types can be classified easily based on the criteria given by (Daset al.2009; Badron et al.2013; Zafar, 2004). Table 5.6 summarize the criteria to classify the rain type.

Table 5.6: Criteria to Differentiate Rain Types Using Radar Data

Stratiform	Convective
1. Reflectivity Ranges (2 - 37dBz)	1. Reflectivity Ranges > 38 dBz)
2. Rainfall Intensity Values (0 - 9.9 mm/hr)	2. Rainfall Intensity Values (>10 mm/hr)
3. Clear Melting Height	3. No Melting Height
4. Rain height between 4 -5 km	4. Rain height > 6 km
5. Slow differences in vertical profile	5. Rapid increase in vertical profile
6. Bright band height for each bin has to be approximated within the same height of the neighbouring bins.	6. Bright band height for each bin is extremely different with theneighbouring bins.
7. Low values of reflectivity gradient	7. High values of reflectivity gradient

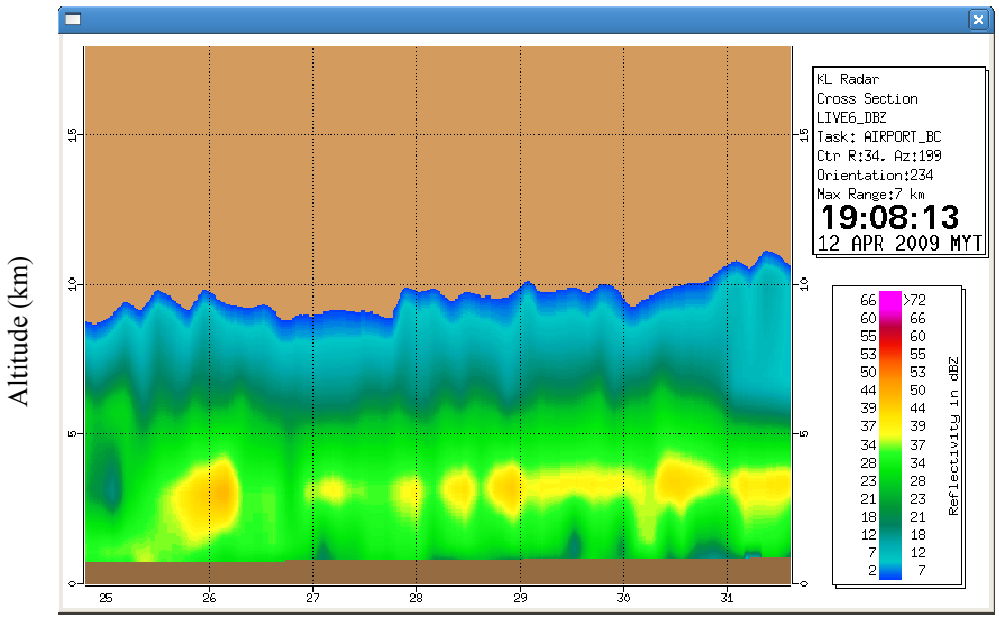

Figure 5.10: Stratiform Event on 12/4/2009 at 19:08:13

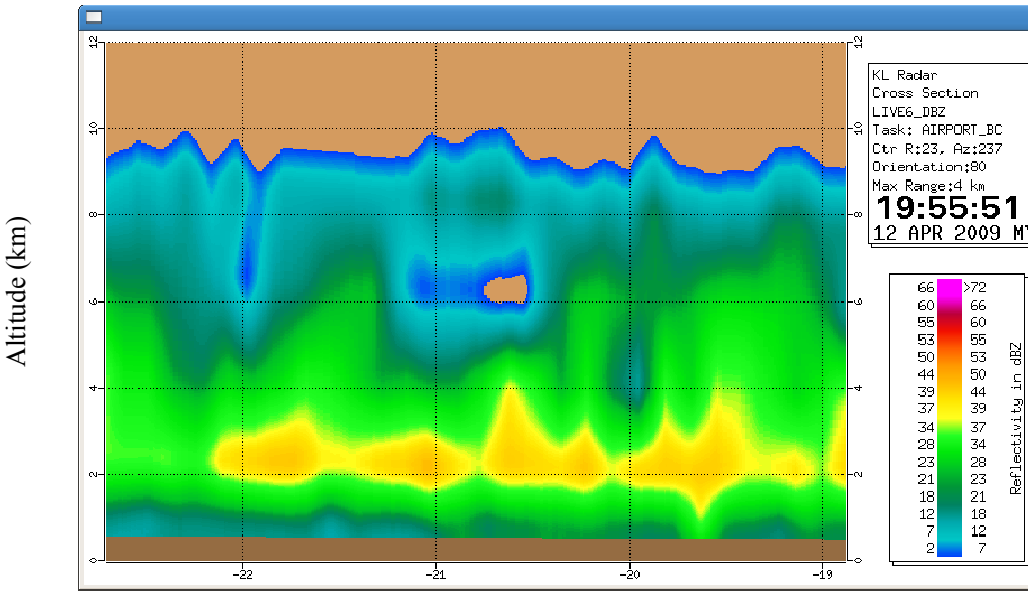

Figure 5.11: Stratiform Event on 12/4/2009 on 19:55:51

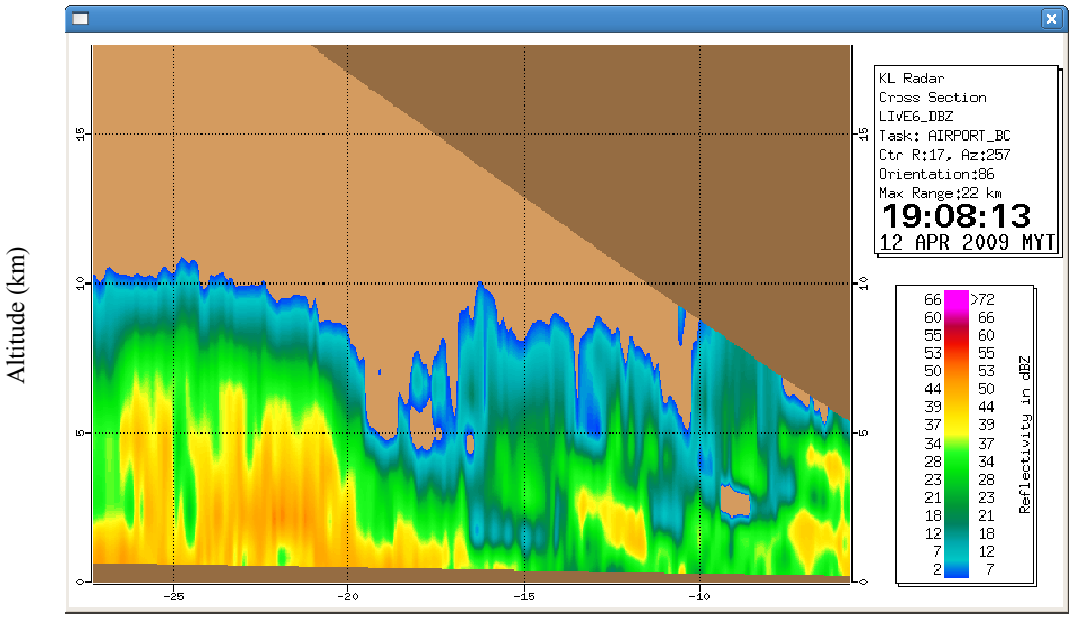

Figure 5.12: Convective Event on 12/04/2009 on 19:08:13

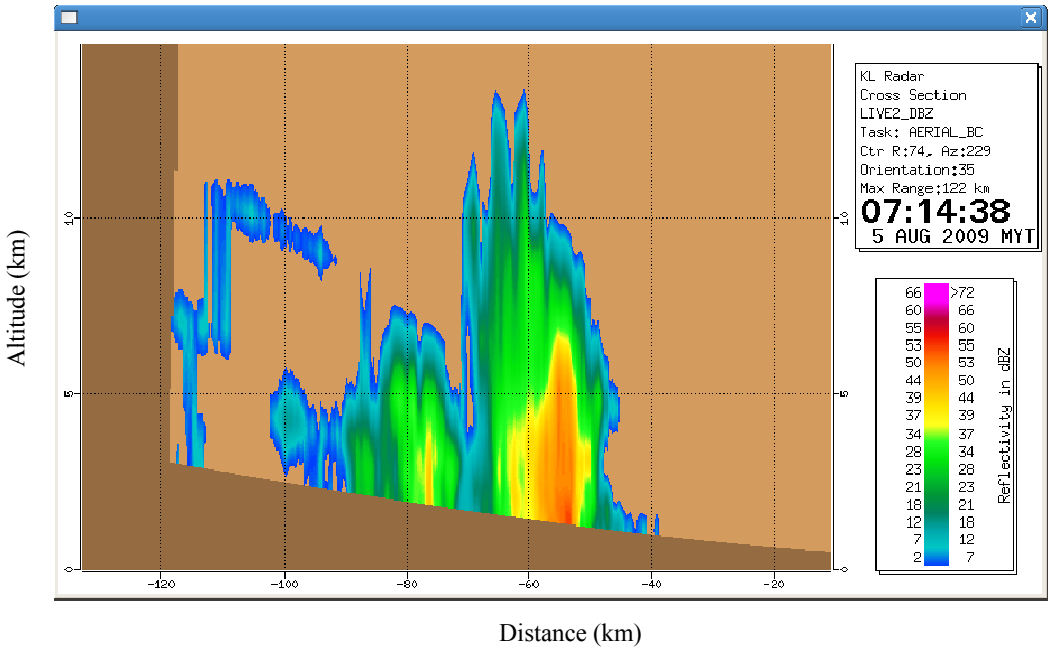

Figure 5.13: Convective Event on 05/8/2009 at 07:14:38

Radar reflectivity, dBZ acquired fromthe radar range-height indicator (RHI) scans have been exploited to derive the attenuation in both the stratiform and convective rain events. The results regarding the types of rain also has been studied and classified. Table 5.7 shows an example of the link measurements for stratiform and convective rain. As results, there are 134 rainy days with total of 308 of rain events. From these events, 73.4% of rains are classified as stratiform and 26.6% are classified as convective.

Table 5.7:Radar Estimated ValueCompared with RazakSAT Link for Rain Attenuations

Events	Path Length (km)	Rain height (km)	Spec. Atten.,γ (dB/ km)	Est Att using radar data (dB)	RazakSAT link attenuation measurement (dB)
Strat	80.16	5.2	0.032	2.56	2.86
Conv	30.37	7.8	0.37	11.14	15.88

5.6 Vertical Profile Reflectivity (VPR) for Convective and Stratiform Rain

It is possible to investigate the exact height of the bright-band using radar measurements.Theoretical step is to detect the height where the melting process happens, which means the height of bright-band. Figure 5.14and5.15 show vertical profile plots during stratiform and convective rain events. Reflectivity profiles in each rain classification seem to have a linear characteristic with height and after applying the regression method; straight lines such plotted on each figure can be approximated with equation:

$$Z = mh + c \qquad (5.14)$$

where Z is given in dB, h in km and m and c are the linear coefficients. The starting height for each range is the height defined by the minimum height of about 416 m not affected by the ground clutter.

Table 5.8: Melting Layer Height for Convective and Stratiform

	Stratiform	Convective
Detected Upper Limits Cloud (km)	4.5	10.2
Melting Layer -Top (km)	8.2	6.2
Melting Layer -Bottom (km)	2.4	3.8

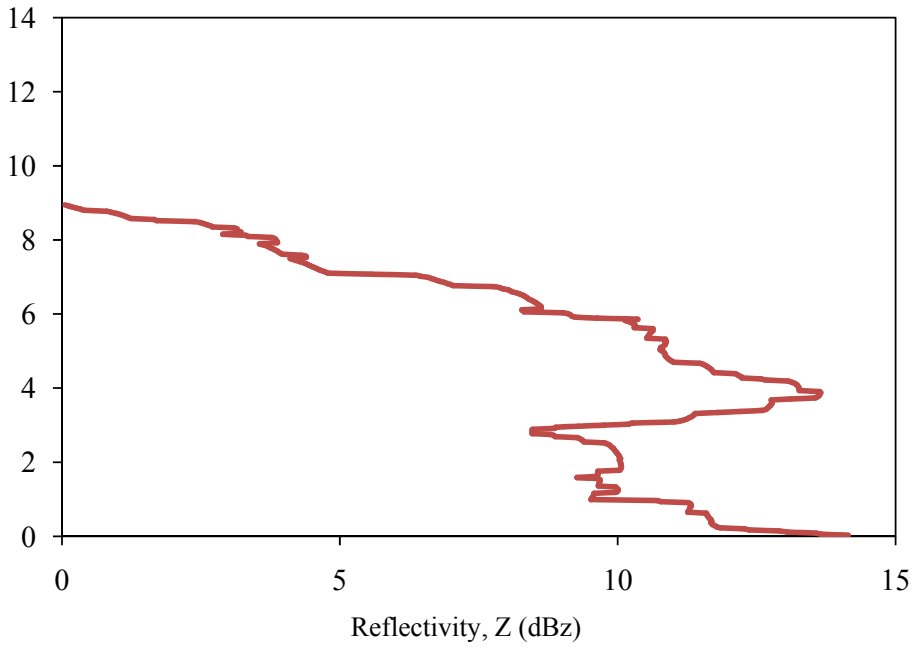

Fig. 5.14: Vertical Reflectivity Profile during a Stratiform Event

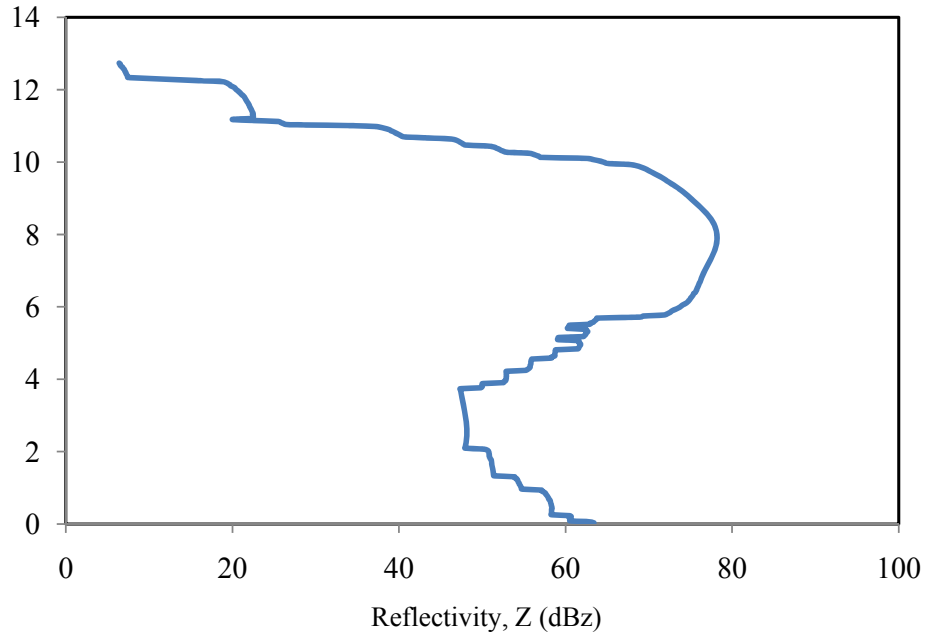

Fig. 5.15: Vertical Reflectivity Profile during a Convective Event

5.7 Summary

It is proved that radar information has the potential to be a reliable technique to estimate the rain attenuation for Earth-satellite link. Comparisons with the satellite link measurements have shown indication that radar reflectivity values can be exploited as an estimator for rain attenuation. Radar is able to provide rainfall spatial information where it is simply not possible by just using rain gauges. The values of the rainfall rate from the radar reflectivity can be estimated at an instantaneous point along the slant path. With the assimilation of the radar reflectivity, appropriate *Z-R* relation and befitting specific attenuation relation, it is suggested that the likely attenuation during convective rain and/or stratiform rain events at any location and time can be predicted. This is important since such rain events are recurrent in tropical regions like Malaysia.The variation of reflectivity with height has been characterised

by taking into account the vertical structure of precipitation in detail. From the studies it can be recommended that the rain height recommendation is about 6.2 km for stratiform and 10.2 km for convective rain in tropical countries.From the analysis presented in this chapter, it is noted that the improvements in rain attenuation estimation technique using radar data have been discovered and capable of producing better prediction values. The new rain attenuation estimation procedure can be very important for satellite engineers and researchers in the effort of planning realistic link budget estimation and set-up.

CHAPTER SIX

ESTIMATION AND VALIDATION OF RAIN ATTENUATION USING RADAR DATA FOR SATELLITE LINK

6.1 Introduction

In satellite communication terminologies, the link availability is defined as percentage of time in a year when the link will perform as per the link's requirement.Fade margin is a parameter that is used in the design of satellite links to ensure optimal performance of the link. For example, military communication satellite requires 99.99% availability for a year, which translates to link accessibility of 8759.1 hours and an unavailability of 0.876 hours (8760 – 8759.1 hours / 8760 hours x 100). Predictions are employed in order to know whether a satisfactory service can be provided at the reception point or area. Furthermore, these parameters are also used for spectrum allocation to avoid mutual interference with other systems occupying the same frequency band. In this chapter, the cumulative distribution function (CDF) for a satellite link will be derived using radar data. These data can be used for the calculation of the fade margin for the system's best performance.

6.2 Assessment of Specific Attenuation (γ) – Reflectivity (Z) Relationship

The information provided by the radar can play important roles in studying the rain-induced propagation effects. For every radar reflectivity-height *Z(h)* profile measured at S-band, the path attenuation at frequency of interest can be derived using equation as follows (Thurai et al.1995; Eastment et al. 1998):

$$A = \left(\sum_{h=0}^{h_R} \alpha_R Z(h)^{\beta_R} dh \right) + \left(\sum_{h=h_R}^{h_m} \alpha_m Z(h)^{\beta_m} dh \right) \quad (6.1)$$

where *dh* is the height resolution of *Z(h)* profile, in this case, is 23 m. On the other hand,h_R and h_m are the heights of the rain and the melting layer respectively. α_R and β_R are the coefficients required for attenuation scaling to frequency of interest. Finally, α_m and β_m are the corresponding coefficients in the melting layer.

Radar scans of rain event in KLIA radar station were used to characterise the rain type. The rain attenuation distributions were then exploited in deriving the relationship between specific attenuation γ and the radar reflectivity, Z. Using the measured rain attenuation distributions and the appropriate reflectivity values at frequencies of interest, the specific attenuation and the radar reflectivity was calculated at different elevation angles.The specific attenuation and reflectivity calculations were used to develop γ-*Z* model using standard regression analysis. Such model can be applied to estimate the specific attenuation using radar reflectivity from radar scans.The availability of an Earth-satellite link in Malaysia was a great opportunity to find the relationship of the specific attenuation, γ and radar reflectivity, *Z*. The X-band RazakSAT link which was available starting 16th July 2009 to December 2009 have been a good indication for measuring rain attenuation in tropical region. The MMD provided the radar data for the said date and time to measure the reflectivity accordingly. The rain attenuation calculation from the RazakSAT link had been explained in detailed in Chapter 4. The method to measure the reflectivity, Z of the specified link can be carried out by adopting processes explained in Step 1-5 in Chapter 5 subsection 5.3. The total reflectivity, Z_{total}along the slant path was then calculated through the numerical summation;

$$Z_{total} = \sum_{i=0}^{n} Z_i \quad (6.2)$$

Where *i* is the bin's number that was affected by rain and *n* is the total number of bins affected by rain based on the elevation angle. The $Z_{total}$is the reflectivity along the specified satellite path to be compared with the RazakSAT link. The rain attenuation of the RazakSAT link at any elevation angle was tabulated against Z_{total} for all samples. The rain attenuation have to be divided to the affected path length to get the specific attenuation,γ. The comparison enables the deduction for equivalent relationship between γ and Z using the regression analysis. In one radar data of 5-minute sampling time, many readings from different angles can be derived. This is because the RazakSAT received power reading is in every second. These samples were paired between the two information and tabulated. The γ-Z relationship for stratiform and convective rain had been deduced. These two categorized relations are hoped to be able to offer better estimation of rain attenuation compared to single relation. The regression analysis of γ-Z is shown in Figure 6.1 and 6.2. The power law coefficients for the best-fit relationships are included in Table 6.1.Two parallel lines are obtained in each figure, which intercept the best-fit line. The power law coefficients for the best-fit relationships are included in Table 6.1.

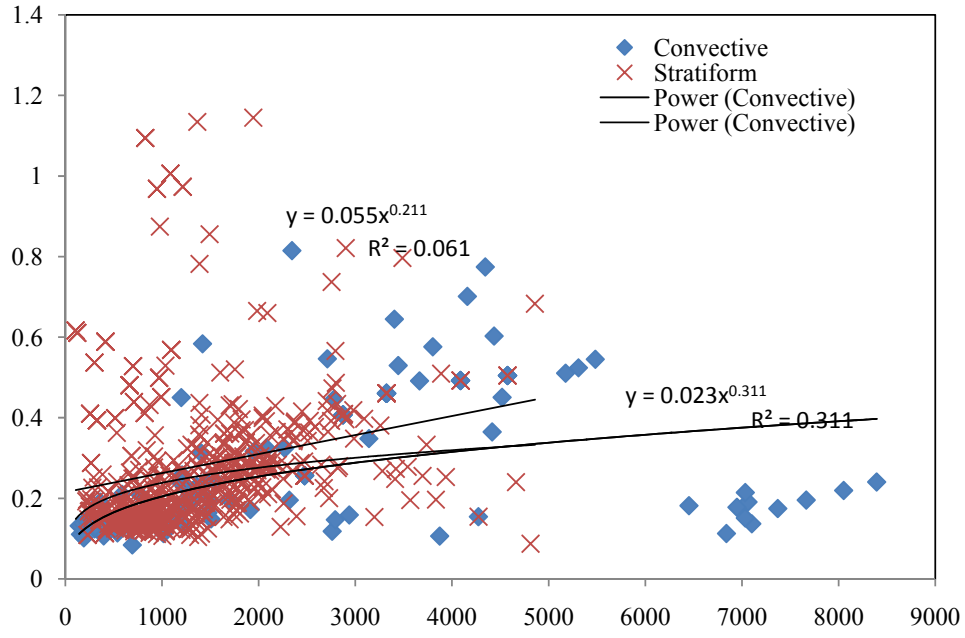

Figure 6.1:Theγ-Z Relationship for Both Convective and Stratiform Events at 8.21GHz

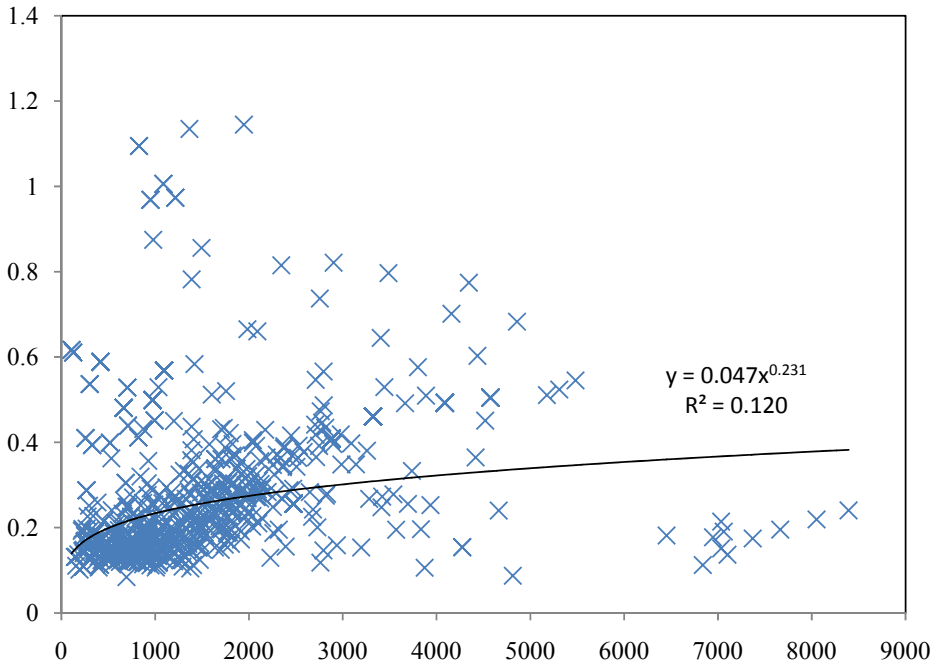

Figure 6.2: Theγ-Z Relationship for Mix Event at 8.21 GHz

Table 6.1: The *a* and *b*Values for the γ-Z Relationships using Power Law Equation

Events	a	b
Stratiform Rain	0.055	0.232
Convective Rain	0.023	0.311
Mix (Convective+ Stratiform)	0.047	0.232

Therefore the γ-Z relationship as obtained in the analysis is equivalent to;

$$\gamma'' = aZ^b \qquad (6.3)$$

Once the relationships were derived, Equation (6.3)can be used in the calculation to predict the attenuation for any link, given the reflectivity, Z. Rain attenuation, *A* is correspondent to;

$$A = \gamma''.\mathrm{Le} \qquad (6.4)$$

where $L_e$is the affected path length.

The newly derived equation of γ-Z is validated by other rainy events. The rain events on 05/10/2009 (Convective Rain Events) at the selected elevation angle as shown in Table 6.2 below and illustrated in Figure 6.3:

Table 6.2: Validation of Newly Derived γ-Z Compared with RazakSAT Rain Attenuation

Elevation Angle	RazakSAT Rain Attenuation	Total Radar Reflectivity	Rain Path Length from RHI	Derived Specific Attenuation from RazakSAT	Rain Attenuation using γ-Z relation (dB)	Variation
10	10.93	7811.00	19.16	0.54	10.25	0.14
20	9.05	7850.50	15.11	0.54	8.11	0.19
30	7.79	7854.50	12.97	0.54	6.96	0.21
40	6.85	7628.00	10.95	0.53	5.79	0.26
50	5.91	5688.00	9.76	0.46	4.45	0.36
60	4.02	4139.00	8.33	0.39	3.24	0.35
70	2.56	2642.00	5.95	0.31	1.85	0.48

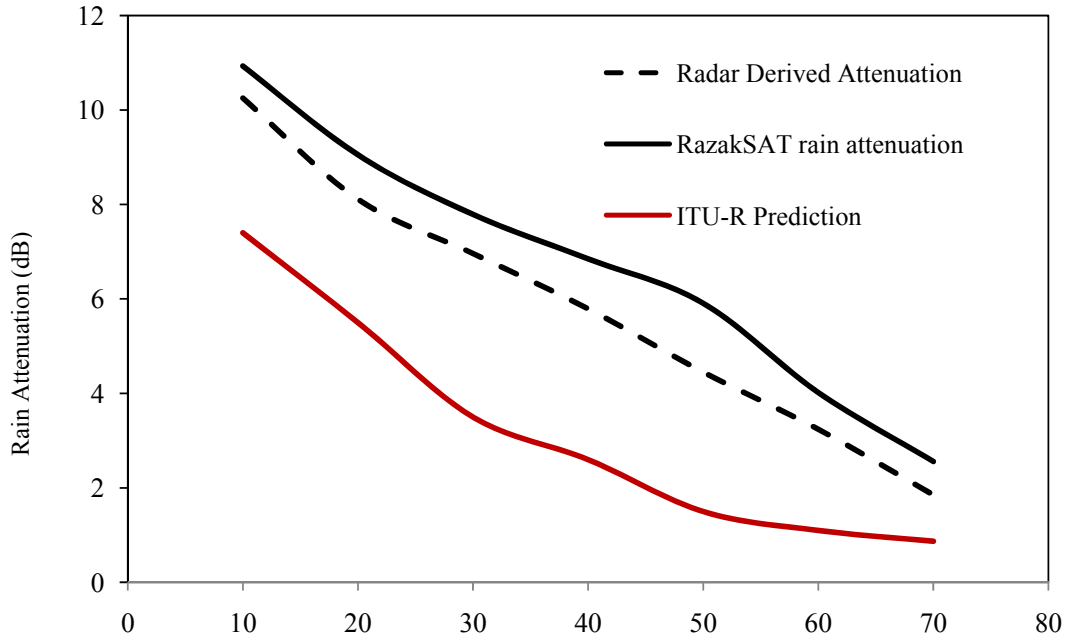

Figure 6.3: X-band Attenuation Prediction from ITU-R Prediction, Radar Derived Estimation and RazakSAT Rain Attenuation.

The newly derived specific attenuation to calculate the rain attenuation from radar information gives small variation as about 0.14% differences compared with ITU-R 618-12 prediction as much as 55% variation for the said events.

6.3 Cumulative Distribution Function Calculation for Techniqueusing Radar Data

The technique to calculate the Cumulative distribution functions(CDF)is described in this section.CDFs are used to specify the distribution of the attenuation level for a given percentage of time. The method to calculate rain attenuation using radar data for Earth-satellite link is described in Chapter 5. The subsequent stepswere used to derive the CDF. Firstly,all attenuation levelswere listed.After that, how many of that level of attenuation occurred is less than or equal to the previous attenuation levelwas calculated. The lower rain attenuation values were added to the next level of rain attenuation values in a cumulative fashion to create the CDF. These numbers of occurrencewere then converted to a percentage time over a year. The CDF of the satellite link, *F(X)* can be expressed as the integral of its probability P(X ≤ x) at each rain attenuation level exist, $p(x_i)$as follow:

$$F(x) = P(X \leq x) = \sum_{x_i \leq x} P(X = x_i) = \sum_{x_i \leq x} p(x_i). \quad (6.5)$$

An integration time of 1-minute is selected by the ITU as a compromise between experimental accuracy and the amount of rainfall data collected. In many countries all over the world, Malaysia included, long-term rain statistics are only available for long integration time of perhaps one hour or more. Since rainfall data at higher than 1-minute integration time are more readily available than 1-minute integration time data,

methods for the conversion of rainfall rate distribution with variable integration time to the equivalent 1-minute would be very helpful. In this study as well, the radar data involved 5 minute integration time and had to be converted to 1-minute integration time. Khairolanuar et al. (2014) suggested a method to convert data with 5-minute integration time to equivalent 1-minute integration time using poly nominal expression as the following:

$$R_1(P)= aR_5(P)^2+bR_5(P)+c \qquad (6.6)$$

where a = 7.8713e^{-4}, b= 0.93176 and c = 1.2345 are empirical constant for 5 minute integration of time. Therefore, to have a better applicability, the 5 minute sampling data is converted to 1 minute sampling data using the Equation (6.6).

The next section will demonstrate how rain fade margin was derived from radar data for X-band and Ku-band.

6.3 Estimations of Fade Margin for Military X-band Satellite Communication Links

The Malaysian Armed Forces (MAF) will be taking a giant leap when it started to operate its own satellite communication to boost the nation's military network's connectivity ("MAF Moves A Step Further With Own Satellite Transponder By 2014", 2013). The satellite communication facility is vital, particularly in ensuring transmission and reception of classified information from other military combat assets, such as fighters and warship. It will also be used specifically to improve the MAF communication capabilities in areas at risk of receiving low communication signals. This is highly useful especially for Unmanned Aerial Vehicle (UAV)

operations, special forces operations and many more. For military communications satellites, the International Telecommunications Union (ITU) has assigned the X band (downlink and uplink frequency band) for sending modulated signals as from 7.25 to 8.4 GHz. However, there are many aspects of X-band that are difficult to realize than of those of at lower frequencies. X-band frequencies certainly have higher atmospheric propagation losses, higher RF losses, and certainly much severe signal degradation due to rain (Allnutt and Peregrinus, 1989). It is would be in the best interest of the satellite designers and engineers alike to accurately appraise the challenges of an X-band SatCom link especially in the case of tropical regions where heavy rains are copious whilst the required technological advancements are in pursuit. Satellite communications (SatCom) can offer rapid establishment of voice and data connectivity. The unique potentials of satellite communications are well suited to fill certain breach of contacts during catastrophic incidents and also in isolated places critical for military operation. Military satellite communication is designed to comprise highly steadfast delivery of voice, data and video services between military headquarters and field units. This sub section highlights an important concern pertaining to the performance predictions of the military X-band satellite communication link especially when facing challenges due to severe rain attenuation in tropical countries. It is proposed that a prediction technique can be employed as well as data acquired from meteorological radars can be exploited to provide estimations of required fade margin for the satellite link. Figure 6.4 explains on how military satellite communications contacted each other.

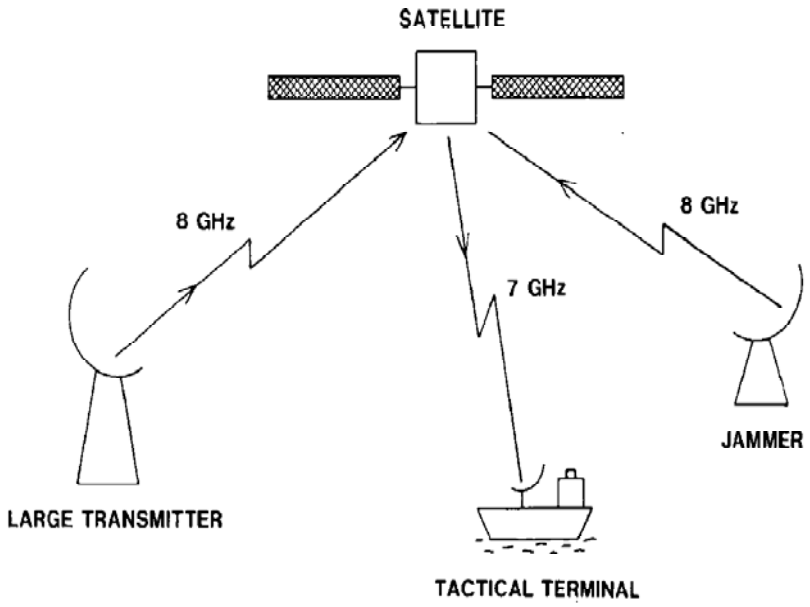

Figure 6.4: Military Satellite Communication

Table 6.3: ITU-R assigned frequency for Malaysian Military Satellite Communications (Frequency Allocation Table, 2010)

Uplink Frequency Band	7.9 to 8.4 GHz
Downlink Frequency Band	7.25 to 7.75 GHz
Local Oscillator Frequency (LNB)	6. 3 GHz
Bandwidth Frequency	0.5 GHz

In communication engineering, this pair of frequency bands may be referred to as the 8 / 7 GHz X-band satellite communications system. The new Malaysian X-band military satellite communication will be using the transponders installed on the recently launched MEASAT-3B satellite positioned at 91.5° E. The Earth terminal ground station is presumed to be established nearby Sg. Lang, Banting, Selangor. The elevation angle from the ground station is then calculated to be 71.5°.

6.3.1 X-band Rain Attenuation Predictions

In this assessment, two different rain attenuation prediction methods are presented. The first method identified as the latest rain attenuation prediction model, the ITU-R P.618-12-"Propagation Data and Prediction Methods Required for the Design of Earth-Space Telecommunication Systems" (2012). This procedure is the most up-to-date ITU-R published method to predict attenuation due to precipitation along a slant propagation path.

The technique currently implemented in ITU-R prediction model is based on the estimation of the attenuation exceeded at 0.01% of the time $A_{0.01}$, which is stipulated from the rainfall rate exceeded at the same time exceedance percentage, $R_{0.01.}$ The specific attenuation $\gamma_R$can be determined for a given value of rainfall rate at time exceedance 0.01%, $R_{0.01}$. Determination of the k and α values using the frequency-dependent coefficients, k_H, k_V, α_H, and α_V from Table 1 of the ITU-R P.838-3.

$$\gamma_R = k\,(R_{0.01})^{\alpha} = 7.2 \text{ dB km}^{-1} \tag{6.7}$$

When multiplied with the effective path length L_E, the corresponding attenuation value at 0.01% time exceedance $A_{0.01}$ can be calculated.

$$A_{0.01} = \gamma_R L_E = 15.92 \text{ dB} \tag{6.8}$$

The estimated attenuation, A to be exceeded for other percentages, p of an average year, in the range 0.001% to 5%, is determined from the attenuation to be exceeded for 0.01% for an average year using Equation (2.23). In the case of the MEASAT-3B,

the elevation angle, θ equivalent to 77.4° and β will be equal to 0.1646 after calculated using ITU-R 618-16 (2012) procedure

The subsequent step is the estimation of the X-band satellite link attenuation by exploiting local radar data acquired from the Malaysian Meteorological Department (MMD). The ability of a radar to scan a wide area around the radar site and not just a particular path made it a very practical for many types of investigations. By using the new technique involving the recently derived γ-Z relationship, the rain attenuation for the said link is calculated. The Cumulative Distribution Function (CDF) is generated by accumulating the attenuation values for every raining events in the year 2009. The amount of raining time is measured and accumulated for the whole year.The CDF from the radar data is compared against the ITU-R P618-12 prediction values. The predicted rain fade estimation using ITU-R recommendation and radar data prediction can be viewed in Figure 6.5. It can be observed that the deduced rain attenuation using radar data is higher than the ITU-R predicted values at all times exceedance.

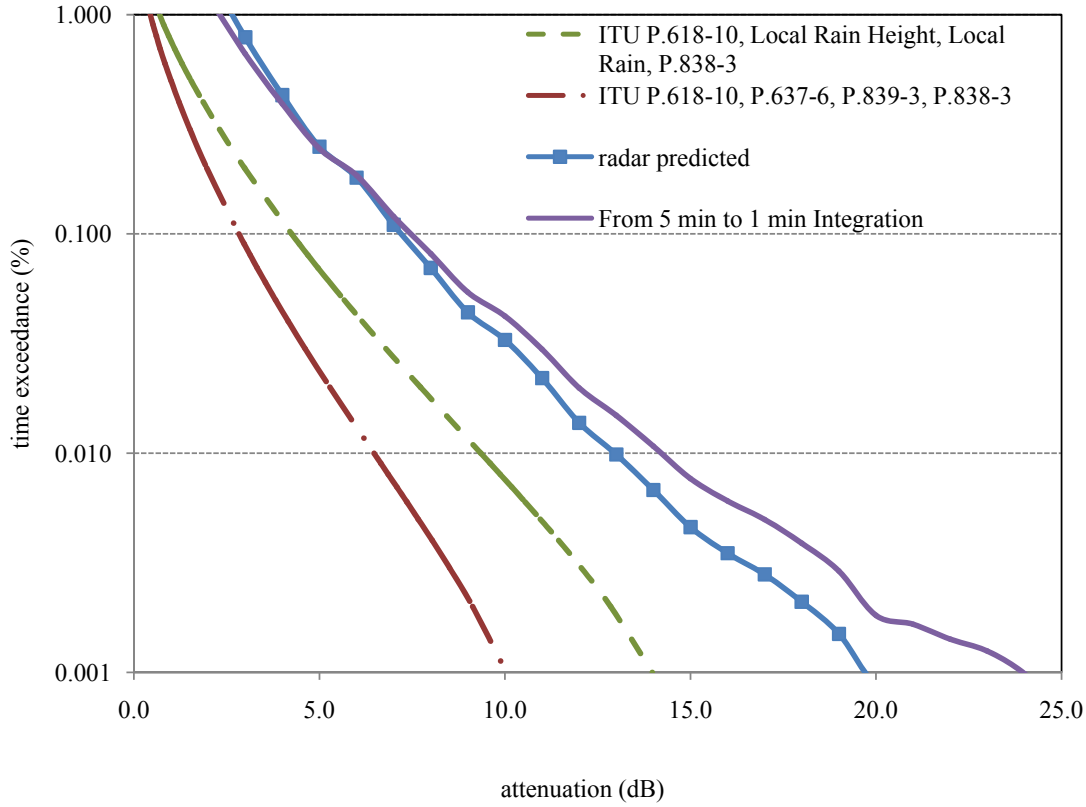

Figure 6.5: Plot of ITU-R Predicted Attenuation Statistics and Radar Derived Attenuation for X-band

Table 6.4 displays select predicted attenuationvalues for the military X-band satellite communication link in Malaysia. These values can be regarded as the required fade margins to overcome the severity of the rain induced attenuation that will be confronted. It can be generalized that the X-band satellite operation in Malaysia and others in tropical region may not be easily achievable to operate at 99.99% availability to concur with the strict communication Quality of Service (QoS) requirement. Considerable substantial margin by today's technological advancement of somewhat more than 6 dB according to ITU-R prediction or more than 13 dB

according to radar derived estimations; has to be incorporated into the communication link in order to cope with rain fading in such severe climate.

Table 6.4: Selected Time Exceedance and Rain Attenuation from ITU-R and Radar Data

Time exceedance (%)	ITU-R 618-12 rain attenuation estimation (dB)	Radar Data Prediction (dB)	Variation
1.000	0.446	2.582	2.136
0.100	2.872	6.005	3.133
0.010	6.461	13.361	6.900
0.001	10.041	20.658	10.617

If X-band satellite communications is to be actually implemented, current and forthcoming studies should be immediately dedicated on identifying integrated solutions in the satellite's design i.e. transmission power level management, determination of appropriate receiver reflector size, antennas configuration, radiating antenna technologies, steerable beam capability, etc. RF engineers can participate in the effort by exploring the use of one or more fading mitigation techniques to lessen the effect of rain induced attenuation.

6.4 Estimations of Fade Margin for the Malaysian MEASAT-3B Ku-Band Link

Communications satellites allow live transmissions of radio, television, and telephone to be sent anywhere in the world. The way humans connect with each otherhave been revolutionize by communication satellites. Direct-broadcast satellite (DBS) or Direct to Home (DTH) is a term used referring for satellite television broadcasts intended for home reception. Using this technique live television channel from other country canbe

easily accessed(Gomez, 2002).This is an alternative to the traditional cable television that have been serving home viewers for decades.MEASAT-3B has been launched on 12 September 2014. MEASAT-3B will be used to expand video and data services across Malaysia, India, Indonesia and Australia. The system is anticipated to increase data connectivity level up by between 10% and 20%, bridging the digital breach in Malaysia ("MEASAT's sixth satellite MEASAT-3B", 2014). MEASAT-3B operates as many as 48 Ku-band transponders simultaneously from the 91.5°E orbital location, where it will be co-located with MEASAT-3 and MEASAT-3A. The ground station of the MEASAT-3B is located at the current MEASAT facility (2.937° N and 101.658° E). Given bearing is 254°08′45″ and elevation angle towards the satellite is 77.4°. It will be a very commanding satellite where there will be more than double the current MEASAT-3A Ku-Band capacity. The satellite will allow the Malaysian operator to meet the increasing requirements and demands of DTH and telecommunications services in the region. MEASAT-3B broadcasting services would be the preferred means over cable TV due to its lower cost, reduced complexity of the set-up, high definition, portability and increased number of channels (Itagaki et al. 2004). Unfortunately, the most severe setback of such DTH service is signal disruptions due to heavy rainfall. The signal discontinuation is the result of microwave radio frequency (RF) signal absorption by atmospheric hydrometeors namely rain. The losses are prevalent at frequencies above 10 GHz (Allnutt and Pregniuss, 1989). Figure 6.6 shows the typical broadcasting satellite set-up.

The estimated annual rain fade statistics using ITU-R recommendation and radar derived rain attenuation prediction can be viewed in Figure 6.7. The measured Ku-band rain fade statistics was also shown in the Figure 6.7. It can be observed that

the deduced rain attenuation statistics values estimated using radar data are higher than the ITU-R predicted values at all times exceedance. Table 6.5 catalogues selected fade margin at specific time exceedances for the MEASAT-3B Ku-band satellite-Earth link in Malaysia.

Figure 6.6: Typical MEASAT Satellite Broadcast Configuration

Table 6.5: Estimated Fade Margins at Selected Time Percentages

Time exceedance	Radar-Derived Attenuation (dB)	ITU-R 618-12 rain attenuation estimation (dB)	RMSE
1.000	3.27	1.26	2.02
0.300	10.4	4.7	1.42
0.100	13	8	1.25
0.010	25	13	3.00
0.001	35	28	1.75

These initial outcomes suggested that due to the severity of the rain induced attenuation that will be confronted, the Ku-band satellite broadcasting operation in Malaysia and others in tropical region may not be easily achievable to operate at 99.97% availability (equivalent to 0. 3% time exceedance) to concur with the strict broadcasting QoS requirement (Public Inquiry Report on The Mandatory Standards

for the Quality of Service, 2002). It is very crucial to be capable of accurately estimate the impairments of the given link in order to devise the services efficiently.

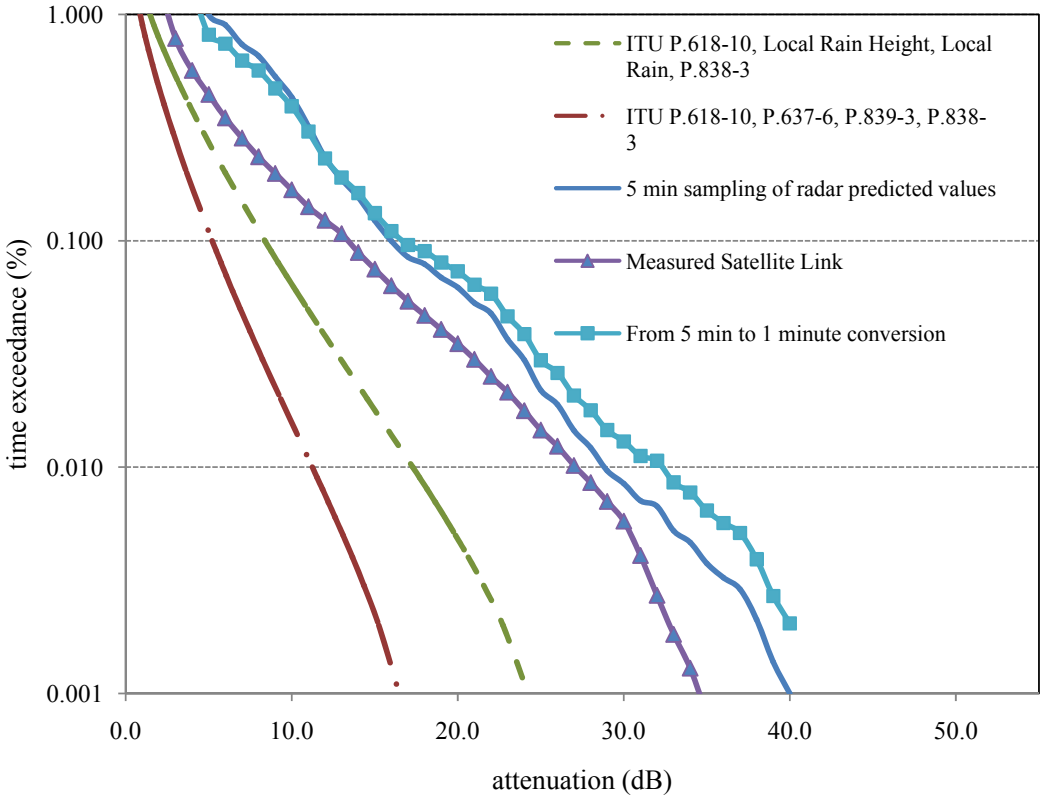

Figure 6.7: Plot of ITU-R Predicted Attenuation Statistics and Radar Derived Attenuation for Ku-Band

6. 5 Conclusion

The S-band single polarization radar reflectivities are able to offer good estimation the rain attenuation for Earth-satellite link. The comparison with the satellite link measurements has proved that the radar reflectivity values can be used as a good estimator for rain attenuation prediction. The advantage of the radar return value is that it is capable of providing aerial precipitation where it is impossible using rain gauges. The values of the rainfall rate from the radar reflectivity are known at any instantaneous point along the slant path. With the assimilation of the radar reflectivity

and the appropriate γ-Z relation, the actual attenuation during convective rain or stratiform rain events at any location and time can be predicted. This is significant since such rain events are frequent in tropical regions like Malaysia. This is very important for the satellite engineers and researchers as an alternative means to plan link budget estimation and set-up.

CHAPTERSEVEN

CONCLUSION AND FUTURE WORK

7.1 Conclusion

Each chapters of this thesis has a self-contained brief conclusion. The aim of this final chapter is to present a comprehensive ending. All the objectives have been achieved. It alsodraws all the ideas within the research work together so that interrelations can be clearly grasped between each seemingly separate section. Studies relating to the prediction of attenuation by rainfall in tropical climates have been presented in this thesis based on 6 months of RazakSAT satellite -Earth link received power signal and 12 months radar data in KLIA, Malaysia. The analyses concerning comparison between measured signals of RazakSAT's Malaysian X-band satellite link and radar derived attenuation using an S-band meteorological radar was presented. RazakSAT's satellite link received power during clear sky and rainy conditions were compared to extract the rain attenuation values. Detected rain events comprise of convective (26.6%) and stratiform (73.4%). The S-band radar horizontal polarization reflectivity information was used to estimate the corresponding rain attenuation along the RazakSAT satellite propagation paths.The first objective to develop the rain attenuation estimation has been achievedusing the derived radar reflectivity information. Newtechniques also have been developed in this study. In the first technique, radar reflectivity values were converted into rainfall rates using the previouslyproposed Z-R relation. The slant path attenuation can then determined using the specific rain attenuation formula and the rainfall rate values. It can be observed that at elevation angle of 60°the radar derived rain attenuation values (0.83 dB) are lower than the measured satellite link signals (1.22 dB). The variation might be due to

unsuitable formula used in converting the rainfall rate value from reflectivity. Standard regression analyses were carried out and a new formulation inclusive of a correction factor of $A'' = 1.33\theta^{-0.10}$ was introduced. VPR for stratiform and convective rain to account the vertical variability of rain specific attenuation with height have been proposed. The analyses were performed in the attempt to determine the applicable rain heights in the tropics, 10.24 km and 6.21 km for convective and stratiform rain respectively. The second method of estimating rain attenuation using radar data involves derivation of specific attenuation(γ) -reflectivity(Z) relationship. The two conditions for stratiform and convective rain are $\gamma = 0.0238Z^{0.3113}$ and $\gamma = 0.0554Z^{0.2112}$ respectively. Both methods introduced in this thesis are capable of offering improved rain attenuation predictions for communication system operating in the tropical region. The first method offers an estimation with only 4.12% variation. The second method which is objective two provides an estimation with 16% variation. As for objective three, a more dependable fade margin was identified from the CDF generated using the first techniques. The value at 0.01% time exceedance is 13.36 dB ; much larger than that of ITU-R's 6.46 dB. The assessment and validation of the two techniques is shown in Chapter 6.

The study is not without its shortcomings. One of the concerns involved reliability of radar data.Limitations of radar measurement needto be highlighted. For example, radar domain cannot besampled at consistent elevations. Beam elevation increases with distanceresulting in ambiguity of low-level precipitation at far away distances.Bin size also increases withdistance, thus suffers incomplete beam filling, smearing of small-scale structure; groundclutter and terrain features may block low

level information.The radar system also has to be calibratedregularly toensure reliable data collection.

One of the first data processing activities was the rejection of permanent echo orpermanent echo check. This was done by taking samples from the radar data and checkwhether there are any instances where there is always a reading at a particular point.This will indicates permanent echo.The operator of the weather radar of the Meteorological Department ofMalaysia explained that they have included echo rejection in their data processingroutines.

7.2 Future Work

Existing propagation models in the temperate regions are well established and are relatively reliable. There are no well-established approaches for tropical region in the millimetre frequency range. In order to respond to this uncertainty, the research carried out in this thesis has been directed on the quantifying propagation characteristics.

Despite some advances in the recent years, ITU-R propagation prediction methods continue to lack of universal applicability, particularly in tropical areas. It is apparent that the latest ITU-R method seriously underestimates the measured attenuation. This could largely due to a shortage of measurement data for these regions of concerned. Hopefully this situation is changing in view of recent efforts to establish appropriate propagation experiments. Especially useful work to further radar measurements in conjunction with satellite beacons.

Rainfall rate and rain height are widely employed in attenuation models to predict signal fading due to rain. Nevertheless, prediction models rarely differentiate

among types of rain parameters despite being considered as factors that can greatly enhance the accuracy in rain attenuation estimates. In this work, the matters have been addressed by studying the correlation of specific attenuation withreflectivity for stratiform and convective precipitation. Further information about the occurrence of each statistics of the rain intensity are needed for an improved rain attenuation model. The initial evaluation of these two factors in Kuala Lumpur has revealed that stratiform precipitation is much more frequent than convective rain and dominates the low availability range statistics. This approach could be extended to include appropriate parameters based upon the type of rain in the propagation model.

Another aspect for further investigation is the modelling of attenuation is the melting layer. The radar parameter Doppler mean velocity, when combined with dBZ and *LDR* can act as sensitive indicator of bright band regions in stratiform and convective events. Dual polarization radar can make the analysis productive. Besides that, the available S-band and X-band frequency from the RazakSAT satellite can be a good indication to analyse the frequency scaling for the γ-Z relationship. DSD derivations are also an important factor that has to be point out. An experiment set-up with a distrometer should be expedite. These facts add additional force to arguments for further radar measurement campaigns. Finally, given the adverse propagation characteristics in tropical regions, it is clearly evident that work to develop fade countermeasures should be undertaken significantly.

REFERENCES

Allnutt, J.E.(1989).*Chapter 4, Satellite-To-Ground Radiowave Propagation*, Peter Peregrinus, Ltd., London.

Allnutt, J.E., and Rogers, D.V. (1990). *The INTELSAT Slant-Path Radiowave Propagation Experiments in Tropical Regions*, International Journal of Satellite Communications, vol.8, pp.181-186

Anagnostou, M.N., Anagnostou, E.N., Vivekanandan, J. (2006). *Correction for Rain Path Specific and Differential Attenuation of X-Band Dual-Polarization Observations*, Geoscience and Remote Sensing, IEEE Transactions on , vol.44, no.9, pp.2470-2480.

Atayero, AAA., Matthew K. L., Orya M. K., Adeyemi A. A, (2011). *Satellite Communications: Impact on Developing Economies.* Journal of Emerging Trends in Computing and Information Sciences, Vol. 2, pp. 574-579.

Ajayi, G.O (Editor) (1996) *URSI Handbook on Radiowave Propagation Related to Satellite Communications in Tropical and Subtropical Countries*, URSI publication

Brost, G.A., Cook, W.G. (2012). Analysis of empirical rain attenuation models for satellite communications at Q to W band frequencies," *Antennas and Propagation (EUCAP), 2012 6th European Conference on* , vol., no., pp.1455-1459, 26-30

Badron, K., Ismail, A.F., Din, J., Tharek, A.R. (2009). Rain induced attenuation studies for V-band frequency in tropical regions," *Antennas & Propagation Conference, 2009. LAPC 2009. Loughborough* , vol., no., pp.689-692, 16-17

Badron, K.; Ismail, A.F.; Ramli, H.A.M.; Ismail, M.; Ooi, S.T.; Jamil, S.F.(2013). *Evaluation of RazakSAT's S-band link signal measurement with the radar derived rain attenuation,* Space Science and Communication (IconSpace), 2013 IEEE International Conference on , vol., no., pp.380,384, 1-3 July 2013.

Baldini, L.; Gorgucci, E.; Romaniello, V.; (2008). *An integrated procedure for rainfall estimation using C-band dual-polarization weather radars*, Radar Conference, 2008. RADAR '08. IEEE , vol., no., pp.1-4, 26-30 May 2008

Bandera, J., Papatsoris, A.D., Watson, P.A., Tozer, T.C., Tan, J. And Gordard, J.W. (1999) *Vertical Path Reduction Factor for High Elevation Communication Systems*, Electronics Letters, vol.35, no.18, 2 Sept. 1999, pp.1584-5. Publisher: IEE, UK

Brussaard, G., and Watson, P.A. (1995), *Chapter 4, Atmospheric Modelling and Millimetre Wave Propagation*, Chapman & Hall, London.

Cakaj, S. Kamo, B., Koliçi V. and Shurdi, O. (2011). *The Range and Horizon Plane Simulation for Ground Stations of Low Earth Orbiting (LEO) Satellites*, International Journal of Communications, Network and System Sciences, Vol. 4 No. 9, pp. 585-589.

Cakaj, Sh. , Keim W. and Malaric, K. (2007) *Communication Duration with Low Earth Orbiting Satellites*, *Proceedings of IEEE*, *IASTED*, 4*th International Conference on Antennas*, *Radar and Wave Propagation*, Montreal, 30 May-1 June 2007, pp. 85-88.

Cakaj, Sh. and Malaric, K. (2005). *Rigorous Analysis on Per-formance of LEO Satellite Ground Station in Urban En-vironment*, International Journal of Satellite Communi-cations and Networking, Vol. 25, No. 6, 2007, pp. 619- 643.

Ciach, G. J. and Krajewski, W. F. (1999). *On the estimation of radar rainfall error variance*. Adv. Water Res., 22(6), 585–595

Crane, R.K. (1980) *Prediction Of Attenuation By Rain*, IEEE Transactions on Communications, COM-28, pp. 1717-1733

Crane, R.K. (1990) *Modelling Attenuation by Rain in Tropical Region*, International Journal of Satellite Communication, vol. 8, pp. 197-210

Currie, N.C., and Brown, C.E. (1987). *Principles and Applications of Millimeter-Wave Radar*, Artech House, Massachusetts, USA

Cherry, S.M., Goddard, J.W. and Hall, M.P.M. (1981) *The Use of Dual Polarisation Radar Data for Evaluation of Attenuation on Satellite-to-EarthPath*. Ann. Telecomm. Vol. 36 pp. 33-39

Crane, R.K. (2003). *A local model for the prediction of rain-rate statistics for rain-attenuation models," Antennas and Propagation,* IEEE Transactions on , vol.51, no.9, pp. 2260- 2273.

Chun, H. J., Kim, B. J., Chang, H. S., Kim, E. E., Park, W. K., Park, S. D. and Arshard, A.S (2006). *RazakSAT – A High Performance Satellite Waiting for Its Mission in Space*, Small Satellite Conference

Creutin, H. A. and Jean, D.(1995). *Identification of Vertical Profiles of Radar Reflectivity for Hydrological Applications Using an Inverse Method. Part I:Formulation*, J. Appl. Meteorol., vol. 34, no. 1, pp. 225–239, 1995.

Dahiya, S., Garg, P.K., Jat, M.K., (2013) *Object oriented approach for building extraction from high resolution satellite images,* in Advance Computing Conference (IACC), 2013 IEEE 3rd International , vol., no., pp.1300-1305, 22-23 Feb. 2013

Das, S.; Shukla, A.K.; Maitra, A.;(2009). *Classification of convective and stratiform types of rain and their characteristics features at a tropical location,* Computers and Devices for Communication, 2009. CODEC 2009. 4th International Conference on , vol., no., pp.1-4, 14-16.

Das, S.; Talukdar, S.; Bhattacharya, A.; Adhikari, A.; Maitra, A. (2011). *Vertical profile of Z- R relationship and its seasonal variation at a tropical location,* in Applied Electromagnetics Conference (AEMC), 2011 IEEE , vol., no., pp.1-4, 18-22

Dalgeish, D.I. (1989). C*hapter 5, An Introduction to Satellite Communications,* Peter Peregrinus, London

Dissanayake, A., Lin, K.T. (2002). *Ka-band rain attenuation estimation using weatherradar*, Journal Space Communications, Vol. 18 Issue 1,2,pages 53-58.

Donald, A.C. (1994). *Meteorology Today, An introduction to Weather, Climate and Environment*, West Publishing, Minnesota

Doviak, R.J., and Zrnic, D.S (1993). 2nd Edition, *Doppler Radar and Weather Observation*, Academic Press, London

Eastment, J.D., Thurai, M., Ladd, D.N., AND Moore, I.N. (1998). *Radiowave Propagation Research in The Tropics Using A Transportable Multiparameter Radar System,* Electronics & Communications Engineering Journal, vol. 10, pp. 4-16

Eastment, J.D (1999) *Polarimetric Doppler Radar*, PhD Thesis, University of Bradford, UK

Eastment, J.D., Thurai, M., Ladd, D.N., and Moore, I.N. (1995) *A Vertically- Pointing Doppler Radar to Measure Precipitation Characteristics in The Tropics*, IEE Transactions on Geoscience and Remote Sensing, vol. 33, pp.1336-1340

Eastment, J.D., Thurai, M., Ladd, D.N., and Moore, I.N. (1998), *Radiowave Propagation Research in The Tropics Using A Transportable Multiparameter Radar System,* Electronics & Communications Engineering Journal, vol. 10, pp. 4-16

Elbert, Bruce R. (2008). *Introduction to Satellite Communication*. Artech House, 3rd. s.l, p. 447

Flavin, R.K. (1982) *Rain Attenuation Consideration for Satellite Paths in Australia*, Australian Telecommunication Research, vol. 16, pp. 11-24

Fukuchi, H. (1992) *Slant Path Attenuation Analysis at 20 GHz for Time-Diversity Reception of Future Satellite Broadcasting*, U.R.S.I. Open Symposium, Wave Propagation and Remote Sensing, Univ. Bradford,pp. 6.5Bradford, UK

Garcia Lopez, J.A., Hernando, J.M., and Selga, J.M. (1988). *Simple Rain Attenuation Prediction Method for Satellite Radio Links*, IEE Transaction of Antenna and Propagation vol. 36 no. 3, pp.444-448

Gayrard, J.D., (2009). *Terabit Satellite: Myth or Reality?,Advances in Satellite and Space Communications, 2009. SPACOMM 2009. First International Conference on* , vol., no., pp.1-6, 20-25.

Geerts, B. and Teferi, D., (2005). *Regional and diurnal variability of the vertical structure of precipitation systems in Africa based on spaceborne radar data*, J. Climatol., vol. 18, pp. 893–916

Godara, L.C. (2001). *Handbook of Antennas in Wireless Communications (Electrical Engineering & Applied Signal Processing Series*) 1st Edition, CRC Press; 1 edition

Gomez, J.M. (2002). *Satellite Broadcast Systems Engineering,* Artech House, 1ST edition, 2002.

Goddard, J.W.F., and Cherry, S.M. (1984). *The Ability of Dual-Polarisation Radar (Co-polar Linear) to Predict Rainfall rate and Microwave Attenuation*, Radio Science, vol. 19, pp. 201-208

Goldhirsh, J., and Katz, I. (1979). *Useful Experimental Results for Earth-Satellite Rain Attenuation Modelling*, IEE Transaction on Antenna and Propagatoin 1979 vol. 27 pp. 413- 415

Habib, E., Krajewski,W.F and Kruger A. (2001). *Sampling Errors of Tipping Bucket Rain Gauge Measurements*, Journal of Hydrologic Engineering, Vol. 6, No. 2, pp.159.

Houze JR, R.A. (1981). *Structures Of Atmospheric Precipitation Systems: A Global Survey,*Radio Science, vol. 16, pp. 671-689

Hall, M.P.M, and Goddard, J.W.F. (1978). *Variation with Height of the Statistics of Radar Reflectivity due to Hydrometeors*, Electronics Letters, vol. 14, no. 17, pp. 224-225

Hodge, D.B. (1973) *The Characteristics Of Millimetre Wavelength Satellite-To-Ground Space Diversity Links*, IEE Conference Publication, vol. 98, pp. 28-32

Houze JR, R.A. (1981) *Structures Of Atmospheric Precipitation Systems: A Global Survey*, Radio Science, vol. 16, pp. 671-689

Hughes, K.A. (1990) *CCIR Data for Slant-Path Propagation in Tropical Regions: A Critical Review*, International Journal of Satellite Communications, vol. 8, pp. 127-139

Hulbert, J. (1973) *Chapter 12, The World's Weather*, Pergamon Press, Oxford

Ippolito, L.J. (1986) *Propagation in Satellite Communications*, Van Nostrand Reinhold, New York

Itagaki, T.; Cosmas, J.; Haque, M., :*An interactive digital television system designed forsynchronised and scalable multi-media content over DVB and IP networks,* Multimedia and Expo, 2004. ICME '04. 2004 IEEE International Conference on , vol.3, no., pp.2155,2158 Vol.3, 27-30 June 2004.

International Telecommunication Union (2010), *Frequency allocation table* Retrieved from https://www.itu.int/ITU-D/asp/CMS/Events/2010/SMS4DC/SMS4DC2_AllocationsV2.pdf

Ismail, AF.; Badron, K.; Yaccop, AAH.; Yao, Y.D.(2013). *Determination of Ku-band specific attenuation parameters based on measurements in the tropics*, Antennas and Propagation Society International Symposium (APSURSI), 2013 IEEE , vol., no., pp.2008,2009, 7-13

Jokanovic, D.; Josipovic, M. (2011). *RF spectrum congestion: Resolving an interference case*, *Microwaves, Communications, Antennas and Electronics Systems (COMCAS), 2011 IEEE International Conference on* , vol., no., pp.1-4, 7-9

Joss, J., and PIittini, A. (1991). *Climatology of Vertical Profiles of Radar Reflectivity*, Proceedings of 25th Conference on Radar Meteorology, pp. 828-831

Joss, J. and Waldvogel, A. (1989) *Precipitation and Vertical Reflectivity Correction*,Proceedings of 24th Conference on Radar Meteorology, pp. 682-688

Kota, S., Giambene, G., and Kim S. (2011). *Satellite component of NGN: Integrated and hybrid networks,* Int. J. Satell. Commun. Network.Vol. 29, pp.:191–208

Khairolanuar, M.H Ismail, A.F, Jusoh,A.Z, Sobli,N.H.M, Badron,K. (2015) *Assessment of Conversion Methods to Acquire 1-Minute Integration Time Rain Intensity Statistic* , Theory and Applications of Applied Electromagnetics ,Lecture Notes in Electrical Engineering Volume 344, 2015, pp 175-183, 14.

Khairolanuar, M.H. Ismail, A.F., Jusoh, A.Z., Sobli, N.H.M., Malek, N.F.A., and Zabidi, S.A.(2014) *New Empirical Conversion Technique for 1-minute Integration Time of Precipitation Intensity in Malaysia*, Aust. J. Basic & Appl. Sci.,8(24):290-295.

Khamis, N. H. H., Sharif, O. A. R., Hanzaz, Z. and Baharom, A. (2006). *Determination of the melting layer from meteorological radar data in Malaysia,* IEEE 2007 Int. Symp. Microwave, Antenna, Propag. EMC Technol. Wirel. Commun. MAPE, pp. 1467– 1470.

Kingsley, S., and Shaun Q. (1992) *Understanding Radar Systems*, McGraw-hill London, UK

Kirby, K., Stratton, J., (2013) *Van Allen Probes: Successful launch campaign and early operations exploring Earth's radiation belts,*Aerospace Conference, 2013 IEEE , vol. 10, no. 1, pp.2-9

Kumar L. S., Y. H. Lee, J. X. Yeo, and J. T. Ong. 2011. "*Tropical Rain Classification and Estimation of Rain from Z-R (Reflectivity-Rain Rate) Relationships*." Progress In Electromagnetics Research B, 32 (July): 107–27.

Kyung Soo Choi; Jae Hoon Kim; Do-Seob Ahn; Nam Ho Jeong; Jeong Ki Pack; (2011). Trends in rain attenuation model in satellite system, *Advanced Communication Technology (ICACT), 2011 13th International Conference on* , vol., no., pp.1530- 1533, 13-16

Harikumar, R., Sampath, S. Sasi, Kumar. V. (2010) *Variation of rain drop size distribution with rain rate at a few coastal and high altitude stations in southern peninsular India*. Advances in Space Research 45, 576-586.

Latef, A.S.A.; Hassan, R. (2011). *Spectrum management system: A study*, *Electrical Engineering and Informatics (ICEEI), 2011 International Conference on* , vol., no., pp.1-6, 17-19.

Ladd, D.N., Wilson, C.L., and Thurai M. (1997). *Radar Measurements from Papua New Guinea and Their Implications for TRMM PR Retrieval Algorithms*. IGARSS'97, International Geoscience and Remote Sensing Symposium, Remote Sensing - A Scientific Vision for Sustainable Development IEEE, vol. 4, pp. 1648-1650 New York, NY, USA.

Leitou, M.J., and Watson, P.A. (1986) *Method for Prediction of Attenuation on Earth-Space Links Based on Radar Measurements of Physical Structure of Rainfall*, IEE Proceedings, vol. 133, pp. 429-440

Lekla, R., Lim, S.L., Watcha, J., and McCormick, K.S. (1995) *Rain Attenuation Measurements in South-East Asia*, Proceedings of URSI-F open symposium, Ahmedabad, India, pp. 241-244.

Llorente, R., Medina, N., Morant, M., Boronat, F., (2011), *Evaluation of UHDTV signal transmission in FTTH networks using next generation WiMedia UWB, Future Network & Mobile Summit (FutureNetw), 2011* , vol., no., pp.1-8, 15-17

Malaysian Communications and Multimedia Commission (2007) Satellite Industry Developments Retrieved from http://www.skmm.gov.my/skmmgovmy/files/attachments/Satellite_Industry_Developments.pdf

Malaysian Communications and Multimedia Commission. (2003). QUALITY OF SERVICE MANDATORY STANDARDS REPORT FOR THE PERIOD ENDING DECEMBER 2003. Retrieved from http://www.skmm.gov.my/skmmgovmy/files/attachments/QoS%20MS2003-FINAL.pdf

Mandeep, J.S., Ooi Wen Hui, Abdullah, M., Tariqul, M.; Ismail, M., Suparta, W., Yatim, B., Menon, P.S., Abdullah, H. (2011). *Modified ITU-R rain attenuation model for equato rial climate, Space Science and Communication (IconSpace), 2011 IEEE Intern ational Conference on , vol., no., pp.89-92, 12-13 July*

Marshall, J.S., and Palmer, W. Mck. (1976) *The Distribution Of Raindrops With Size*, Journal Meteorology, vol. 5, pp. 16-166

Matricianni, E. (1997) *Prediction of Orbital Diversity Performance in Satellite Communication Systems Affected by Rain Attenuation*, International Journal of Satellitte Communications, vol. 15, pp. 45-50

Maekawa, Y.; Miyamoto, S.; Sawai, K.; Shibagaki, Y.; Sato, T.; Yamamoto, M.; Hashiguchi, H.; Fukao, S., (2009).*Estimation of rain attenuation characteristics of satellite communication links using x-band meteorological radars*, ICCAS-SICE, 2009 , vol., no., pp.1320,1323, 18-21 Aug.

Measat-3B (2013). Retrieved From http://www.measat.com/3b/overview/mission.html Available Online.

Measat-3B :Largest satellite ever ordered by Malaysian operator MEASAT (2012) Retrieved Fromhttp://www.astrium.eads.net/en/programme/-measat-3b.html Available Online. Retrieved 2nd Mar 2014

Moupfama, F. (1987) *Rain Induced Attenuation Prediction Model for Terrestrial and Satellite-Earth Microwave Links*, Annual Telecommunications, vol. 42, no. 9-10, pp.539-550

Moupfama, F. (1997) *A New Theoretical Formulation for Calculation of the Specific Attenuation Due to Precipitation Particles on Terrestrial and Satellite Radio Links*, International Journal of Satellite Communications, vol. 15, pp. 89-99

Mori, S.; Marzano, F.S.; Montopoli, M.; Pulvirenti, L.; Pierdicca, N.; Weinman, J.A. (2011). Modelling polarimetric effects of precipitation on spaceborne side-looking aperture radar response," *Antennas and Propagation (EUCAP), Proceedings of the 5th Europ ean Conference on* , vol., no., pp.29-33, 11-15

Oguchi, T. (1983) *Electromagnetic Wave Propagation and Scattering in Rain and Other Hydrometeors*, Proceedings of the IEEE, vol. 71, pp. 1029-1078

Olsen, R.L., Rogers, D.V., and Hodge, D.B. (1978) *The aRb Relation in the Calculation of Rain Attenuation*, IEEE Transactions on Antennas and Propagation, AP-26, 1978, pp. 318-32 9

Ong, J.T., Timothy, K.I., Choo, E.B.L., and Carron, W.L. (2000) *Effective Rain Height Statistics for Slant Path Attenuation Prediction in Singapore*, Electronics Letters, vol.36, no. 7, pp. 661-663. Publisher: IEE, UK.

Ong, J.T., and Shan, Y.Y. (1997) *Rain Drop Size Distribution Models for Singapore – Comparison with Results from Different Regions*, Proceedings of the 10th International Conference on Antennas and Propagation (ICAP'97), p.p. 2.281-2.285, Edinburgh UK

Otsu, T., Toshiniaga, H., Matsuda, M., Kazama, H. (1998). *A study on global multimedia satellit e communication system*, *Global Telecommunications Conference, 1998. GLOBECOM 1998. The Bridge to Global Integration. IEEE* , vol.5, no., pp.2960,2965 vol.5.

Otto, T.; Russchenberg, H.W.J. (2011). *Estimation of Specific Differential Phase and Differential Backscatter Phase From Polarimetric Weather Radar Measurements of Rain*, *Geoscience and Remote Sensing Letters, IEEE* , vol.8, no.5, pp.988-992.

Panagopoulos, A.D., Arapoglou, P.D.M., Chatzarakis, G.E., Kanellopoulos, J.D., Cottis, P.G., (2006) *Coexistence of the broadcasting satellite service with fixed service systems in frequency bands above 10 GHz*, *Broadcasting, IEEE Transactions on* , vol.52, no.1, pp. 100- 107.

Performance Management & Delivery Unit (PEMANDU). (2011). National Key Econo mic Area Retrieved from http://etp.pemandu.gov.my/annualreport2011/12_National_Key_Economic_Areas-@- 12_National_Key_Economic_Areas.aspx

Pillai, S.U. Himed, B., Yong, L.K. (2006). *Effect of earth's rotation and range foldover on space-based radar performance,*Aerospace and Electronic Systems, IEEE Transactions on , vol.42, no.3, pp.917-932, July

Pratt, T., and Bostan, C.W. (1986) *Satellite Communications*, John Wiley & Sons, New York.

Prentiss, S. (1987) *Satellite Communications*, Tab Books, United States

Pritchard, W.L., and Sciulli, J.A. (1986) *Satellite Communication Systems Engineering*, Prentice Hall, New Jersey, USA

Recommendation ITU-R P.618-5 (1997) *Propagation Data and Prediction Methods Required for the Design of Earth-Space Telecommunication Systems*

Recommendation ITU-R P.618-12 (2015) *Propagation Data and Prediction Methods Required for the Design of Earth-Space Telecommunication Systems*

Recommendation ITU-R P.679-4 (2015) *Propagation Data Required for the Design of Broadcasting-Satellite Systems*

Recommendation ITU-R P.837-1 (1994) *Characteristics of Precipitation for Propagation Modelling*

Recommendation ITU-R P.837-6 (2012) *Characteristics of Precipitation for Propagation Modelling*

Recommendation ITU-R P.838-3 (2005) *Specific Attenuation Model for Rain for Use in Prediction Methods*

Recommendation ITU-R P.839-4 (2014) *Rain Height Model for Prediction Methods*

RadiocommunicationBureau (1996) *Handbook on Radiometeorology*, Geneva

Richharia, M. (1999) *Satellite Communication Systems*, McGraw Hill, New York 1999

Riley, D., and Spolton, L. (1974) *Part 3, World Weather and Climate*, Cambridge University Press, London

Rogers, D.V., and Olsen, R.L. (1976) *Calculation of Radiowave Attenuation Due to Rain a t Frequencies Up to 1000 GHz*, CRC report No. 1299. Communication Research centre, Department of Communications, Ottawa, Canada

Romo, J.A.; Maruri, M.; Perez-Fontan, F.; Fernandez, I. (2012) *Characterization of Maximum Radar Reflectivity Height During Stratiform Rain Events*, in Antennas and Propagation, IEEE Transactions on , vol.60, no.10, pp.4884-4891, Oct.

Roddy, D. (2006) *Satellite Communications,* McGraw Hill, New York

Savageot, H. (1992), *Radar Meteorology*, Artech House, Massachusetts, USA

Segal, B. (1986) *The Influence Of Rain gauge Integration Time on Measured Rainfall- Intensity Distribution Functions*, Journal of atmospheric and Oceanic Technology, pp. 662-671

Sevruk, B. and Klemm, S. (1989). *Catalogue of national standard precipitation gauges.* World Meteorological Organization, *Instruments and Observing Methods Rep.,* WMO/TD-No. 313, 50 pp.

Shan, Y.Y, (1996) *Study On Rain Attenuation Effects on Microwave Signals*, M.Eng. Thesis, Nanyang Technology, University, Singapore 1996

Sklar, B. (2001). *Digital Communications: Fundamentals & Applications, Second Edition*. Bernard Goodwin. Prentice Hall; 2 edition

Singh, M. S J; Hassan, S.I.S.; Ain, M.F.; Igarashi, K.; Tanaka, K.; Iida, M., (2005). *Proposed Rain Attenuation Model Revised from ITU Used for Prediction in Tropical Climates, Information,* Communications and Signal Processing, 2005 Fifth International Conference on , vol., no., pp.994,996,

Schnabl, G., (1988*). Polarimetric Radar Measurements of Rain and Radar Derived Attenuation and Depolarization in Rain at 20/30 GHz,* Microwave Conference, 1988. 18th European , vol., no., pp.436,441, 12-15 Sept.

Steiner, M., Houze, R. and Yuter. S. E. (1995). *Climatological Characterization of Three- Dimensional Storm Structure from Operational Radar and Rain Gauge Data*," Journal of Applied Meteorology, vol. 34. pp. 1978–2007, 1995.

Sudarshana, K.P.S.; Samarasinghe, A.T.L.K.(2011) *Rain rate and rain attenuation estima tion for Ku band satellite communications over Sri Lanka*, Industrial and Information Systems (ICIIS), 2011 6th IEEE International Confer ence on , vol., no., pp.1-6, 16-19

Tan, J. and Goddard, J. W. (1999). *Vertical variation of reflectivity and specific attenuation in stratiform and convective rainstorms*, vol. 35, no. 7, pp. 599–600.

Thurai,M., Eastment, J.D., Ladd, D.N. and Moore, I.N. (1995) *A Vertically-Pointing Doppler Radar to Study the Precipitation Characteristics in the Tropics*. Interna tional Geoscience and Remote Sensing Symposium, IGARSS '95. Quantitative Remote Sensing for Science and ApplicationsIEEE. Part vol.3, 1995, pp.1669 vol.3. New York, NY, USA.

Tri, T. (1990) *Digital Satellite Communication*, McGraw-Hill, New Jersey

Vilar, E., Montanari, C., Pontes, M.S., Silva Mello, L.A.R., Lorente, J., and Codina, B. (1997) *Scattering and Extinction: Dependence Upon Raindrop Size Distribution in Temperate (Barcelona) and Tropical (Belem) Regions*. Tenth International Conference on Antennas and Propagation, IEE, vol. 2, pp. 230-233, London, UK

Vivekanandan, J.; Turk, J.; Bringi, V.N.; (1993). *Comparisons of precipitation measurements by the Advanced Microwave Precipitation Radiometer and multiparameter radar*," Geoscience and Remote Sensing, IEEE Transactions *on* , vol.31, no.4, pp.860-870,

Vivekanandan, J.; Zhang, G.; Politovich, M.K. (2000*). Estimation of cloud droplet size and liquid water content using dual-wavelength radar measurements*,Geoscience and Remote Sensing Symposium, 2000. Proceedings. IGARSS 2000. IEEE 2000 International , vol.5, no., pp.1813-1816 vol.5

Watson, P.A. (1997) *Effect of Rain on SHF/EHF Terrestrial Systems*, Radio Propagation Prediction IDGS Lectures

Wiliamson, M. (1990) *The Communications Satellite*, Adam Hilger, Bristol, UK

Watson, P.A. and Allnutt, J.E. (1998) C*hapter 7, VSAT Book*, University of York

Wood, J. (1994) *Satellite Communications Pocket Book*, Newnes Butterworth-Heinemann, Oxford.

Wilson, C., and Tan, J. (2001). *The Characteristic of Rain fall and Melting Layer in Singapore: Experimental Results From Radar and Ground Instruments*. IEE, 11th International Conference on Antenna and Propagation,17-20 April 2001.

Wilson, C. , Tan, J., Goddard, J. W. and Ong, J. T. (2001). *Radar Vertical Profiles and Melting Layer Studies From an S-band Doppler Polarisation-Diversity Radar Campaign in Singapore*, in 30th INTERNATIONAL CONFERENCE ON RADAR METEOROLOGY- AME, 2001, no. July, p. 21.

Yaccop, A. A. H., Yao, Y. D., Ismail, A. F. and Badron, K. (2013). *Comparison of Ku-Band Satellite Rain Attenuation with ITU-R Prediction Models in the Tropics*, Antenna Propag. Symp., pp. 2006–2007.

Yeo, J.X., Lee, Y.H., Kumar, L.S., Ong, J.T.; (2012). *Comparison of S-Band Radar Attenuation Prediction With Beacon Measurements*, Antennas and Propagation, IEEE Transactions on , vol.60, no.10, pp.4892-4900, Oct. 2012.

Yeo, J.X., Lee, Y.H., Ong, J.T., (2009). *Modified ITU-R slant path rain attenuation model for the tropical region*, Information, Communications and Signal Processing, 2009. ICICS 2009. 7th International Conference on , vol., no., pp.1-4, 8-10

Zabidi, S.A., Md Rafiqul, I., Wajdi, A.K., (2013). *Rain attenuation prediction of optical wireless system in tropical region,* 2013 IEEE International Conference on Smart Instrumentation, Measurement and Applications (ICSIMA), , vol., no., pp.1,5, 25-27

Zafar, B.J., Chandrasekar, V., (2004) *Classification of precipitation type from space borne precipitation radar data and 2D wavelet analysis*, *Geoscience and Remote Sensing Symposium, 2004. IGARSS '04. Proceedings. 2004 IEEE International* , vol.5, no., pp. 3570- 3573 vol.5, 20-24

Zee, R. E. and Stibrany, P. (2002) *The MOST Microsatellite: A Low-Cost Enabling Technology for Future Space Science and Technology Missions*,Canadian Aeronautics and Space Journal, Vol. 48, No. 1, , pp. 1-10

Zvanovec, S., Pechac, P., (2006*). Rain Spatial Classification for Availability Studies of Point- to-Multipoint Systems,*Antennas and Propagation, IEEE Transactions on , vol.54, no.12, pp.3789-3796.

PUBLICATIONS

- **Journals**

1. Badron, K., Ismail, A.F., Ismail, M. Estimating tropical rain attenuation on the Earth-satellite path using radar data (2015**) International Journal of Remote Sensing**, 36 (24), pp. 6101-6115. **(WoS -Q2)**

2. K.Badron, A.F. Ismail, Mazslan Ismail, O.S.Teng and T.J Daim., Assessment of X-band Earth-Satellite link Rain Attenuation Prediction in Malaysia. **Aust. J. Basic & Appl. Sci**., 8(24): 254-259, 2014 **(SCOPUS)**

3. K. Badron, A. F. Ismail, A. Z. Jusoh, N. H. M. Sobli, M. Ismail, and W. Hashim, "Comparison of Radar Derived Rain Attenuation with the RazakSAT's X-Band Link Signal Measurement," ***International Journal of Computer and Communication Engineering***vol. 2, no. 4, pp. 428-432, 2013A. **(INSPEC, IET)**

4. C. M. Nuroddin, A. F. Ismail, K. Abdullah, K. Badron, M. Ismail, and W. Hashim, "Rain Fade Estimations for the X-Band Satellite Communication Link in the Tropics**,"** ***International Journal of Computer and Communication Engineering***vol. 2, no. 4, pp. 408-412, 2013. **(INSPEC, IET)**

- **Books Chapters**

1. Badron, K., Ismail, A.F., Asnawi, A., Nordin, M.A.W., Zahirul Alam, A.H.M., Khan, S. Classification of precipitation types detected in Malaysia (2015) Lecture Notes in Electrical Engineering, 344, pp. 13-21. **Theory and Applications of Applied Electromagnetics (SCOPUS)**

2. Badron, K., Ismail, A.F., Nordin, M.A.W., Isa, F.N.M., Asnawi, A. Fade margin estimation technique using radar data for satellite link (2015) Lecture Notes in Electrical Engineering, 344, pp. 247-253. **Theory and Applications of Applied Electromagnetics (SCOPUS)**

3. Badron, K., Ismail, A.F., Asnawi, A.L., Malek, N.F.A., Abidin, S.Z., Islam, M.R. Estimations of fade margin for the new malaysian MEASAT-3B Ku-band link (2015) Lecture Notes in Electrical Engineering, 344, pp. 95-103. **Theory and Applications of Applied Electromagnetics (SCOPUS)**

- **Conference Papers**

1. Badron, Khairayu and Ismail, Ahmad Fadzil and Asnawi, Ani Liza and Ismail, Madzlan and Salim, Hamid and Mustafa, Hafidzah (2014) *Comparison of X-band satellite link measurements with radar derived rain attenuation in the tropics.* In: The 3rd International Conference on Computer Engineering & Mathematical Sciences (ICCEMS 2014), 4th-5th December 2014, Aseania Resort & Spa, Langkawi, Malaysia. (**Scopus)**

2. Badron, Khairayu and Ismail, Ahmad Fadzil and Wan Nordin, Mimi Aminah and Zainal Abidin, Suriza and Ismail , Maszlan and Ooi, Sock Teng (2014) *Fade margin estimations for military X-band satellite communication links in tropical region.* In: The 3rd International Conference on Computer Engineering and Mathematical Sciences (ICCEMS14) , 4-5th December 2014, Langkawi, Malaysia. (**Scopus**)

3. Badron, K., Ismail, A.F., Ramli, H.A.M., Ismail, M., Ooi, S.T., Jamil, S.F. Evaluation of RazakSAT's S-band link signal measurement with the radar derived rain attenuation (2013) International Conference on Space Science and Communication, IconSpace, pp. 380-384. **(WoS)**

4. Nuroddin, A.C.M., Ismail, A.F., Badron, K., Zulkurnain, N.F., Ismail, M., Salim, H. Rain induced attenuation studies using RazakSAT space-earth links (2013) International Conference on Space Science and Communication, IconSpace, pp. 402-406. (**Wos**)